Development of environment-friendly adsorbents and adsorption of heavy metals

2016

PANG Meiling

Doctoral program in Advanced Materials Science and Technology

Graduate School of Science and Technology

Niigata University

Contents

Chapter 1

1.1 Background ..... - 2 -

1.2 Heavy Metals ..... - 3 -

1.3 Adsorbents ..... - 6 -

1.4 Theory ..... - 9 -

1.5 The Purpose and Outline of the Thesis ..... - 12 -

Chapter 2

2.1 Introduction ..... - 16 -

2.2 Experimental Section ..... - 17 -

2.2.1 Materials ..... - 17 -

2.2.2 Apparatus ..... - 18 -

2.2.3 Modification of Activated Carbon with $KMnO_4$ ..... - 19 -

2.2.4 Characterization of ACs (Activated Carbons) ..... - 19 -

2.2.5 Adsorption experiments of heavy metal ions and REEs using modified activated carbon ..... - 19 -

2.2.6 Effect of competitive cations on the adsorption of Pb^{2+} ..... - 21 -

2.2.7 Effect of competitive anions on the adsorption of Cr (VI) ..... - 21 -

2.2.8 Effect of competitive metal ions on the adsorption of heavy metals - 21 -

2.2.9 Regeneration studies ..... - 22 -

2.3 Results and Discussion ..... - 23 -

2.3.1 Characterization of the modified activated carbon ..... - 23 -

2.3.2 Adsorption of lead on modified activated carbon ..... - 24 -

2.3.3 Adsorption of Cr (VI) on modified activated carbon ..... - 26 -

2.3.4 Adsorption of REEs on modified activated carbon..... - 28 -

2.3.5 Adsorption Isotherms ..... - 29 -

2.3.6 Kinetic Studies ..... - 30 -

2.3.7 Desorption performance of heavy metal from ACs ..... - 31 -

2.4 Conclusions ..... - 32 -

Chapter 3

3.1 Introduction ..... - 54 -

3.2 Experimental section..... - 55 -

3.2.1 Materials ..... - 55 -

3.2.2 Synthesis of ZCHC ..... - 56 -

3.2.3 Characterization of ZCHC ..... - 57 -

3.2.4 Adsorption experiment for heavy metal and REEs Using ZCHC.... - 57 -

3.3 Results and Discussion ..... - 58 -

3.3.1 Characterization of ZCHC ..... - 58 -

3.3.2 Adsorption of Pb^{2+} on zeolite and ZCHC ..... - 58 -

3.3.3 Adsorption of Cr (VI) on ZCHC ..... - 60 -

3.3.4 Adsorption of REEs on ZCHC..... - 62 -

3.3.5 Adsorption isotherms..... - 64 -

3.3.6 Kinetic Studies ..... - 65 -

3.4 Mechanism ..... - 67 -

3.5 Conclusions ..... - 67 -

Chapter 4

Conclusions..... - 86 -

References……-92 -

Acknowledgements……-106 -

Chapter 1 General Introduction

1.1 Background

With the rapid development of industry, the water pollution is becoming more and more serious in the world. Based on the type of mining, the kinds and the concentrations of metal ions are many and varied. Thus the minimization and recovery of harmful pollutants, such as heavy metals in natural environment is very significant as well as monitoring and determination of the pollutants from the viewpoint of environmental protection [1, 2]. On the other hand, the demand of metallic elements in modern society has increased remarkably over the past years. However, the shortage of metals including REEs has been concerned in recent years, and the establishment of the new recovery method for the rare metals is important from the viewpoint of resources recovery [3].

There are many processes for the treatment of metal-contaminated wastewaters, including chemical precipitation, membrane filtration, reverse osmosis, ion exchange, and adsorption [4-8]. However these technologies become expensive or inefficient for the treatment of metal ions with high concentrations. Then, it is important to develop new methods for the removal and recovery of metals from such effluents, and thus reduce the concentration of these metal ions to low levels. Adsorption has been proved as one of the most efficient methods for the removal of heavy metals from aqueous media [9-13].

The most problematic contaminants include heavy metals, pesticides and other organic compounds which can be toxic to wildlife and humans in small concentration. Recently, an extensive body of research has found that a wide variety of commonly

discarded waste including chitosan [14], eggshells [15, 16], seaweed [17, 18], yeast [19] and carrot peels [20] can efficiently remove toxic heavy metal ions from contaminated water. In addition, adsorbing biomass, or biosorbents can also remove other harmful metals like: arsenic [21, 22], lead, cadmium [16, 23], cobalt [24], chromium [25] and uranium[26]. Adsorbent based on biological materials may be used as an environmentally friendly filtering technique.

1.2 Heavy Metals

A toxic heavy metal is any relatively dense metal or metalloid that is noted for its potential toxicity, especially in environmental. The term has particular application to cadmium, mercury, lead and arsenic, all of which appear in the World Health Organisation's list of 10 chemicals of major public concern [27, 28]. Other examples include manganese, chromium, cobalt, nickel, copper, zinc, selenium, silver, antimony and thallium.

Heavy metals are found naturally in the earth, and become concentrated as a result of human caused activities. Common sources are from mining and industrial wastes; vehicle emissions; lead-acid batteries; fertilisers; paints; treated woods; aging water supply infrastructure; and microplastics floating in the world's oceans [29]. Arsenic, cadmium and lead may be present in children's toys at levels that exceed regulatory standards [21, 23]. Lead can be used in toys as a stabilizer, color enhancer, or anti-corrosive agent. Cadmium is sometimes employed as a stabilizer, or to increase the mass and luster of toy jewelry. Regular imbibers of illegally distilled alcohol may be exposed to arsenic or lead poisoning the source of which is arsenic-contaminated lead used to solder the distilling apparatus. Rat poison used in grain and mash stores

may be another source of the arsenic.

Lead (Pb)

Lead is a chemical element in the carbon group and atomic number 82. It is used in building construction, lead-acid batteries, bullets and shot, weights, as part of solders, pewters, fusible alloys, and as a radiation shield. If ingested or inhaled, lead and its compounds are poisonous to animals and humans. Lead is a neurotoxin that accumulates both in soft tissues and the bones, intestines, kidneys, damaging the nervous system and causing brain disorders. It interferes with the development of the nervous system and is therefore particularly toxic to children, causing potentially permanent learning and behavior disorders [30].

Studies have shown that lead does not readily accumulate in the fruiting parts of vegetable and fruit crops (e.g., corn, beans, squash, tomatoes, strawberries, and apples). Higher concentrations are more likely to be found in leafy vegetables (e.g., lettuce) and on the surface of root crops (e.g., carrots). Generally, the risk of lead poisoning through the food chain increases as the lead level in soil rises above 300 ppm [31, 32]. Then it is necessary to removal the contaminated water or soil by lead.

Chromium (Cr)

Chromium (Cr) is the first element in transition metal of group VIB in the periodic table. It is the seventh most abundant element on earth and is found in rocks, animals, plants, and soils. Cr consists of two stable oxidation states such as trivalent state Cr(III) and hexavalent state Cr(VI) in natural aqueous environment. It is well known that, Cr(III) is essential materials for living organisms, is the other main form of chromium, and is essential for living organisms. Both can transform each other under certain conditions. whereas, Cr(VI) is more toxic, carcinogenic and mutagenic [33-37]. After chromium (VI) enters the body then reaches the blood stream, it damages the

kidneys, the liver and blood cells through oxidation reactions. Among the toxic metals, hexavalent chromium (Cr(VI)) containing wastes are considered as severe pollutants due to high water-solubility and toxicity [38]. The maximum levels permitted in wastewater are 5 $mg \cdot dm^{-3}$ for trivalent and 0.05 $mg \cdot dm^{-3}$ for hexavalent chromium [39]. Cr(VI) may be present in the form of CrO_4^{2-} or $HCrO_4^-$, whereas, Cr(III) tends to form $[Cr(H_2O)_6]^{3+}$, $Cr(H_2O)_5(OH)^{2+}$, $Cr(H_2O)_4(OH)_2^+$, or Cr(III) organic complexes [36, 40].

As chromium compounds were used in dyes and paints, these compounds are often found in soil and groundwater at abandoned industrial sites, so it is necessary and urge to cleanup and remediate the land. From above-mentioned, the minimization and recovery of harmful pollutants such as Cr(VI) in natural environment is very significant.

Rare earth elements (REEs)

In particular, water pollution due to heavy metal has become one of the largest problems in recent years. On the other hand, the demand of rare earth elements (REEs; Scandium (Sc), Yttrium (Y) and fifteen lanthanides) in modern technology has increased remarkably over the past years. However, the shortage of trace metals including REEs (and the problem of stable supply for these metals) has been concerned in recent years. Therefore, the establishment of the removal or recovery method for the trace metals is important from the viewpoint of resources recovery as well as environmental protection.

In recent decades, geochemical processes controlling metal migration and deposition in the earth`s surface environment has been intensively and increasingly attracting much interests of scientists [41-43]. The lanthanide elements traditionally have been divided into two groups, the light rare earth elements (LREEs) are

lanthanum through europium (Z = 57 through 63), and the heavy rare earth elements (HREEs) are gadolinium through lutetium (Z = 64 through 71). Although yttrium (Y) is the lightest REE, it is usually grouped to the HREEs because of chemically and physically similar properties[44, 45].

Mining, refining, and recycling of rare earths have serious environmental consequences if not properly managed. At the same time, the REEs are often found together, and are difficult to extract and separate each other. Commercial market remands for REEs have arisen due to widely application in industry and agriculture such as catalysis of engine, permanent magnet, phosphor of illumination and so on in recent years [46, 47], so the shortage of trace metals including REEs (and the problem of stable supply for these metals) has been concerned. Therefore, it is require us to remove these REEs within the scope of permissible concentration before discharge into subsurface environments. Considering the technical, economical and health-related points, the adsorption process seems to be a more appropriate technology for the removal of REEs from pollutants.

1.3 Adsorbents

There are many processes for the treatment of metalcontaminated wastewaters including chemical precipitation, membrane filtration, reverse osmosis, ion exchange, and adsorption. However, their use is limited due to various disadvantages. Among environmentally friendly technologies for the removal of heavy metals from aquatic effluent, biosorption has attracted increasing research interest recently [48-50]. The major advantages of biosorption are its high effectiveness in reducing the heavy

metals and the use of inexpensive biosorbents [50]. Biosorption studies using various low cost biomass as adsorbents have been currently performed widely for the removal of heavy metals from aquatic effluent [51-58].

Activated carbon

Activated carbon, also called activated charcoal, or activated coal, is a form of carbon processed to have small, low-volume pores that increase the surface area available for adsorption or chemical reactions [59]. Carbon adsorption has numerous applications in removing pollutants from air or water streams both in the field and in industrial processes such as: spill cleanup, groundwater remediation, drinking water filtration, air purification [3, 8, 37].

Activated carbon has shown great potential for the removal of various inorganic and organic pollutants and radionuclides due to properties such as large surface area, microporous structure, and high adsorption capacity [59, 60]. As a promising material among nanostructured carbon materials, powdered activated charcoal (AC) continues to attract tremendous attention due to its unique physical and chemical properties [10, 13]. In particular, the chemical functionalization of AC can modify its physical and chemical properties, leading to an improved performance in various applications [59, 61].

Zeolite

Zeolites are microporous, aluminosilicate minerals commonly used as commercial adsorbents and catalysts [62]. Zeolites have uses in advanced

reprocessing methods, where their micro-porous ability to capture some ions while allowing others to pass freely, allowing many fission products to be efficiently removed from nuclear waste and permanently trapped. Zeolites are also used in the management of leaks of radioactive materials. For example, in the aftermath of the Fukushima Daiichi nuclear disaster, sandbags of zeolite were dropped into the seawater near the power plant to adsorb radioactive caesium which was present in high levels [63]. Natural zeolites have been used as cationic exchange materials for the remediation of heavy metals and other contaminants due to their excellent properties as adsorbents [64, 65]. They also have the advantages of being very abundant in nature and possessing high chemical stability.

During the last decade, alternative and novel modifications have been exploited to give zeolites new properties that can increase their applications. In fact, modifications with cationic surfactants, such as high molecular-weight quaternary ammonium salts, have rapidly become important because they provide zeolites with the potential to behave as anionic exchangers [64, 66].

Chitosan

Chitosan is a linear polysaccharide composed of randomly distributed β-(1-4)-linked D-glucosamine (deacetylated unit) and N-acetyl-D-glucosamine (acetylated unit). It is made by treating shrimp and other crustacean shells with the alkali, sodium hydroxide [67]. Chitosan is a naturally occurring substance that is chemically similar to the plant fibre called cellulose. Unlike plant fibre, Chitosan possesses a positive ionic charge that can achieve remarkable results – the ability to

attract digested fat, heavy metal and toxic substances which are negatively charged into a large mass. Chitosan is a safe ingredient that is biodegradable [68] and environmentally biocompatible [69]. It has been safely used in many fields.

Among many biosorbents, chitosan can be an excellent biosorbent for metals because its amine ($-NH_2$) and hydroxyl (-OH) groups may serve as coordination sites to form complexes with various heavy metal ions [70, 71]. Uses of chitosan on the removal of various pollutants have been adequately reviewed.

1.4 Theory

Adsorption isotherms

Adsorption is usually described through isotherms, that is, the amount of adsorbate on the adsorbent as a function of its pressure (if gas) or concentration (if liquid) at constant temperature. The quantity adsorbed is nearly always normalized by the mass of the adsorbent to allow comparison of different materials [20, 28, 72]. Two common adsorption model, Langmuir and Freundlich isotherm model was applied to evaluate the adsorption data obtained in this study.

Langmuir model assumes monolayer sorption onto a surface and is given by

$$\frac{C_e}{q_e} = \frac{C_e}{q_{\max}} + \frac{1}{K_L q_{\max}} \qquad (2)$$

where C_e is the concentration of Cr(III) in a batch system at equilibrium ($mg \cdot L^{-1}$), q_e is the amount of adsorption of Cr(III) at equilibrium ($mg \cdot g^{-1}$), q_{max} is the maximum adsorption capacity on the surface of activated carbon ($mg \cdot g^{-1}$), K_L is the equilibrium adsorption constant ($L \cdot mg^{-1}$). A plot of C_e/q_e versus C_e gives a straight line with slope

of $1/q_{max}$, and intercept is $1/ (K_L q_{max})$, K_L can be related to the adsorption free energy ΔG_{ads} ($J \cdot mol^{-1}$), by the following equation:

$$n\Delta G_{ads} = -RT \ln K_L \qquad (3)$$

where R is the gas constant (8.314 $J \cdot K^{-1} mol^{-1}$), T is the absolute temperature at equilibrium (K), and K_L is the equilibrium constant at temperature T.

The equilibrium constant, b can be calculated from:

$$K_L = q_e / C_e \qquad (4)$$

Where C_e and q_e were same as mentioned above in Eq.(2).

The equilibrium adsorption constant [73, 74] (K_L) can be used to determine the suitability of the adsorbent to adsorbate by using dimensionless parameter, Hall separation factor [75] (R_L), which is defined as

$$R_L = \left(\frac{1}{1 + K_L C_0}\right) \qquad (5)$$

where C_o ($mg \cdot L^{-1}$) is the initial concentration.

The linearized Freundlich model isotherm is represented by the following equation:

$$\log_{10} q_e = \log_{10} K_F + (1/n) \log_{10} C_e \qquad (7)$$

The plots of q_e versus C_e in log scale can be plotted to determine values of $1/n$ and K_F from power equation depicting the constants of Freundlich model.

Kinetic Model

The rate equation for a chemical reaction is an equation that links the reaction rate with concentrations or pressures of reactants and constant parameters (normally rate coefficients and partial reaction orders) . For many reactions the rate is given by a power law such [76] as

$$r = k[\mathrm{A}]^x[\mathrm{B}]^y \qquad (8)$$

where [A] and [B] express the concentration of the species A and B, respectively (usually in moles per liter (molarity, M)). The exponents x and y are the partial reaction orders and must be determined experimentally; they are often not equal to the stoichiometric coefficients. The constant k is the rate coefficient or rate constant of the reaction. The value of this coefficient k may depend on conditions such as temperature, ionic strength, surface area of an adsorbent or light irradiation.

Kinetic models have been proposed to determine the mechanism of the adsorption process which provide useful data to improve the efficiency of the adsorption and feasibility of process scale-up [18, 77]. In the present investigation, the mechanism of the adsorption process was studied by fitting pseudo first-order and second-order reactions to the experimental data.

The pseudo first-order model is given by the following equation:

$$\ln(q_e - q_t) = \ln(q_e) - k_1 t \qquad (9)$$

where q_e and q_t are the adsorption capacities of Cr(III) and Cr(VI) using chitosan at equilibrium and time t, respectively ($mol \cdot g^{-1}$), and k_1 is the rate constant of the pseudo-first-order adsorption (h^{-1}).

The linear form of the pseudo second-order rate equation is given as follows:

$$\frac{t}{q_t} = \frac{1}{kq_e^2} + \frac{t}{q_e} \qquad (10)$$

where q_e and q_t are the adsorption capacities of Cr(III) and Cr(VI) using chitosan at equilibrium and time t, respectively ($mol \cdot g^{-1}$), and k is the rate constant of the pseudo-second-order adsorption ($g \cdot mol^{-1} \cdot h^{-1}$).

1.5 The Purpose and Outline of the Thesis

In this thesis, the objective elements are mainly lead (Pb), chromium (Cr), REEs (lanthanides, as well as scandium (Sc) and yttrium (Y)) and the objective material for adsorption using activated carbon modified with $KMnO_4$.

The purpose of present study is to investigate the recovery and/or eliminate method of Pb, Cr, and REEs by shell biomass. The adsorption agent can be applied to the fields of treatment of the heavy metal waste water, restoration of heavy metal polluted water bodies, and the like. The ultimate aim in this study is to investigate the efficiency of the charcoal as adsorbent for heavy metals and REEs for more practical use in future.

In this paper, there are 4 chapters.

In Chapter 1, the general introduction was stated.

In Chapter 2, adsorption of heavy metal and REEs onto activated carbon modified with Potassium permanganate. This study investigated the adsorption of Pb, Cr, and REEs by activated carbon modified with potassium permanganate. Adsorption experiments from aqueous solutions containing known amounts of Pb, Cr, and REEs were explored in a batch system. The amount of Pb, Cr, and REEs adsorbed at different pH values, initial concentrations, sorbent dosages, contact times, and temperature were determined by ICP-AES or ICP-MS in order to determine the optimum conditions for Pb, Cr, and REEs adsorption. The metals adsorption on modified and unmodified activated carbon conformed to the Langmuir isothermal adsorption equation. Overall the modified activated carbon exhibited a higher adsorption capacity and stronger chemical affinity than pristine activated carbon. The rates of adsorption were found to conform to pseudo-second order kinetics. Furthermore, to evaluate the characteristics of the sample used in this work, the

surface morphology of the carbon (both modified and pristine carbon) was determined by N_2-BET, SEM and FT-IR.

In Chapter 3, adsorption of heavy metals and REEs by zeolite/zhitosan hybrid composite (ZCHC). This study investigated the adsorption ability of ZCHC as adsorbent for aqueous Pb, Cr, and REEs, ZCHC was prepared with sol-gel method by mixing zeolite and chitosan, and the surface morphology of the zeolite, chitosan and ZCHC was determined by N_2-BET, SEM and FT-IR. Adsorption experiments as above chapter 1.

In Chapter 4, the conclusions of the thesis are presented.

Table 1-1 REEs, atomic numbers, abundances and applications [45, 78]

Atomic Number	Element (Symbol)	Upper Crust Abundance /*ppm*	Applications
21	Scandium(Sc)	5.0	Light aluminium-scandium alloy for aerospace components, additive in Mercury-vapor lamps
39	Yttrium(Y)	22	Yttrium-aluminium garnet (YAG) laser, yttrium vanadate (YVO4) as host for europium in TV red phosphor, YBCO high-temperature superconductors, yttrium iron garnet (YIG) microwave filters, energy-efficient light bulbs
57	Lanthanum(La)	30	High refractive index glass, flint, hydrogen storage, battery-electrodes, camera lenses, fluid catalytic cracking catalyst for oil refineries
58	Cerium(Ce)	64	Chemical oxidizing agent, polishing powder, yellow colors in glass and ceramics, catalyst for self-cleaning ovens, fluid catalytic cracking catalyst for oil refineries, ferrocerium flints for lighters
59	Praseodymium(Pr)	7.1	Rare-earth magnets, lasers, core material for carbon arc lighting, colorant in glasses and enamels, additive in didymium glass used in welding goggles, ferrocerium firesteel (flint) products.
60	Neodymium(Nd)	26	Rare-earth magnets, lasers, violet colors in glass and ceramics, ceramic capacitors
61	Promethium(Pm)	-	Nuclear batteries
62	Samarium(Sm)	4.5	Rare-earth magnets, lasers, neutron capture, masers
63	Europium(Eu)	0.88	Red and blue phosphors, lasers, mercury-vapor lamps, NMR relaxation agent
64	Gadolinium(Gd)	3.8	Rare-earth magnets, high refractive index glass or garnets, lasers, X-ray tubes, computer memories, neutron capture, MRI contrast agent, NMR relaxation agent
65	Terbium(Tb)	0.64	Green phosphors, lasers, fluorescent lamps
66	Dysprosium(Dy)	3.5	Rare-earth magnets, lasers
67	Holmium(Ho)	0.80	Lasers
68	Erbium(Er)	2.3	Lasers, vanadium steel
69	Thulium(Tm)	0.33	Portable X-ray machines
70	Ytterbium(Yb)	2.2	Infrared lasers, chemical reducing agent
71	Lutetium(Lu)	0.32	PET Scan detectors, high refractive index glass

Chapter 2 Adsorption of heavy metal and REEs onto activated carbon modified with potassium permanganate

2.1 Introduction

The amount of heavy metal ions released into the environment has been increased due to industrial activities and technological development. Furthermore, indiscriminate disposal has caused worldwide concern for many years because of the toxicity, accumulation in the food chain, persistence in nature, and concentration by organisms [9, 10,79]. Heavy metals are not biodegradable and tend to accumulate in living organisms, causing various diseases and disorders [78, 80]. It is, therefore, important to reduce the levels of toxic metals or to completely remove them from wastewaters before being discharged into the environment [7]. Then, the minimization and assessment of harmful pollutants such as lead (Pb) and uranium (U) in the environment are very significant from the viewpoint of environmental protection.

Recently, adsorption based on carbonaceous materials including activated carbon (AC)[81], biochar [26], and carbon nanotubes [82] has been gradually applied to this area. Activated carbon has shown great potential for the removal of various inorganic and organic pollutants and radionuclides due to properties such as large surface area, microporous structure, and high adsorption capacity. The mechanisms of heavy metal ion adsorption on ACs are very complicated and appear attributable to physical adsorption, electrostatic attraction, precipitation and chemical interaction between the heavy metal ions and the surface functional groups of ACs. Among these, chemical interaction between the heavy metal ions and the surface functional groups of ACs is the major adsorption mechanism (see **Fig. 2-1**) [8, 83, 84]. The activation of AC is

known to play a key role.

Surface functional group density, rather than total surface area, becomes the primary determinant of inorganic pollutant adsorption capacity. Activation of ACs plays an important role in enhancing the maximum adsorption capacity because of the modification in the surface morphology and surface functional groups. Activation of ACs under oxidizing conditions with chemicals such as $KMnO_4$, HNO_3, H_2O_2, NaClO, H_2SO_4, KOH, and NaOH have been widely reported [85, 86].

Considering the above discussion, uptake experiments for the adsorption of Pb^{2+} from aqueous solutions by activated carbon modified with potassium permanganate ($KMnO_4$) was carried out in this work. Two concentrations of $KMnO_4$ (0.01 mol/L and 0.03 mol/L) were used. Furthermore, to evaluate the characteristics of the activated carbon modified with $KMnO_4$, the surface morphology, specific surface area, and functional groups of the material were determined by scanning electron microscope (SEM), Brunaeur–Emmet–Teller (BET) method, and FT-IR, respectively.

2.2 Experimental Section

2.2.1 Materials

Activated carbon used in the study was purchased from the Sigma-Aldrich, Inc., USA. This product is an untreated, granular carbon with a particle size of less than 75 microns (80%-90%) (100-400 mesh). The carbon is prepared from wood which has been chemically activated. Solutions containing competitive ions (Na^+, K^+, Ca^{2+}, or Mg^{2+}) were individually prepared using nitrate salts: $NaNO_3$, KNO_3, $Ca(NO_3)_2$, and

$Mg(NO_3)_2$. Chemical reagents including $KMnO_4$ were purchased from Kanto Chemical Co., Inc. (Japan). For all experiments, each stock solution was suitably diluted with deionized water for use. All reagents used were of analytical grade, and water (> 18.2 MΩ) which was treated by an ultrapure water system (Advantec aquarius: RFU 424TA) was employed throughout the work. The pH meter (HORIBA F-72) was used for measurement of pH while adjusting the pH of the solutions using 0.1 mol/L NH_4OH aqueous/0.1 mol/L HNO_3.

2.2.2 Apparatus

The concentration of Pb and Cr/or REEs in the filtrate was determined with an atomic absorption spectrophotometer (AAS) and inductively coupled plasma-atomic emission spectrometry (ICP-AES), respectively. The operating condition of ICP-AES is shown in **Table 2-1**. Characterization of the structure of the chitosan was carried out by N_2 adsorption/desorption tests (Micromeritics TriStar 3020). The Brunaeur, Emmet and Teller (BET) method was applied to determine the surface area. The pore volume was calculated from the amount of N_2 adsorbed at the relative pressure of 0.99. The surface morphology of chitosan was surveyed using a scanning electron microscope (SEM) from (JEOL (Japan Electron Optics Laboratory), JSM-5800, Japan). The ACs were characterized bands of graphite structure using Fourier transform infrared (FT-IR) spectroscopy (FTIR-4200, Jasco, Japan) in pressed KBr pellets. The measurement of pH in solution was carried out using a pH meter (HORIBA, F-21, Japan).

2.2.3 Modification of Activated Carbon with $KMnO_4$

The AC was washed by deionized water (at 80 °C) to remove fine powder and contaminants, and then dried at 110 °C for 2 h before use. 5 g of the activated carbon were placed in a 200 mL conical flask which containing 50 mL $KMnO_4$ solution (0.01 or 0.03 mol/L). Adjusting the temperature to 25 °C and stirring for 12 h, the resulting solution was filtrated through 0.45 μm membrane filter. Then, the filtrate was washed with deionized water until the pH (of the filtrate) is constant. The activated carbon was dried at 70 °C for 6 h. The pristine and modified (i.e., modified with 0.01 mol/L and 0.03 mol/L KMnO4 solution) activated carbons were described as AC0, AC_{K1} and AC_{K3}, respectively.

2.2.4 Characterization of ACs (Activated Carbons)

Various characterization methods have been used to determine physicochemical properties of pristine and modified activated carbons. The surface morphologies of these ACs were surveyed by using a SEM (Hitachi S-4300). Surface areas and pore volumes of these ACs before and after Cr (VI) adsorption was carried out by N_2 adsorption/ desorption tests (Micromeritics TriStar 3020). Surface functional groups were identified by FT-IR spectrometer (FTIR-4200, Jasco, Japan).

2.2.5 Adsorption experiments of heavy metal ions and REEs using modified activated carbon

For investigating the effects of pH, contact time, sorbent dose and initial

concentration on the adsorption of Pb^{2+}, Cr (VI), REEs, the following adsorption experiments were performed using modified activated carbons. Activated carbons were thoroughly mixed with 50 mL of containing known amount of Pb^{2+}, Cr (VI), REEs, in a 200 mL conical flask, and the suspensions were shaken in a water bath at room temperature (25±2 □), respectively. Adsorption experiments were conducted in the pH range of 3–7, adsorbent dosage 0.1–1.5 $g \cdot L^{-1}$, contact time from 1h to 24h, and initial concentration from 20 to 200 $mg \cdot L^{-1}$. The pH of each solution was adjusted by using 0.1 $mol \cdot L^{-1}$ NH_3 aq / 0.1 $mol \cdot L^{-1}$ HNO_3.

Following each adsorption experiment, the suspension containing carbon and the above standard solution was filtered through a 0.45 μm membrane filter (Advantec Mixed Cellulose Ester, 47 mm) to remove Pb^{2+}, Cr (VI), REEs that have been adsorbed into the activated carbon, and the concentration of Pb in the filtrate was determined with an AAS or ICP-AES.

The metal uptake by the activated carbons was calculated using the following equation:

$$q = \frac{(C_i - C_e)}{m} \cdot V \qquad (1)$$

where q is the adsorption capacities of Pb^{2+}, Cr(VI), REEs using modified activated carbon at equilibrium ($mg \cdot g^{-1}$), C_i and C_e are the initial and equilibrium concentrations of metal ions in a batch system respectively ($mg \cdot L^{-1}$), V is the volume of the solution (L), and m is the weight of adsorbent (g).

2.2.6 Effect of competitive cations on the adsorption of Pb^{2+}

The effect of competitive ion on the adsorption of Pb^{2+} was studied as the following experiment under the optimum conditions which was obtained from **2.2.5**. The initial Pb^{2+} concentration was taken as 100 $mg \cdot L^{-1}$ based on preliminary experiments. In a 200 ml conical flask, each activated carbon sample (50 mg) was contacted with 50 mL of Pb^{2+} solution under the different concentrations (i.e., 0, 10, 20, 50, 100, 200 and 500 $mg \cdot L^{-1}$) of sodium (Na), potassium (K), calcium (Ca) or magnesium (Mg) ion separately and in combinations of all 4 ions (where the concentrations of each ion were 0, 10, 20, 50, 100, 200 and 500 $mg \cdot L^{-1}$). Other experimental conditions and methods were basically the same as that mentioned in section *2.2.5*.

2.2.7 Effect of competitive anions on the adsorption of Cr (VI)

The effect of competitive metal ions (ie., Fe^{3+}, Co^{2+}, Ni^{2+}, Zn^{2+}) on the adsorption of Pb^{2+} and Cr (VI) were studied as the following experiment. In this experiment, the initial concentration of Pb^{2+} and Cr (VI) was taken as 100 $mg \cdot dm^{-3}$ based on preliminary experiments [32]. In a 200 ml conical flask, each ACs (0.1 g) was contacted with 100 cm^3 of Pb^{2+} and Cr (VI) solution under the presence of iron (Fe^{3+}), cobalt (Co^{2+}) , nickel (Ni^{2+}) and zinc (Zn^{2+}) ion at different concentrations 10, 50 and 100 $mg \cdot dm^{-3}$. Other experimental conditions and methods were basically the same as that mentioned above in section *2.2.5*.

2.2.8 Effect of competitive metal ions on the adsorption of heavy metals

The effect of competitive anions on the adsorption of Cr (VI) was studied as the following experiment. In this experiment, the initial concentration of Cr (VI) was taken as 100 mg×dm-3 based on preliminary experiments [32]. In a 200 ml conical flask, each ACs (0.1 g) was contacted with 100 cm3 of Cr (VI) solution under the presence of chloride (Cl-), nitric acid (NO3-) and sulfuric acid (SO42-) ion at different concentrations 50, 100 and 200 mg×dm-3. Other experimental conditions and methods were basically the same as that mentioned above in section 2.2.5.

2.2.9 Regeneration studies

From industrial and technological point of view, it is desirable to recover the adsorbed material along with the adsorbent in wastewater treatment processes [76]. AC was exhausted with 100 mg·dm^{-3} Pb^{2+} and 100 μg·dm^{-3}Cr (VI) and La(III) at pH 3 before regeneration, respectively. In each desorption experiment, 50 mg of the spent adsorbent was treated with 50ml of desorption agent, then filtered and finally Pb^{2+}, Cr (VI) and La(III) content in the filtrate was determined. Adsorption–desorption studies were continued during the five cycles by using 5%, 10% HCl, 5%, 10% HNO_3 and 5%, 10% NaOH at 90□ for 4h as eluent, respectively.

2.3 Results and Discussion

2.3.1 Characterization of the modified activated carbon

The FT-IR spectra of the pristine and modified activated carbon (i.e., AC_0, AC_{K1} and AC_{K3}) are shown in **Fig. 2-2**. The pristine and modified activated carbon displayed the characteristic bands of the graphite structure of carbon at 1615 cm^{-1} [32, 60, 87]. Moreover, an OH stretching band, one of the typical peaks of activated carbon, was found at 3300 to 3500 cm^{-1}. The peak at 3433 cm^{-1} was related to the hydroxyl groups (-OH) stretch from deprotonated pristine and modified activated carbon. The wide peak at 1550 to 1750 cm^{-1} shows the asymmetric stretch of the carboxylate (-COO-) group [60].

The surface properties of the activated carbon were investigated by N_2 adsorption (TriStar II 3020 Micromeritics), and the analytical results for the adsorption/desorption isotherms are shown in **Table2-2**.

The pore volume was calculated from the amount of N_2 adsorbed at the relative pressure of 0.99. The pore size was calculated from the adsorption average pore width (4V/A by BET) in this work. From **Table 2-2**, it is found that the pore volume and pore size as well as the specific surface area decreased significantly after modification with $KMnO_4$. The isotherm showed a type H1 isotherm with a clear hysteretic loop, characteristic of disordered micro-porous materials.

The SEM micrographs of the activated carbon are shown in **Fig. 2-3**. The modified AC (**Fig. 2-3B and 2-3C**) seemed to exhibit a more compact stacking

morphology than the pristine AC (**Fig. 2-3A**), due to cohesive forces, which may be generated from the introduction of oxygen containing functional groups. These results are consistent with those of the N_2 adsorption-desorption experiment. The decrease of the pore volume and pore size may be related to the increase of acidic groups on the surface of activated carbon treated with $KMnO_4$.

2.3.2 Adsorption of lead on modified activated carbon

Effect of pH

To investigate the effect of solution pH on Pb^{2+} adsorption efficiency, the pH of the solution was varied from 3 to 7, while the Pb^{2+} concentration was kept constant at 100 $mg \cdot L^{-1}$. The experimental results are presented in **Fig.2-4**. The Pb^{2+} adsorption efficiency was at pH 5 regardless of the kind of adsorbent (Figure 3). The uptake of Pb^{2+} increased from 50.8% at pH 3 to 90.0% at pH 5, and at higher pH value, it remained almost constant (or decreased only slightly). Notably the adsorption capacities decreased at low pH values due to the competition of protons with metal ions for active binding. On the other hand, lead precipitated from the solution at higher pH values as lead hydroxide. From the FT-IR spectra of AC (**Fig. 2-2**), it was clear that, the hydroxyl groups (-OH) were introduced onto AC. We hypothesized that the Pb^{2+} adsorption occurred predominantly by cation exchange reaction between the H^+ of the hydroxyl groups on modified AC and cationic Pb^{2+} species. However, it is possibile that Pb^{2+} was removed to some extent via precipitation at higher pH values rather than by adsorption on the modified AC. Hence, pH 5 was utilized for further

experiments.

Effect of contact time

The effect of contact time on Pb^{2+} adsorption efficiency using 1.0 $g \cdot L^{-1}$ AC_{K3} (100 $mg \cdot L^{-1}$ of solution) was investigated at pH 5.

More than 80% Pb was removed within 1 h, and it gradually increased at 2 h. Approximately 90% of Pb was removed from the solution at the contact time of 2 h. After 2 h, there was no appreciable change. Therefore, 2 h was chosen as the optimized contact time for the rest of the experimental work.

Effect of adsorbent dosage

Under the optimized pH conditions (i.e., pH 5) and contact time (i.e., 2 h), the adsorption behavior of AC_{K3} at different dosages (from 0.1 to 1.5 $g \cdot L^{-1}$) was studied in 100 $mg \cdot L^{-3}$ Pb^{2+} solution.

More than 90 % of Pb^{2+} was removed with a dosage of 1.0 $g \cdot L^{-1}$ (**Fig. 2-5**). The removal increased remarkably with higher dosage rates, but no remarkable increase was observed at dosages greater than 1.0 $g \cdot L^{-1}$. Therefore, 1.0 $g \cdot L^{-1}$ was considered as the optimum dosage for the remainder of the study.

Effect of temperature

Study was carried out by varying temperature from 20℃ to 40℃ for contact time of 8h with a dosage of 50 mg at pH 5, concentration at 100 mg/L. The results are shown in **Fig. 2-6**. The highest uptake was observed at 25℃, and there is no appreciable change of the uptake of Pb^{2+} with increasing temperatures. Hence, 25℃ was selected for the rest of this study.

Effect of competitive ions

Competitive experiments were conducted under the optimized pH conditions (i.e., pH 5), contact time (i.e., time 2 h), and sorbent dosage (i.e., 1 g/L) using different concentrations of Na^+, K^+, Ca^{2+}, or Mg^{2+} separately and combination of all 4 ions (i.e., 0, 10, 20, 50, 100, 200, and 500 $mg \cdot L^{-1}$). The percent removal of Pb^{2+} decreased in the presence of Na^+, K^+, Ca^{2+}, or Mg^{2+} with concentrations from 0 to 500 $mg \cdot L^{-1}$ (**Fig. 2-7**). A remarkable decrease in the adsorption capacity of Pb^{2+} was not observed, even with common ions at concentrations of 100 $mg \cdot L^{-1}$ (i.e., more than 80% Pb^{2+} was removed; **Fig. 2-7**). This implied that activated carbon was an efficient adsorbent for Pb^{2+}, although further investigations are required for the realization of practical application.

2.3.3 Adsorption of Cr (VI) on modified activated carbon

Effect of pH

The removal of metallic species from water by an adsorbent is highly dependent on the pH of the solution, which affects the surface charge of the adsorbent, the degree of ionization and the chemical speciation of the adsorbate species [88]. To investigate the effect of solution pH on Cr(VI) adsorption efficiency, the pH of the solution was varied from 3 to 7, while the Cr(VI) concentration was kept constant at 100 $\mu g \cdot L^{-1}$. The experimental results are presented in **Fig. 2-8.** From **Fig. 2-8**, it is obviously found that Cr(VI) adsorption was strongly pH dependent, and that Cr(VI) adsorption was superior at low pH [75]. The distribution of Cr(VI) at different pH is shown in **Fig. 2-9**. Cr(VI) exists as hydrogen chromate anions ($HCrO_4^-$) between pH

2.0 and pH 6.5 and it exists as chromate ions (CrO_4^{2-}) at pH 8 according to the following Eqs. (1)-(3) [75]:

$$HCrO_4^- \leftrightarrow CrO_4^{2-} + H^+ \text{ (6), p}Ka = 5.9 \quad (1)$$

$$H_2CrO_4 \leftrightarrow HCrO_4^- + H^+ \text{ (7), p}Ka = 4.1 \quad (2)$$

$$Cr_2O_7^{2-} + H_2O \leftrightarrow 2HCrO_4^- \text{ (8), p}Ka = 2.2 \quad (3)$$

On the other hand, the possible reactions on carbon surface with increasing pH can be expressed as follows [89]:

$$AC\text{-}OH_2^+ \leftrightarrow AC(OH)^0 + H^+ \quad (4)$$

$$AC(OH)^0 \leftrightarrow AC\text{-}O^- + H^+ \quad (5)$$

The protonated carbon surface shows great affinity to the anions because of the electrostatic attraction. Therefore, it promotes the adsorption of the negatively charged hydrogen chromate ions from the solution. Proton dissociation occurs with increasing pH, and consequently, deprotonated surface repulses the hydrogen chromate ions. Cr (VI) exists as chromate ion (CrO_4^{2-}) at pH above 6.5. At pH 8, the uptake capacities are very low. This could be explained as competitiveness between chromate and hydroxyl ions.

Hence, pH 3 was taken for further experimental work.

Effect of Contact Time

The effect of contact time on Cr(VI) adsorption efficiency using 1.0 $g \cdot L^{-1}$ AC_{K3} (100 $mg \cdot L^{-1}$ of solution) is investigated at pH 3.

The removal of Cr (VI) more than 85% was observed within 1h, and it gradually increased up to the contact time of 2 h. Approximately 95% of Cr (VI) removal from

the solution was observed at the contact time of 4 h, and after that there was no appreciable change. Hence, 4 h was chosen as the optimized contact time for the rest of the experimental work.

2.3.4 Adsorption of REEs on modified activated carbon

Strong surface complexation and/or chemisorption are considered as the main adsorption mechanism of radionuclides such as Eu(III) [159] adsorption on ACs. Radionuclide is bound to ACs in two forms at least, fast adsorption on the outer surfaces of ACs and slow adsorption in the inner channel of ACs, the distribution of which is time-dependent [90]. More and more radionuclide enters the inner channel of ACs with increasing time and forms strong complexes in the central channel of ACs (as shown in **Fig. 2-10**). The radionuclides in the inner channel of ACs are difficult to be desorbed from ACs, whereas the adsorbed radionuclides on the outer surfaces of ACs can be easily desorbed from ACs to aqueous solution in acidic solution. Comparing to other adsorbents, the irreversible adsorption of radionuclides on ACs is much more important for radionuclides disposal for long time. As for oxidized ACs, it has been found that the lanthanide ions likely coordinate to these nanotubes through the increased number of oxygen atoms, forming predominantly ionic bonding arrangements.

Effect of pH

Aqueous solution pH can affect the surface charge of the adsorbent, the degree of ionization and speciation of metal ions and surface metal binding sites [91, 92]. The effect of initial pH on the adsorption was investigated over a pH range 2-8, the uptake

of REEs on the ACs at the initial concentrations of 100 μg·L^{-1}, and the corresponding data are contained also in **Fig. 2-11**. The pH was adjusted using diluted nitric acid and sodium hydroxide (0.1 mol·L^{-1}). At this concentration, the pH range was kept below 7.0 in order to avoid any bulk precipitation of REE hydroxides. It is seen that by increasing the aqueous solution pH up to 3, the adsorption percentage increases, that modified activated carbon showed the highest capacity, and beyond pH of 3.0 the uptake more than 80%. This pH dependency can be described by considering a decrease in the positive surface charges by aqueous solution pH [14, 93]. The results allowed choosing initial pH 3 as the optimum value for continuing the extraction experiments.

Effect of contact time

In order to optimize the time required for access to equilibrium condition, a series of single component sorption experiments for removal of REEs (initial concentration 100 μg·L^{-1}) from aqueous solutions adjusted at pH 3 by using 50 mg of ACs, respectively, by contacting the phases for 30 min to 12 h were performed (**Fig. 2-12,** take Sc for example). This investigation lets also verifying the kinetics of process, which will be discussed later in section 2.3.5. The results reveal a relatively fast adsorption process of both ions onto AC_{K1} and AC_{K3} with respect to the kinetics of the adsorption by AC_0. Based on the obtained results, we used 8 h for adsorption of the studied ions by ACs.

2.3.5 Adsorption Isotherms

Adsorption isotherms are commonly used to reflect the performance of

adsorbents in adsorption processes. In this paper, Langmuir and Freundlich isotherms were applied to the data obtained in this work. The linear plots of C_e/q_e-C_e and $\lg q_e$-$\lg C_e$ were presented for Langmuir (**Fig. 2-13, Fig. 2-14, Fig. 2-16)** and Freundlich (**Fig. 2-15**) models, and the coefficient of both isotherms are shown in **Table 2-3**-**Table 2-5**.

From **Table 2-3**, it is also found that R^2 value for each adsorbent is comparatively large. On average, the Langmuir model correlation coefficients were found to be closer to unity with generally raise standard deviations compared to the Freundlich isotherm model. However, due to the nature of the material, multiple binding sites are available, thus the Langmuir isothermal is adopted. That is to say, favorable adsorption for Pb^{2+}, Cr (VI), REEs by the activated carbon is presented. This result suggests that the both physical and chemical adsorptions are existing in these ACs, that the adsorption of heavy metals and REEs on zeolite, chitosan and ZCHC mainly occurred by monolayer reaction.

2.3.6 Kinetic Studies

The linear plot of t/q_t versus t for metal adsorption system under the optimized experimental conditions is shown in **Fig. 2-17-Fig. 2-19**. The pseudo-second-order rate constant (k) and the amount of adsorbed lead (q_e), obtained from the intercept and slope of the plot of t/q_t vs. t are listed in **Table 2-6-Table 2-8** along with the regression coefficients (R^2).

Considering the values of correlation coefficients, the pseudo secondorder kinetic model provided an impressive and comparable correlation for the adsorption

of ions. The comparison of the evaluated adsorption capacity considering the pseudo second-order equation (q_e) and that found experimentally (q_{exp}) confirms also the validity of the proposed model. It suggests that the rate determining step might be chemical and the adsorption process involves the valency forces through sharing electrons between the metal ions and adsorbent.

The suggests that for the most part, the adsorption takes place in two steps. The first linear region represents the stage of film diffusion, which is the diffusion of Pb^{2+}, Cr (VI), REEs from the bulk solution to the external surface of the ACs. The second region can be attributed to intraparticle diffusion stage due to the rough surface and voids within the ACs. The film diffusion stage is larger than the intraparticle diffusion stage, which is represented by a larger slope (k_p). The lower slope for the intraparticle diffusion indicates a more gradual process, which is consistent with the parameters of Weber's intraparticle diffusion model [3]. Most of the plots do not pass through the origin, indicating the intraparticle diffusion is not the rate limiting step[94]. The intercept (C_{IP}) reflects the boundary layer effect, that is, the larger the intercept, the greater the contribution of the surface adsorption in the rate controlling steps[95].

2.3.7 Desorption performance of heavy metal from ACs

Adsorption–desorption studies were continued during the five cycles by using 5%, 10% HCl, 5%, 10% HNO_3 and 5%, 10% NaOH at 90℃ for 4h as eluen, the ACs was filtered, the solution was analyzed by ICP-AES and the percent desorbed determined. The percent adsorbed and desorbed for each cycle is shown in **Fig. 2-20 Fig. 2-21 and Fig. 2-22.** It is clear that the desorption performance depends upon the

nature of the solution. The results are promising, showing 92% and 78% desorption for all Pb^{2+}, Cr (VI) and La(III) tested using 10% HNO_3.

Then, the repeated availability of AC_{K3} through five cycles of adsorption/desorption was investigated by using 10% HNO_3 as desorbing reagent. The results are shown in **Fig. 2-20 Fig. 2-21 and Fig. 2-22**. The adsorption capacity of AC_{K3} towards Pb^{2+}, Cr (VI) and La (III) decreases from 92%, 85% and 71% to 37%, 23% and 9% after four cycles, respectively. The results indicate that ACs still present the high adsorption capacity (about 70% relative to original) towards Pb^{2+}, Cr (VI) and La(III) through three cycles of adsorption/desorption behavior.

2.3.8 Adsorption of polymetallic mixture from ACs

Competitive experiment for Pb^{2+} and Cr (VI) was performed at optimized under the presence of common ions (Pb^{2+}, Fe^{3+}, Co^{2+}, Ni^{2+}, Zn^{2+}) at concentrations 100 $mgdm^{-3}$. The adsorption capacity of Pb^{2+} and Cr (VI) was decreased obviously, along with the increasing concentration of common metal ions.

2.4 Conclusions

Carbon based materials have been extensively examined and applied for adsorption of aqueous heavy metals. In this study, the efficiency of activated carbon modified by $KMnO_4$ as adsorbent for Pb^{2+}, Cr (VI), REEs was investigated by batch techniques. The results show that Pb^{2+}, Cr (VI), REEs adsorption capacity of AC_{K1} and AC_{K3} were increased after the modification with $KMnO_4$. Adsorption of heavy

metals and REEs onto such materials can generally be attributed to ion exchange with carboxylic and phenolic hydroxyl functional groups.

The ACs showed excellent adsorption capacity even if large amount of competitive ions exist in system. Particularly, ACs modified with $KMnO_4$ still showed highest adsorption capacity.

The adsorption isotherm of Pb^{2+}, Cr (VI), REEs by ACs was well interpreted by Langmuir and Freundlich models. However, the experimental data of the adsorption of the studied ions onto ACs was suitably described by Langmuir isotherm, which suggests a monolayer chemical adsorption of Pb^{2+}, Cr (VI), REEs on ACs. The comparison evaluated correlation coefficients based on the studied kinetic models allowed considering the pseudo-second order model suitable for describing the adsorption processes. This analysis revealed the rate determining step might be chemical and the adsorption processes involved the valency forces through sharing electron between the metal ions and adsorbents.

Desorption of Pb^{2+}, Cr (VI) and La (lanthanum (III)) from the adsorbent has been found to depend upon the nature of the extracting solution, and ACs still present the high adsorption capacity towards heavy metals through several cycles of adsorption/desorption behavior. ACs could be an efficient adsorbent for heavy metals and REEs.

From this work, it was quantitatively clarified to some extent ACs could be an efficient adsorbent for heavy metal and REEs. It is very significant information from the viewpoint of environmental protection, and can be used for treating industrial

waste waters including pollutants.

Tables

Table 2-1 Operating conditions of the ICP-AES

Parameters	
Plasma conditions	
Rf frequency (MHz)	27.12
Incident power (kW)	1.3
Gas conditions	
Outer gas (Ar) flow rate (dm^3 min^{-1})	17
Intermediate gas (Ar) flow rate (dm^3 min^{-1})	0.55
Carrier gas (Ar) flow rate (dm^3 min^{-1})	0.58
Sampling conditions	
Observation height (mm)	10.3
Integration time (s)	3
Detection wavelength (nm)	Cr: 206.15; La: 379.48; Eu: 381.97; Lu: 261.54; Yb: 328.94; Y: 371.03; Sc: 361.38.

Table 2-2 Textural characteristics of activated carbon

Adsorbent	BET surface area [$m^2 \cdot g^{-1}$]	Pore volume [$cm^3 \cdot g^{-1}$]	Pore size [nm]
AC_0	381	0.402	4.23
AC_{K1}	373	0.390	4.18
AC_{K3}	346	0.348	4.03

Table 2-3 Coefficient of Langmuir isotherm for Pb^{2+} using AC.

adsorbent	q_{max} [$mg \cdot g^{-1}$]	K_L [$L \cdot mg^{-1}$]	R
AC_0	25.1	0.0452	0.983
AC_{K1}	80.0	0.435	0.998
AC_{K3}	101	4.60	1.00

Table 2-4 Coefficient of Langmuir and Freundlich isotherms for Cr(VI) using ACs

	Langmuir isotherm			Freundlich isotherm		
	q_{max} ($mg \cdot g^{-1}$)	K_L ($dm^{-3} \cdot mg^{-1}$)	R^2	K_F ($(mg \cdot g^{-1}) \cdot (dm^{-3} \cdot mg^{-1})^{1/n}$)	n	R^2
AC_0	43.0	1.72E-02	0.998	3.44	1.68	0.975
AC_{K1}	109	1.88E-01	0.910	38.9	1.73	0.994
AC_{K3}	134	4.42E-01	0.988	61.7	2.01	0.987

Table 2-5 Coefficient of Langmuir and Freundlich isotherms for REEs

		Langmuir isotherm			Freundlich isotherm		
		q_{max} [$\mu g \cdot g^{-1}$]	K_L [$L \cdot \mu g^{-1}$]	R^2	K_F [$(\mu g \cdot g^{-1}) \cdot (L \cdot \mu g^{-1})^{1/n}$]	1/n	R^2
La	AC_0	48.0	0.291	0.992	11.9	0.334	0.779
	AC_{K1}	57.9	0.341	0.998	23.8	0.245	0.773
	AC_{K3}	71.0	1.11	0.999	28.2	0.252	0.763
Yb	AC_0	53.1	0.250	0.996	15.3	0.282	0.912
	AC_{K1}	70.8	0.418	0.999	21.0	0.304	0.844
	AC_{K3}	84.6	0.612	0.999	31.4	0.261	0.845
Lu	AC_0	52.7	0.257	0.993	15.1	0.289	0.859
	AC_{K1}	62.4	1.48	0.999	26.4	0.238	0.828
	AC_{K3}	75.9	1.78	1.00	31.0	0.247	0.820
Eu	AC_0	38.4	0.378	0.996	18.2	0.282	0.957
	AC_{K1}	80.6	0.433	1.00	25.2	0.300	0.821

	AC_{K3}	97.2	0.176	1.00	42.8	0.235	0.837
	AC_0	57.4	0.182	0.993	13.2	0.342	0.839
Y	AC_{K1}	71.2	0.559	0.999	23.0	0.286	0.873
	AC_{K3}	89.5	0.601	0.999	33.5	0.256	0.882
	AC_0	69.3	0.330	0.996	26.7	0.367	0.974
Sc	AC_{K1}	93.0	0.797	1.00	43.0	0.301	0.985
	AC_{K3}	121.5	1.22	1.00	58.1	0.288	0.982

Table 2-6 Kinetic coefficients for Pb^{2+} adsorption on ACs

Activated carbon	q_e [$mg \cdot g^{-1}$]	k [$g \cdot mol^{-1} \cdot h^{-1}$]	R
AC_0	26.4	2.87×10^{-3}	0.999
AC_{K1}	81.8	1.16×10^{-2}	0.999
AC_{K3}	101	4.51×10^{-2}	0.999

Table 2-7 Kinetic coefficient for Cr (VI) adsorption on activated carbon.

Activated carbon	q_e ($mg \cdot g^{-1}$)	k ($g \cdot mol^{-1} \cdot h^{-1}$)	R
AC_0	39.5	1.29×10^{-4}	0.998
AC_{K1}	93.2	1.15×10^{-3}	0.999
AC_{K3}	99.5	5.14×10^{-3}	0.997

Table 2-8 Kinetic coefficient for REEs adsorption on adsorbents

		pseudo-first-order			pseudo-second-order		
		q_e ($\mu g \cdot g^{-1}$)	k_1 (h^{-1})	R^2	q_e ($\mu g \cdot g^{-1}$)	k_2 ($10^{-2} \cdot g \cdot \mu g^{-1} \cdot h^{-1}$)	R^2
La	AC_0	46.6	0.394	0.981	83.5	0.776	0.995
	AC_{K1}	49.7	0.401	0.980	92.9	1.39	0.999
	AC_{K3}	69.7	0.440	0.959	99.9	1.56	0.999
Yb	AC_0	43.9	0.377	0.955	82.7	0.126	0.995
	AC_{K1}	60.0	0.390	0.979	97.6	1.08	0.999
	AC_{K3}	85.0	0.428	0.959	102	1.80	1.00
Lu	AC_0	38.4	0.337	0.954	58.8	0.236	0.964
	AC_{K1}	50.8	0.339	0.959	95.1	1.26	0.999
	AC_{K3}	66.0	0.381	0.907	99.1	1.99	0.99
Eu	AC_0	39.1	0.432	0.992	79.4	0.378	0.994
	AC_{K1}	50.6	0.457	0.951	101	1.22	0.998
	AC_{K3}	82.1	0.529	0.968	104	2.41	1.00
Y	AC_0	45.9	0.288	0.986	93.5	0.471	0.993
	AC_{K1}	48.0	0.440	0.954	97.8	1.41	1.00
	AC_{K3}	79.3	0.462	0.959	103	1.63	0.999
Sc	AC_0	8.48	0.261	0.957	91.3	0.942	0.993
	AC_{K1}	51.3	0.477	0.968	98.9	1.54	0.996
	AC_{K3}	66.7	0.553	0.951	100	1.90	1.00

Figures

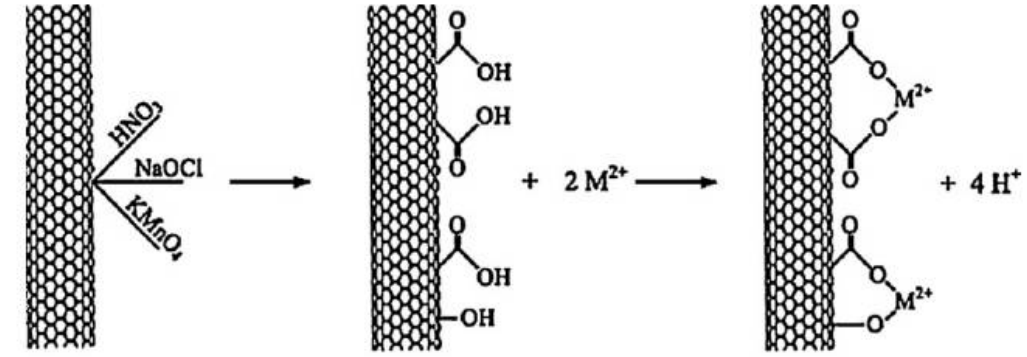

Raw AC **Oxidized AC** **Ion exchange on AC surface**

Fig. 2-1 Schematic of the major mechanism for sorption of metal ions onto AC surfaces

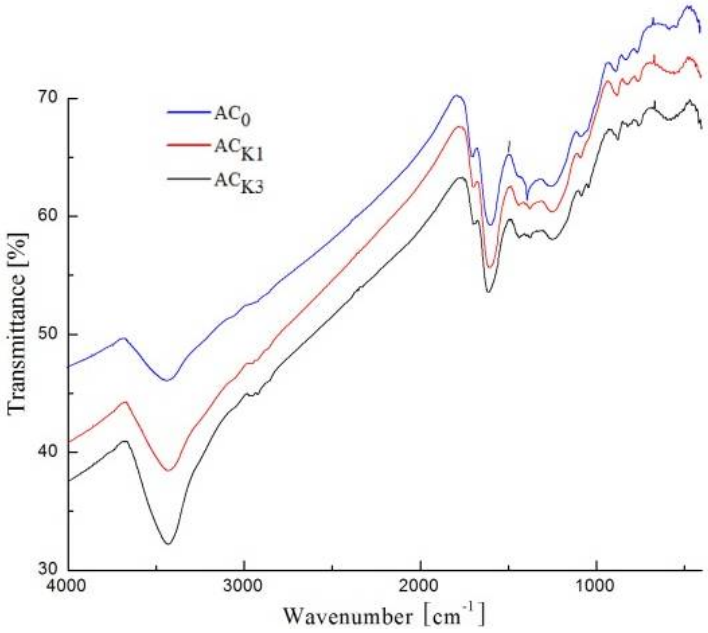

Fig. 2-2 FT-IR spectra of AC_0, AC_{K1}, and AC_{K3}

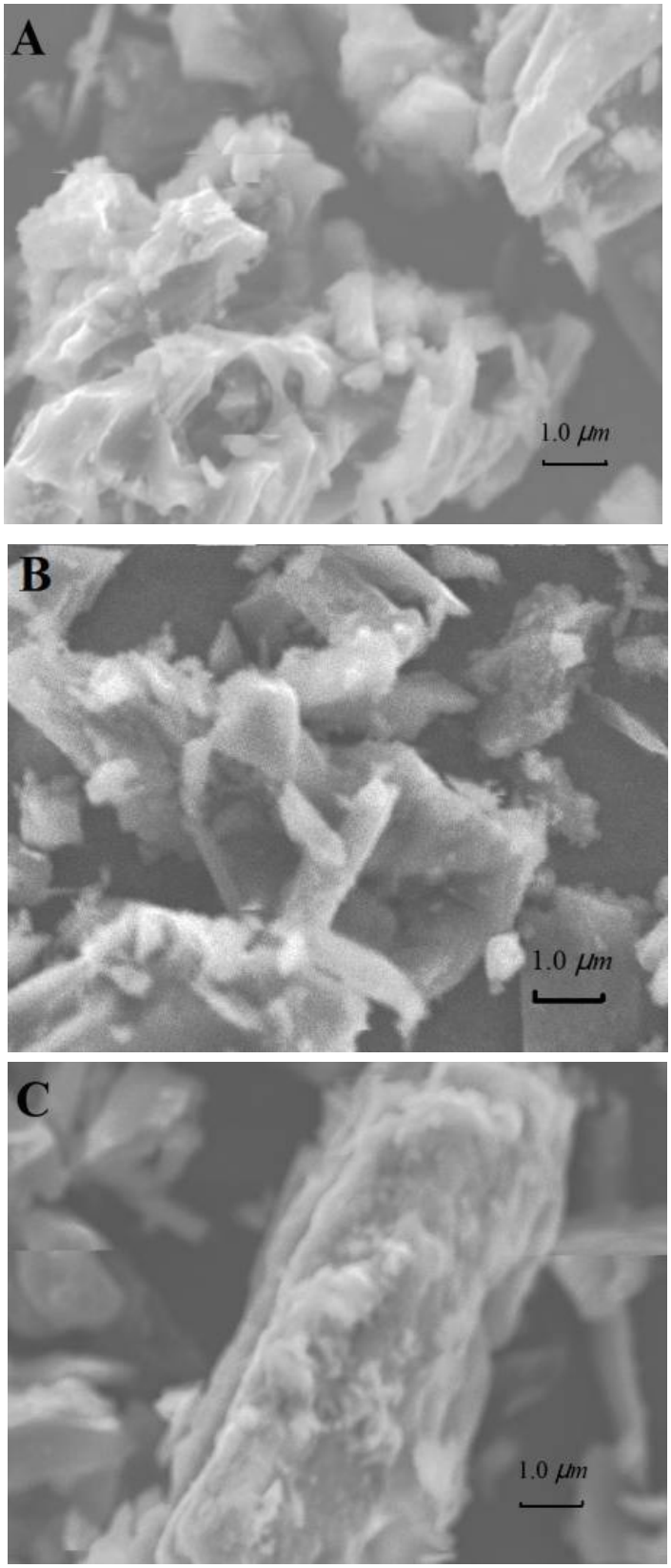

Fig. 2-3 SEM micrographs of the surface of activated carbon:

(A) unmodified; (B) modified with 0.01 mol/L $KMnO_4$; (C) modified with 0.03 mol/L $KMnO_4$

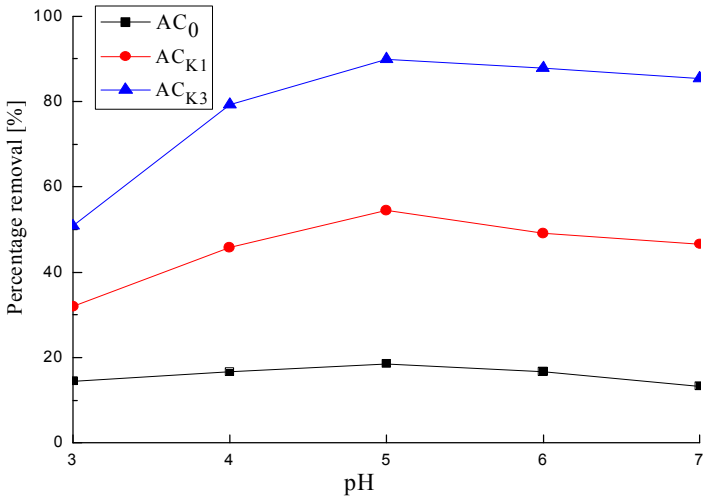

Fig. 2-4 Effect of pH on the removal of Pb^{2+} (%) using modified activated carbon

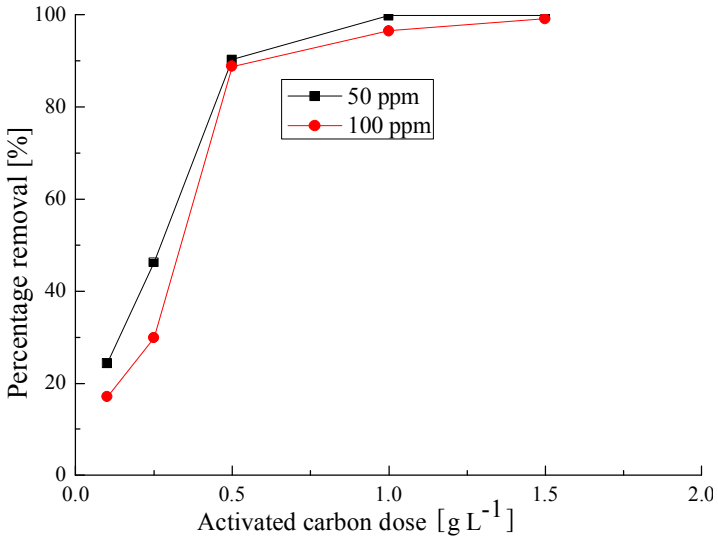

Fig. 2-5 Effect of sorbent dosage on percent removal of Pb^{2+} using AC_{K3}

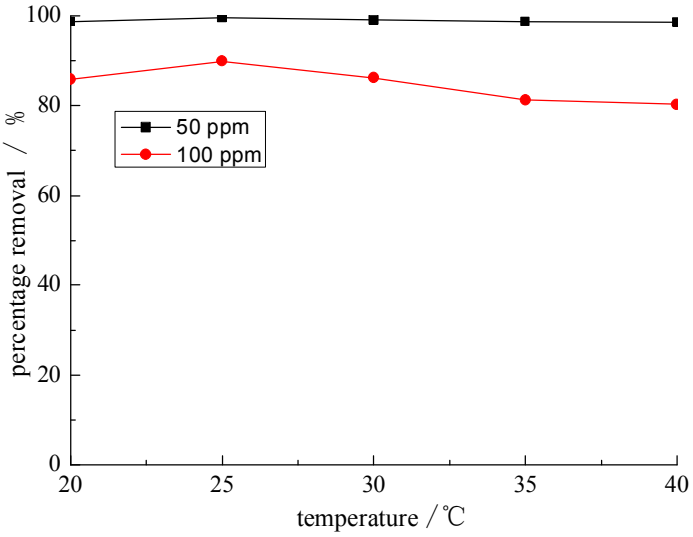

Fig. 2-6 Effect of temperature on percent removal of Pb^{2+} using AC_{K3}

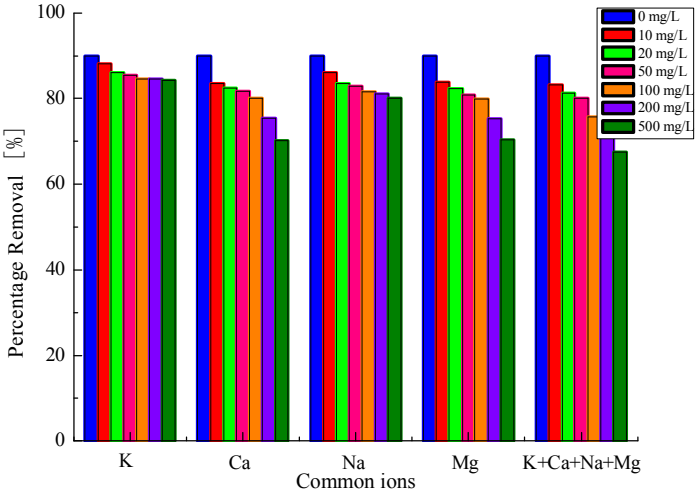

Fig. 2-7 Effect of competitive ions on percent removal of Pb^{2+} using AC_{K3}

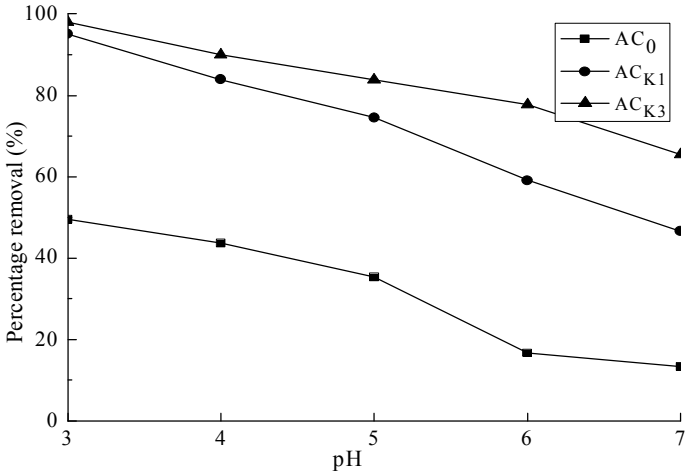

Fig. 2-8 Effect of pH on percent removal of Cr (VI) using modified activated carbon.

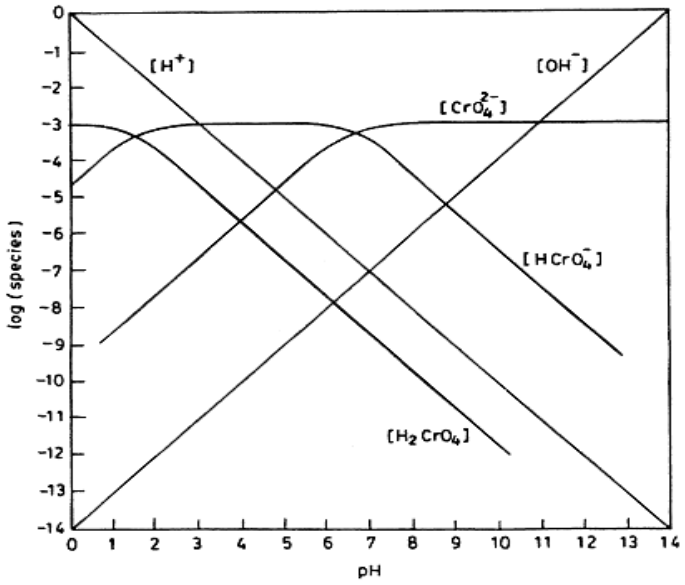

Fig. 2-9 Logarithmic concentration diagram for 10^{-3} M $H_2Cr_2O_4$ solution

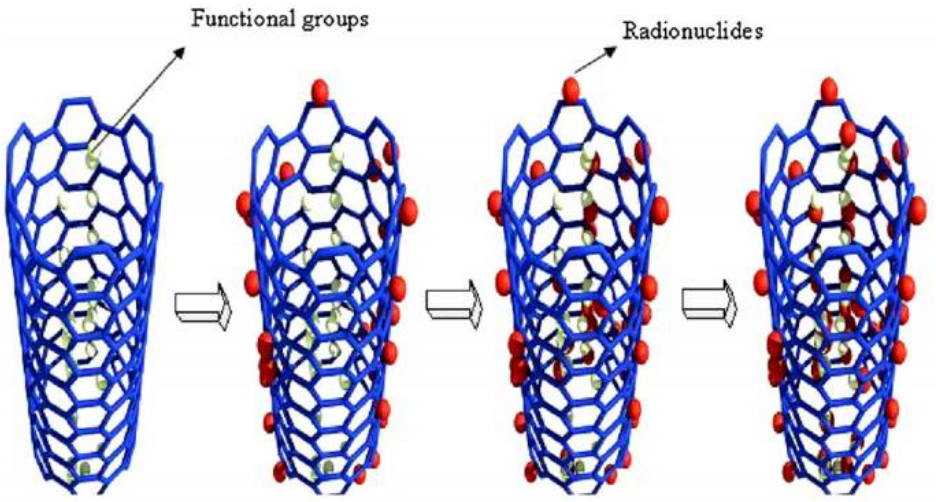

Fig. 2-10 The possible process of Eu(III) adsorption diagram on CNTs

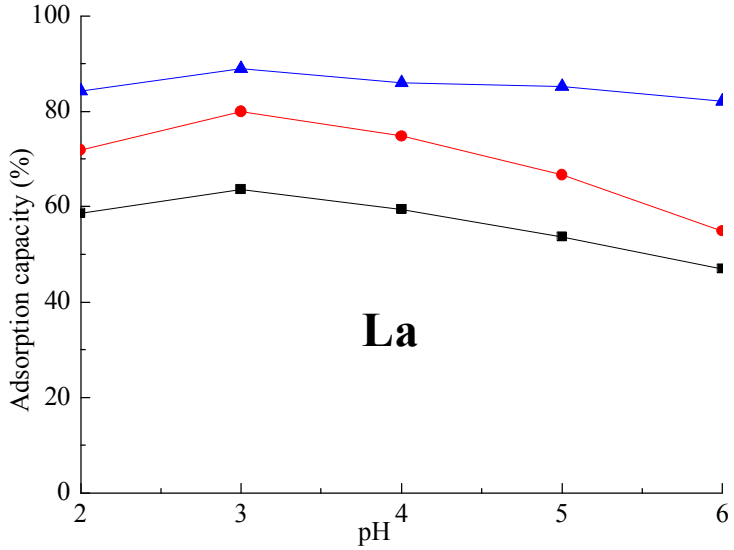

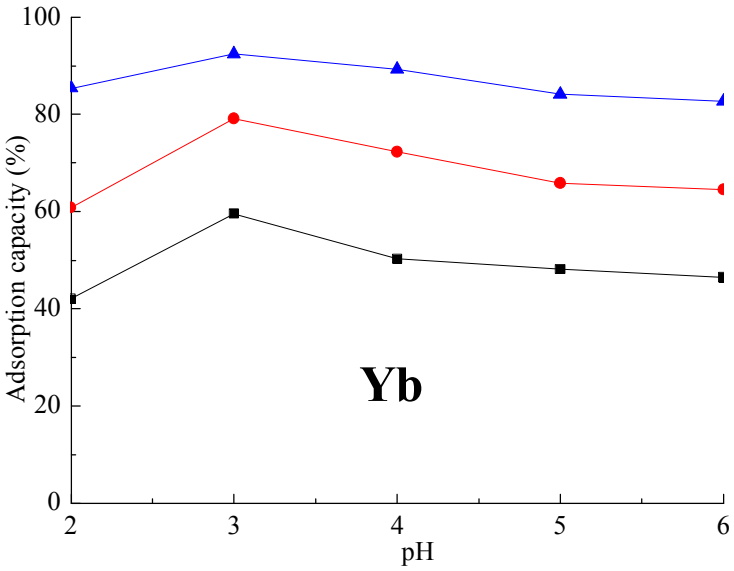

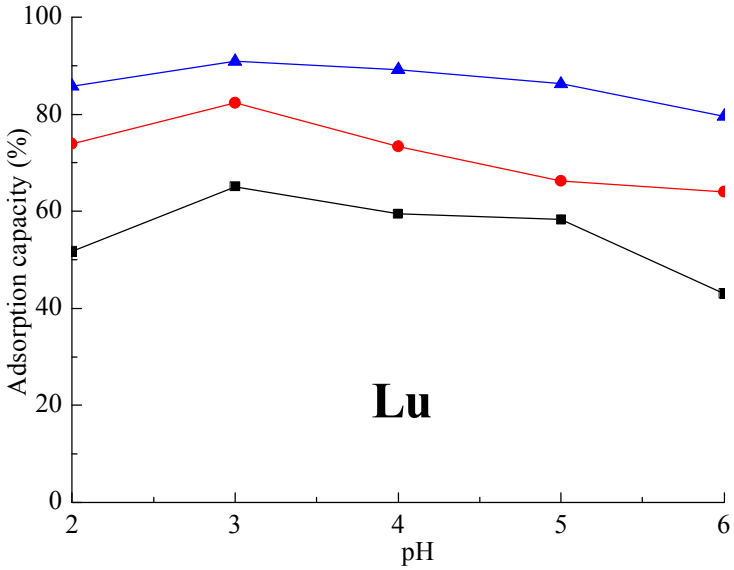
100
80
60
40
20
0
Adsorption capacity (%)
Lu
2
3
4
5
6
pH

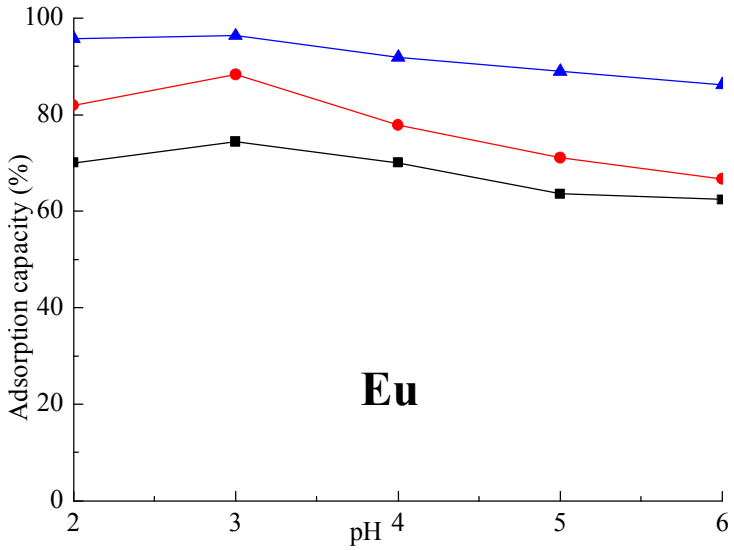
100
80
60
40
20
0
Adsorption capacity (%)
Eu
2
3
pH
4
5
6

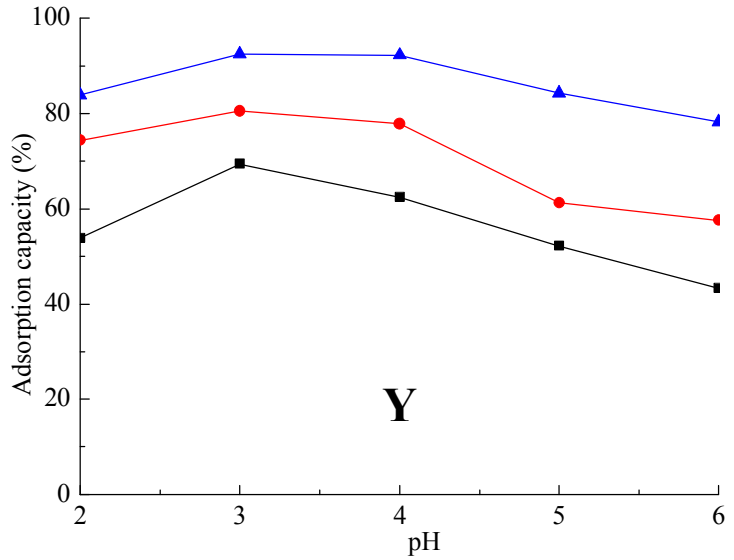
100
80
60
40
20
0
Adsorption capacity (%)
Y
2
3
4
5
6
pH

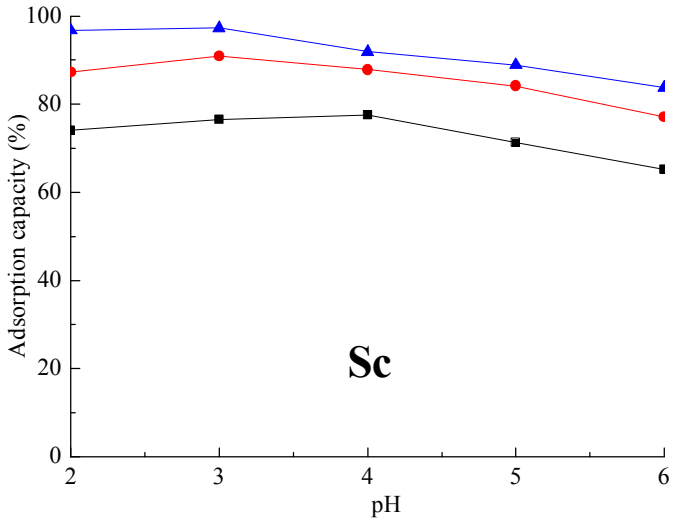

Fig. 2-11 Effect of pH on the removal of REEs using ACs (▲: AC_0; ●:AC_{K1}; ■: AC_{K3})

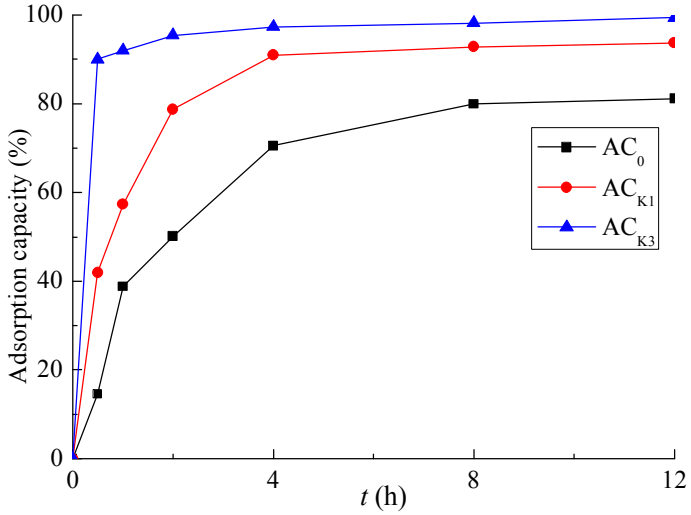

Fig. 2-12 Effect of contact time on the removal of Sc using ACs

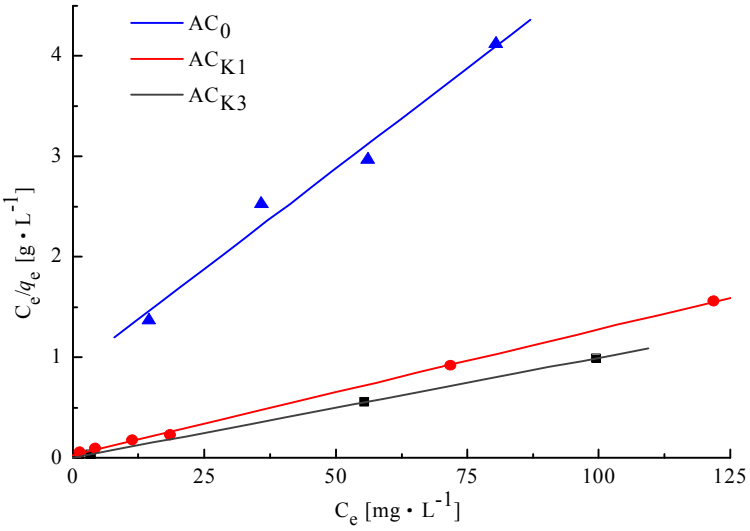

Fig.2-13 Langmuir isotherm of Pb^{2+} adsorption on AC

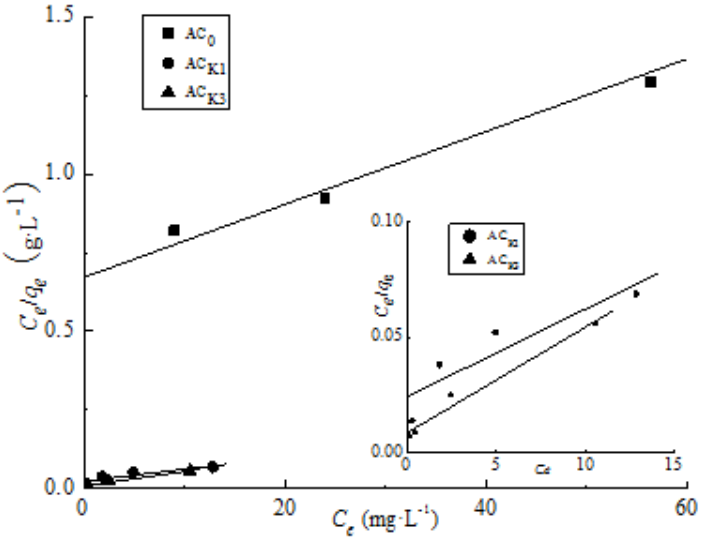

Fig. 2-14 Langmiur isotherm of Cr (VI) adsorption onto activated carbon

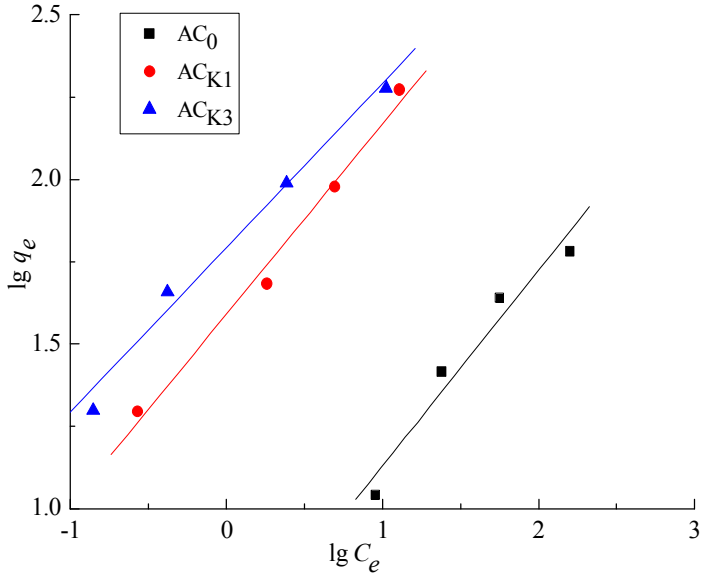

Fig. 2-15 Freundlich isotherm of Cr(VI) adsorption onto ACs

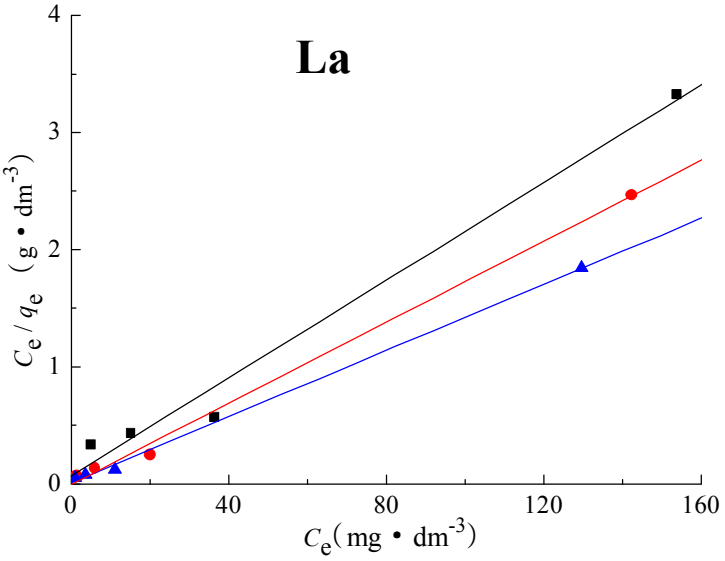

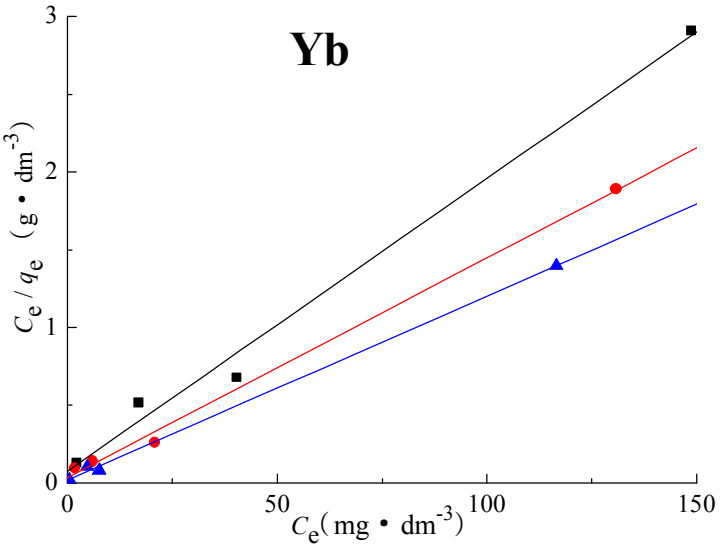
Yb
C_e / q_e (g • dm^{-3})
C_e(mg • dm^{-3})
0
1
2
3
0
50
100
150

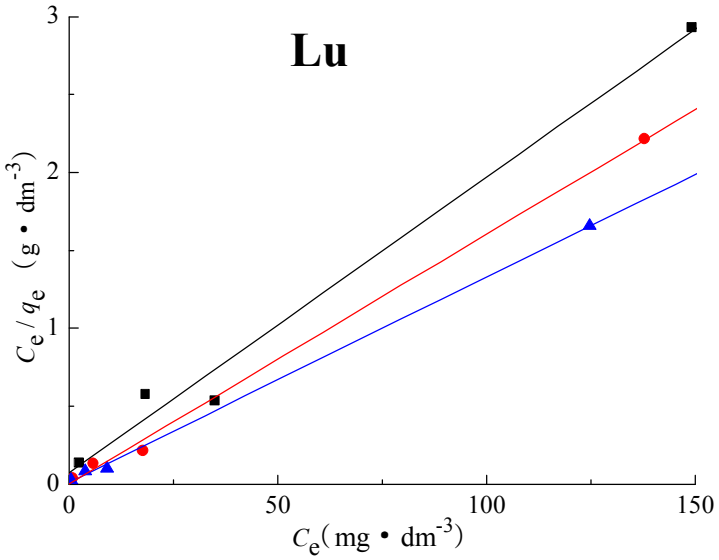
Lu
C_e / q_e (g • dm^{-3})
C_e(mg • dm^{-3})
0
1
2
3
0
50
100
150

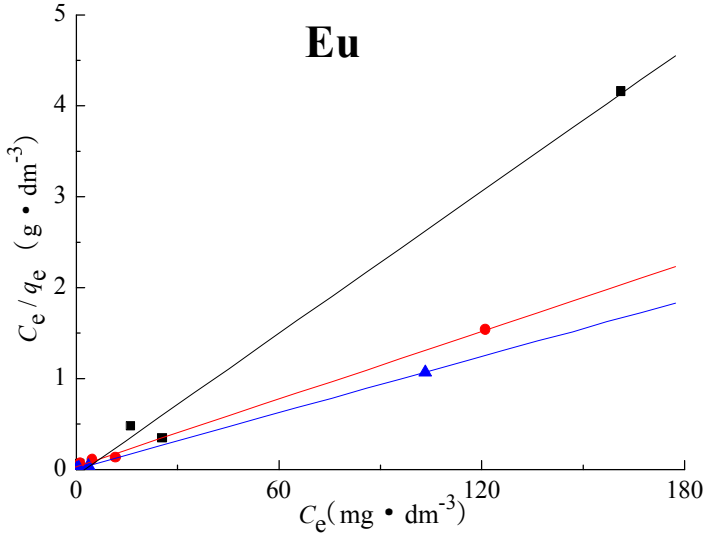
Eu
C_e / q_e (g • dm^{-3})
C_e(mg • dm^{-3})
0
1
2
3
4
5
0
60
120
180

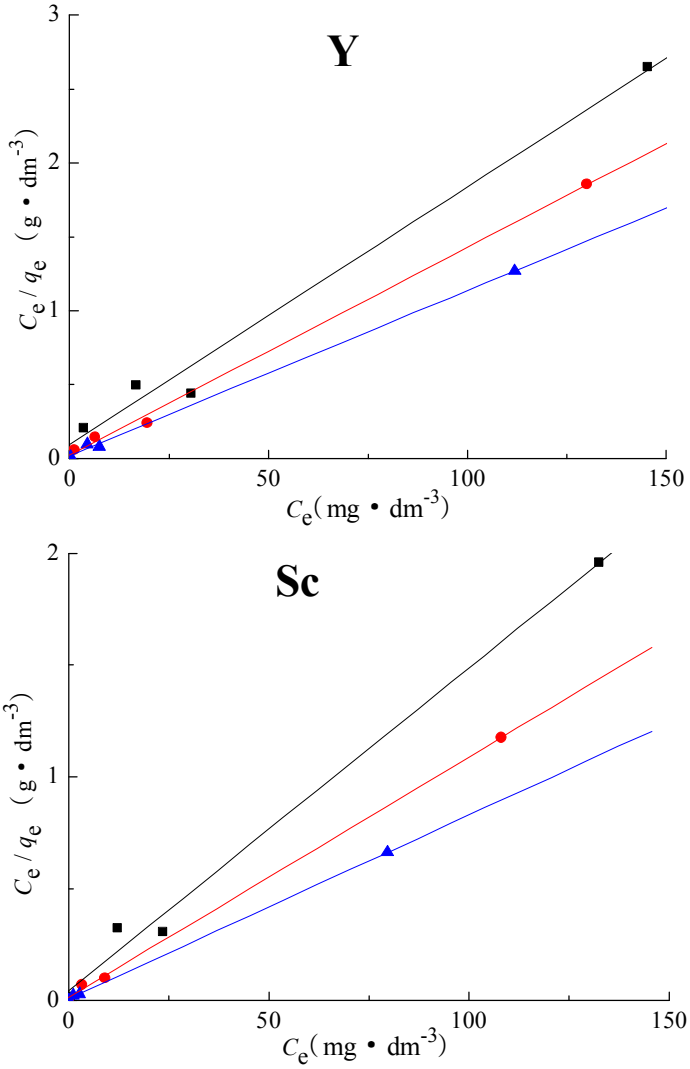

Fig. 2-16 Langmiur isotherm of REEs adsorption onto ACs (▲: AC_0; ●:AC_{K1}; ■: AC_{K3})

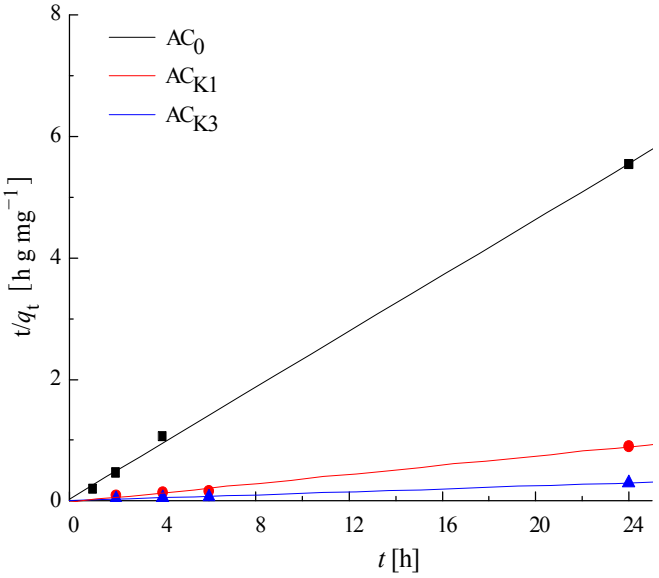

Fig.2-17 The pseudo second-order kinetic model for Pb^{2+} adsorption on ACs

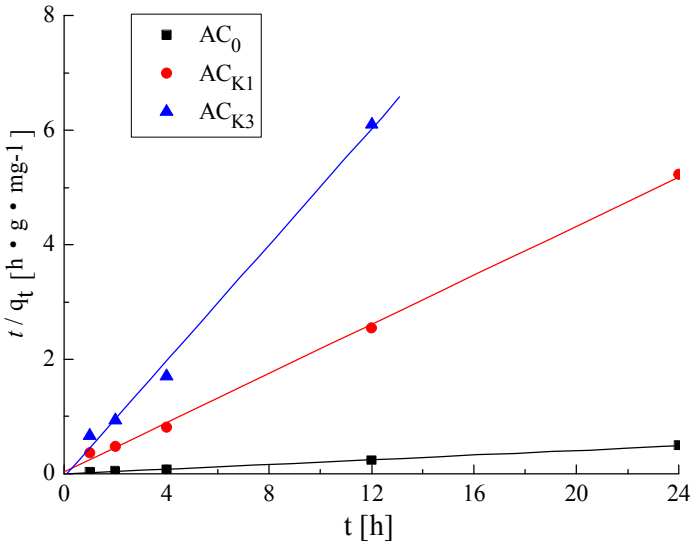

Fig. 2-18 The pseudo second-order kinetic model for activated carbons

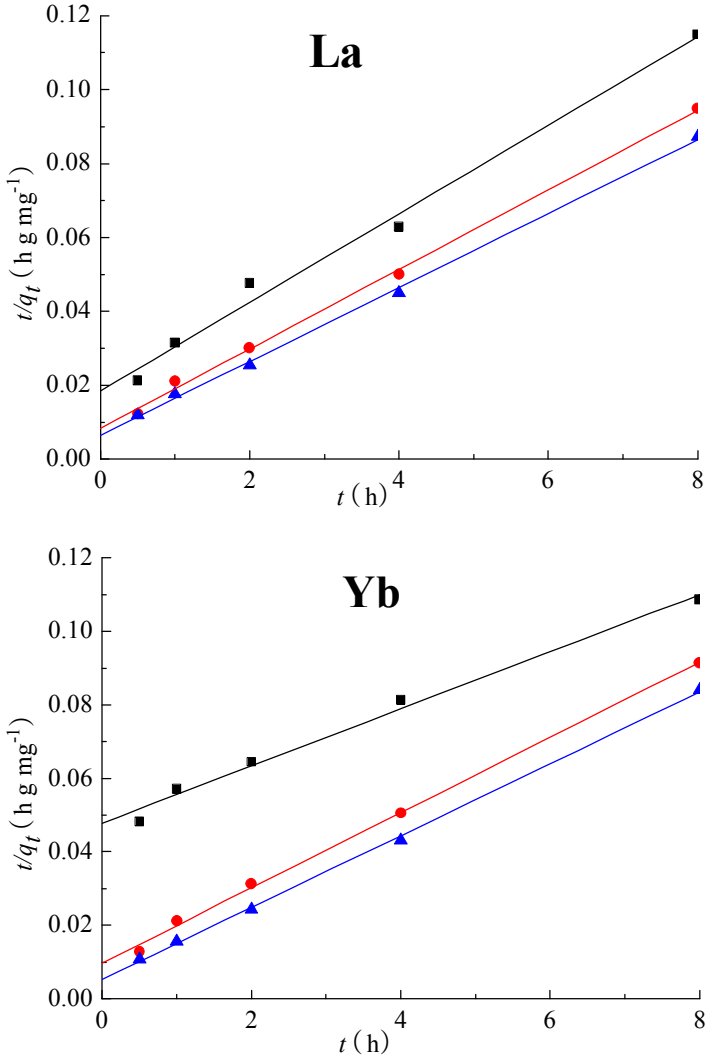

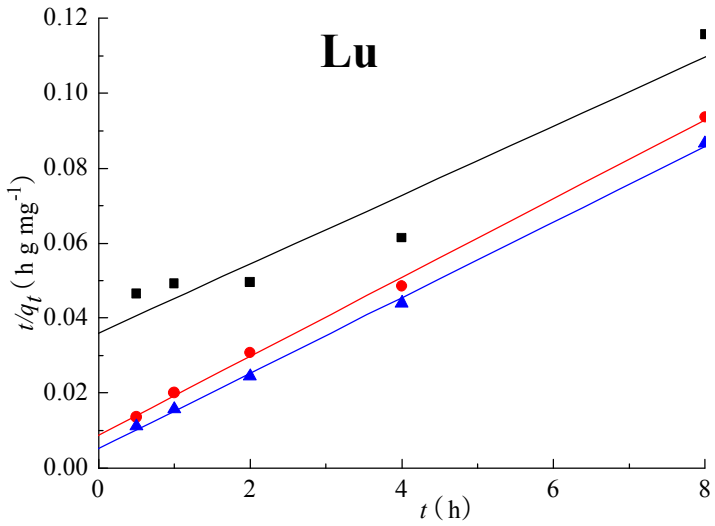
Lu
0.12
0.10
0.08
0.06
0.04
0.02
0.00
t/q_t (h g mg^{-1})
0
2
4
6
8
t (h)

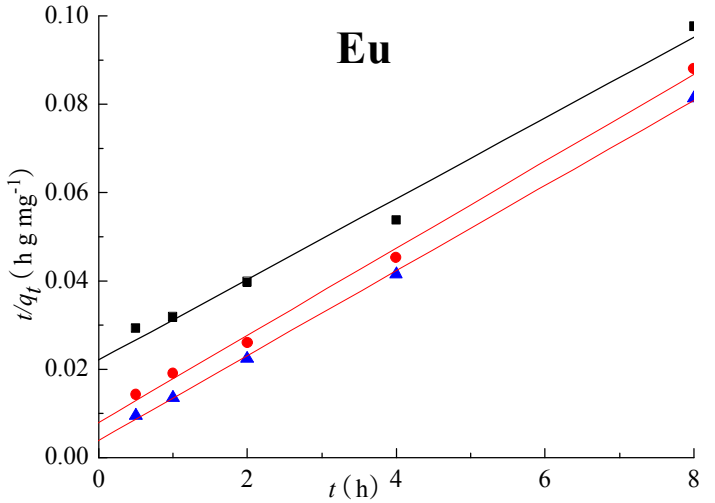
Eu
0.10
0.08
0.06
0.04
0.02
0.00
t/q_t (h g mg^{-1})
0
2
4
6
8
t (h)

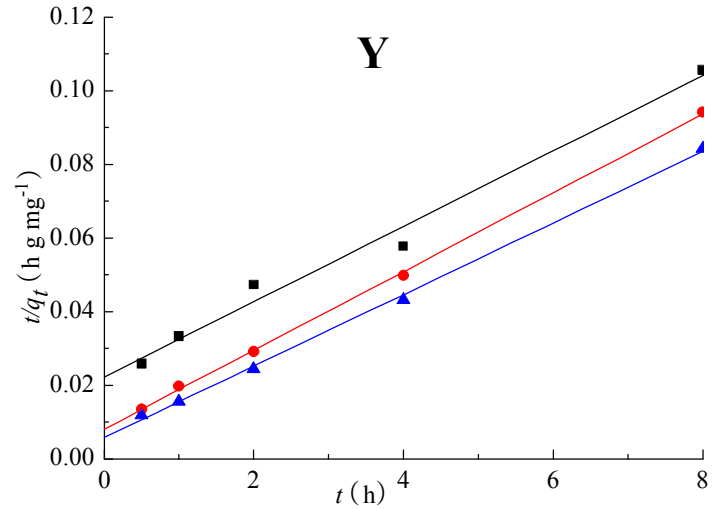
Y
0.12
0.10
0.08
0.06
0.04
0.02
0.00
t/q_t (h g mg^{-1})
0
2
4
6
8
t (h)

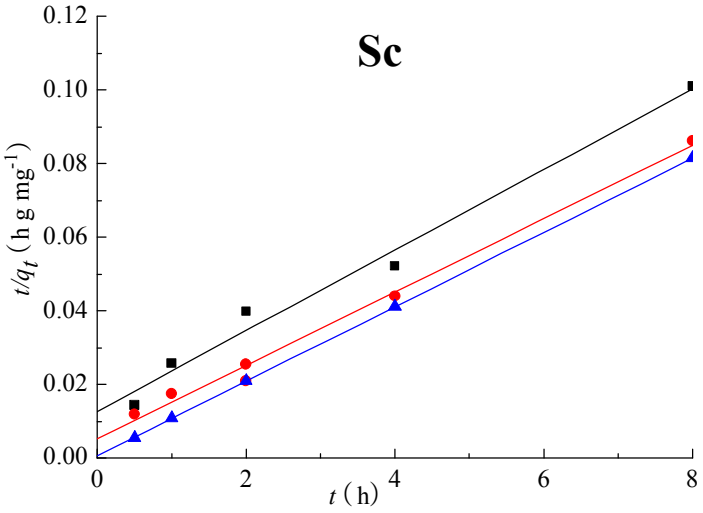

Fig. 2-19 The pseudo-second-order kinetic model of REEs for ACs (▲: AC_0; ●:AC_{K1}; ■: AC_{K3})

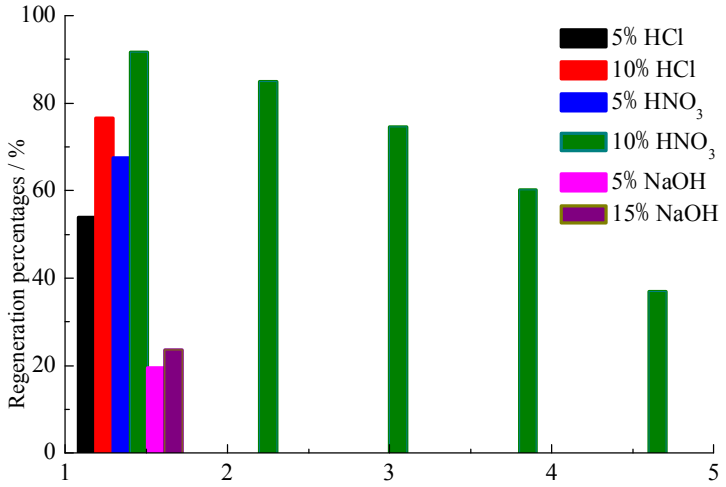

Fig. 2-20. The adsorption capacity after desorption using various leaching agents for Pb^{2+}

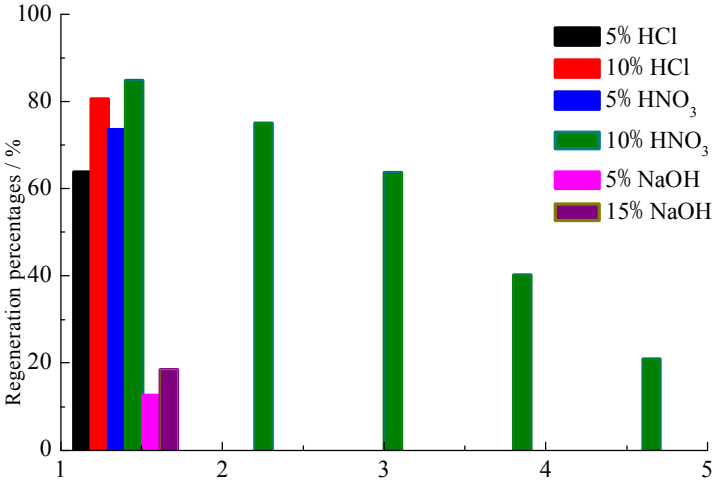

Fig. 2-21.The adsorption capacity after desorption using various leaching agents for Cr (VI)

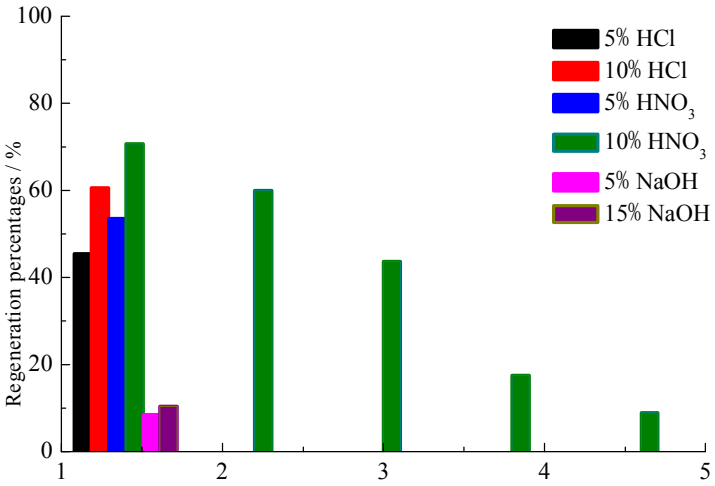

Fig. 2-22.The adsorption capacity after desorption using various leaching agents for La (III)

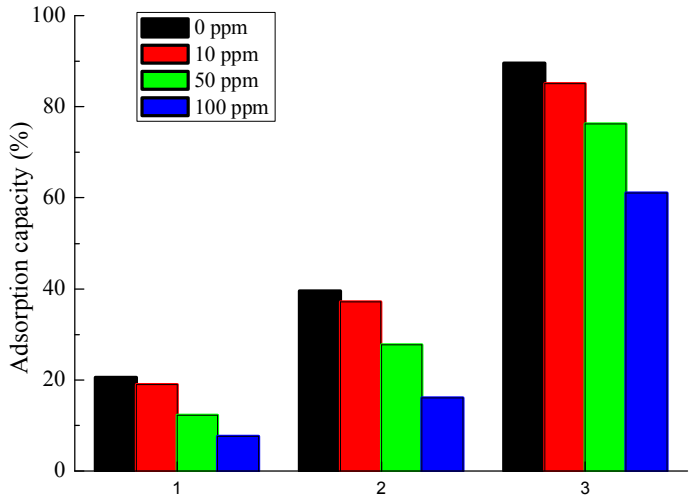

Fig. 2-23. The effect of competitive ions on the adsorption of of Pb^{2+}
(1: AC_0; 2: AC_{K1}; 3:AC_{K3})

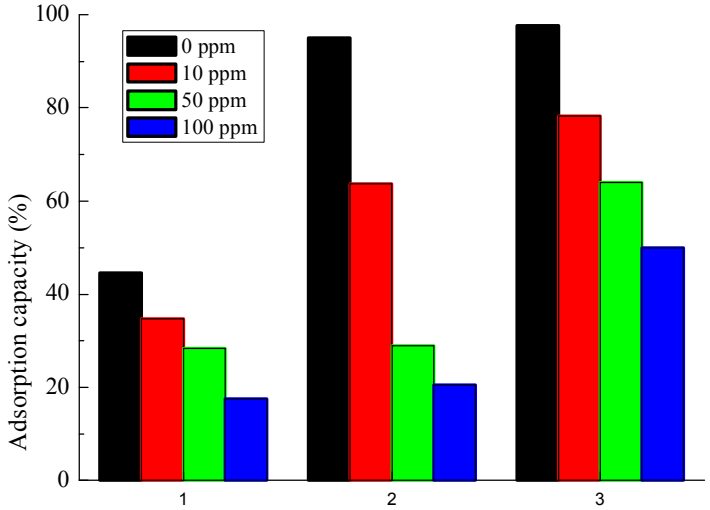

Fig. 2-24. Effect of competitive ions on the adsorption of of Cr (VI)
(1: AC_0; 2: AC_{K1}; 3:AC_{K3})

Chapter 3 Adsorption of heavy metals and REEs by zeolite/zhitosan hybrid composite (ZCHC)

3.1 Introduction

Nowadays, environmental pollution including water pollution due to heavy metals, nutrients, organic materials etc. is one of the most important problems throughout the world.

Of all pollutants, Cr (VI)-containing wastes are considered one of the most severe. In order to assess and minimize harmful pollutants such as Cr(VI) , ecological restoration techniques using minerals [96], microbes [97], and organic substances [98], are needed and very significant from the viewpoint of environmental protection.

Furthermore, the demand of rare earth elements (REEs) in modern technology has increased remarkably over the past years. However, the supply of trace metals including REEs has been restricted for particular countries, and the shortage of these metals has been concerned in recent years, the establishment of the new recovery method for the trace metals seems more and more important from the viewpoint of resources recovery [47, 48, 99].

Zeolites are three dimensional aluminosilicate minerals with a porous structure that have valuable merits, such as cation exchange, molecular sieving, catalysis and adsorption [65, 100]. However, in many cases, these materials do not exhibit high adsorption efficiencies for target metals and therefore their modification has been reported to enhance their adsorption potential [71, 101]. Therefore, the development of alternative adsorbents has been under an intensive study in recent decades.

Chitosan, as an abundant natural polysaccharide, has attracted much attention in the biomaterial area because of its biocompatibility, biodegradability and

non-antigenicity [66, 102]. In this study, chitosan is a hydrophilic and cationic polymer product of chitin and was used to form a composite with zeolite, which is an alumino-silicate with three-dimensional framework structure containing AlO_4 and SiO_4 [67, 103]. Modifications were made in order to improve pore size, mechanical strength, chemical stability, and hydrophilicity of chitosan[104, 105]. Then, it is expected that the zeolite/chitosan hybrid material (ZCHC), which can incorporate the merits of both materials, may exhibit promising capability for the removal of lead from aqueous solution. Therefore, chitosan and zeolite are the composite materials and have good developmental prospects.

This study investigated the adsorption ability of ZCHC as adsorbent for aqueous Pb, Cr, and REEs, ZCHC was prepared with sol-gel method by mixing zeolite and chitosan. Finally the further developments of ZCHC as composition adsorbent with the future of application in the environmental chemistry are foretold.

3.2 Experimental section

3.2.1 Materials

Chitosan (50-100mPa·s; 0.5% in 0.5% Acetic acid at 20℃) was purchased from Tokyo chemical industry Co., Ltd. The small granule zeolite, which particle size is largely 0.84~1.68 mm (≧80.0%) and some of more than 1.68 mm (≦80.0%), was purchased from Kanto chemical Co., Inc. (Japan).

Chemical reagents including $Pb(NO_3)_2$ were purchased from Kanto Chemical Co., Inc. (Japan). Cr(VI) standard solutions were prepared by diluting a standard

solution (1,000 $mg \cdot dm^{-3}$ $K_2Cr_2O_7$ solution) purchased from Kanto Chemical Co.. REEs standard solutions were prepared by diluting a 10 $mg \cdot dm^{-3}$ custom assurance standard solution purchased from Spex CertiPrep. Each stock solution was diluted with deionized water. All other chemical reagents were also purchased from Kanto Chemical Co.. All reagents were of analytical grade, and water (>18.2 MΩ) treated by an ultrapure water system (Advantec aquarius: RFU 424TA) was employed throughout the work.

3.2.2 Synthesis of ZCHC

Zeolite were heated at 700℃ for 3 h to activate the surface in a muffle furnace, and then washed with hydrochloric acid (5%, volume) and deionized water (at 80℃) to remove fine powders and contaminants, and was then dried at 110℃ for 2 h before use.

ZCHC was prepared by mixing solutions of chitosan and dispersions of zeolite in water. The general procedure of the synthesis is as follows: firstly, 1 g chitosan was dissolved in 20 mL of 0.2 M acetic acid with constant stirring at temperature of 50 ℃. The 10 mL of deionized water was added into 10mL chitosan sol solution, heated and stirred for 1 h. These solutions were mixed, while zeolite was dispersed in the chitosan solution with constant stirring for 5 h at temperature of 50℃. Then the solution was transferred into five 10 mL centrifuge tubes, which were centrifuged at 9000 rpm for 5 min, and then washed with deionized water to remove contaminants. The mixed solutions were put on Petri dishes, and left to dry at room temperature for 24 h. The obtained films with their thickness 0.1 mm were used for the following

adsorption experiments.

3.2.3 Characterization of ZCHC

Characterization of the structure of zeolite, chitosan and ZCHC was carried out by N_2 adsorption/desorption tests (Micromeritics TriStar 3020). The pore volume was calculated from the amount of N_2 adsorbed at the relative pressure of 0.99. The pore size was calculated from the adsorption average pore width (4V/A by BET) in this work. The surface morphology of ZCHC before and after Pb^{2+} adsorption was surveyed using a Scanning Electron Microscope (SEM, JCM-6000).

3.2.4 Adsorption experiment for heavy metal and REEs Using ZCHC

For obtaining the optimum conditions regarding the adsorption of heavy metal and REEs, were studied by varying pH, contact time, adsorbent dose, and initial concentration on the adsorption of heavy metal and REEs. The pH of each solution was adjusted by using 0.1 mol·dm^{-3} NH3aq (aqueous solution)/0.1 mol·dm^{-3} HNO_3.

Following each adsorption experiment, the suspension containing adsorbent and the above standard solution was filtered through a 0.1 μm membrane filter (Advantec Mixed Cellulose Ester, 47 mm) to remove heavy metal and REEs that have been adsorbed into the adsorbent, and the concentration of this metal in the filtrate was determined with an AAS or ICP-AES.

The metal uptake by the adsorbent was calculated using the Eq. (1):

$$q = \frac{(C_0 - C_e)}{W} \cdot V \quad [\mathrm{mg \cdot g^{-1}}] \qquad (1)$$

where, q is the adsorption capacities of REEs at equilibrium ($\mu g \cdot g^{-1}$), C0 and Ce are the initial and equilibrium concentrations of heavy metal and REEs in a batch system respectively ($\mu g \cdot dm^{-3}$), V is the volume of the solution (dm^3), and W is the dry weight of each adsorbent (g).

3.3 Results and Discussion

3.3.1 Characterization of ZCHC

The surface properties of zeolite, chitosan and ZCHC were investigated by N_2 adsorption (TriStar II 3020, Micromeritics), and the analytical results for the adsorption/desorption isotherms are shown in **Table 3-1**. The pore volume was calculated from the amount of N2 adsorbed at the relative pressure of 0.99. The pore size was calculated from the adsorption average pore width (4 V/A by BET) in this work. The SEM pictures of the chitosan and ZCHC are shown in **Fig. 3-1**. By comparing the surface structure chitosan and ZCHC, the zeolite treatment REEs to a remarkable increase in the surface area and mesoporous volume of ZCHC sample. Then ZCHC can be a good adsorbent for heavy metals and REEs. These results are consistent with those of the N_2 adsorption-desorption experiment.

3.3.2 Adsorption of Pb^{2+} on zeolite and ZCHC

The surface properties of ZCHC before and after Pb^{2+} adsorption were investigated by N_2 adsorption (TriStar II 3020, Micromeritics), and the analytical results for the adsorption/desorption isotherms are shown in **Table 3-2**.

The SEM micrographs of the ZCHC before and after Pb^{2+}adsorption ZCHC are

shown in **Fig 3-2**. From **Fig. 3-2,** it is found that the morphology of ZCHC surface has hardly changed even after exposing Pb^{2+}, although the SEM picture after Pb^{2+} adsorption slightly exhibit a more compact stacking morphology than the that before adsorption (**Fig 3-2B**). From the above observation, ZCHC should be predicted to withstand the repeated use; and hence it can be a good adsorbent for heavy metals such as Pb^{2+}.

Effect of pH

With the aim of obtaining the optimum conditions, the effects of pH value, and contact time in the case of a fixed dosage of adsorbent (ie., 1.0 $g \cdot L^{-1}$) on the removal of Pb^{2+} from the aqueous solution were investigated. The effect of pH on Pb^{2+} adsorption onto zeolite and ZCHC are shown in **Fig 3-3**.

From **Fig 3-3,** the uptake of Pb^{2+} increased from 56.7% at pH 3 to 95.6% at pH 5, and at higher pH value, it remained almost constant (or decreased slightly). Notably, the adsorption capacities decreased at low pH values due to the competition of protons with metal ions for active binding. On the other hand, lead precipitated from the solution at higher pH values as lead hydroxide [9]. Hence, pH 5 was utilized for further experiments.

Effect of contact time

The effect of contact time on Pb^{2+} adsorption onto zeolite and ZCHC are shown in **Fig 3-4**. Approximately 90% of Pb was removed from the solution with ZCHC at the contact time of 1 h, and it gradually increased at 4 h as shown in **Fig 3-4**. More that 95% of Pb was removed from the solution at the contact time of 4 h. After 4 h,

there was no appreciable change. On the other hand, contact time of 8h was needed to attain at equilibrium in case of zeolite. Therefore, 8 h was chosen as the optimized contact time for more certainty for these samples at the rest of the experimental work.

Effect of adsorbent dosage

Under optimized condition of pH and contact time, adsorption behaviors onto adsorbents at different dosages from 0.1 $g \cdot dm^{-3}$ to 2.0 $g \cdot dm^{-3}$ have been studied in 100 $\mu g \cdot dm^{-3}$ of Pb^{2+} solution, the results are shown in **Fig 3-5**. The removal of Pb^{2+} more than 90% was observed for 1.0 $g \cdot dm^{-3}$ dosage, but no remarkable increase is observed at a dosage more than 1.0 $g \cdot dm^{-3}$. Therefore, 1.0 $g \cdot dm^{-3}$ was considered as optimum dosage for the removal of Pb^{2+} in our study.

3.3.3 Adsorption of Cr (VI) on ZCHC

For obtaining the optimum conditions regarding the adsorption of Cr(VI), the effects of pH, contact time and dosage of adsorbents ((i.e., zeolite, chitosan and ZCHC) on the removal of Cr(VI) from the aqueous solution were investigated.

Effect of pH

Solution pH is one of the most important parameters affecting adsorption characteristics. In many cases, the dominant chemical species alter as pH varies. To investigate the effect of solution pH on Cr(VI) removal efficiency by ZCHC, the pH of the solution was varied from 2-8 (in 100 $mg \cdot dm^{-3}$ of solution using 1.0 $g \cdot dm^{-3}$ ZCHC dosage for contact time of 6h). The experimental results using ZCHC are shown in **Fig.3-6** along with that by chitosan.

Cr (VI) exists as hydrogen chromate anions ($HCrO_4^-$) between pH 2.0 and pH 6.5, and it exists as chromate ions (CrO_4^{2-}) at pH 8 according to the following Eqs. (6) - (8) [75,106, 107]:

$$HCrO_4^- \leftrightarrow CrO_4^{2-} + H^+ \quad pKa = 5.9 \qquad (6)$$

$$H_2CrO_4 \leftrightarrow HCrO_4^- + H^+ \quad pKa = 4.1 \qquad (7)$$

$$Cr_2O_7^{2-} + H_2O \leftrightarrow 2HCrO_4^- \quad pKa = 2.2 \qquad (8)$$

The adsorption capacity of Cr (VI) reached maximum at pH 3 in case of using ZCHC (whereas at pH 4 for zeolite and chitosan), where Cr (VI) may exist as $HCrO_4^-$ or ($Cr_2O_7^{2-}$). This anion species has a tendency to bind to the protonated active sites of the chitosan in solution at optimum pH[108]. Cr (VI) exists as chromate ion (CrO_4^{2-}) at pH above 6.5. At pH 8, the uptake capacities are very low. This could be explained as competitiveness between chromate and hydroxyl ions. Then, pH 3 was taken for the removal of Cr (VI) by ZCHC (and pH 4 was used for zeolite and chitosan) for further experiments.

Effect of contact time

The effect of contact time on the adsorption capacity of Cr (VI) using 1.0 $g \cdot dm^{-3}$ adsorbent (100 $\mu g \cdot dm^{-3}$ of solution) is investigated.

The adsorption capacity of adsorbents for Cr (VI) is shown in **Fig.3-7**. More than 50% (in case of zeolite), 60% (in case of chitosan) and 80% (in case of ZCHC) adsorption was observed within first 30 min, and approximately 80% (in case of zeolite and chitosan) and 95% (in case of ZCHC) was obtained at 240 min (i.e., 4 h) and after that there is no appreciable increase. Hence, the optimized contact time was

taken 4 h for the removal of Cr (VI) in our experimental work.

Effect of adsorbent dosage

Under optimized condition of pH and contact time, adsorption behaviors onto adsorbents at different dosages from 0.1 $g \cdot dm^{-3}$ to 2.0 $g \cdot dm^{-3}$ have been studied in 100 $mg \cdot dm^{-3}$ of Cr solution. The removal of Cr (VI) more than 90% was observed for 1.0 $g \cdot dm^{-3}$ dosage, but no remarkable increase is observed at a dosage more than 1.0 $g \cdot dm^{-3}$. Therefore, 1.0 $g \cdot dm^{-3}$ was considered as optimum dosage for the removal of Cr (VI) in our study.

Effect of initial concentration

Study was carried out by varying initial concentrations from 20 $mg \cdot dm^{-3}$ to 200 $mg \cdot dm^{-3}$ under optimized conditions of pH 4, contact time (i.e., time 4 h) and adsorbent dosage (i.e., 1.0 $g \cdot dm^{-3}$). There was a continuous increase in the uptake of Cr (VI) per gram of adsorbent up to the concentration of 100 $mg \cdot dm^{-3}$, but the uptake is almost constant at further higher concentration for Cr (VI). Data obtained from the variation of initial concentrations were fitted for adsorption isotherms [9] to estimate the relevant parameters mentioned in Section 2.4.

3.3.4 Adsorption of REEs on ZCHC

Effect of pH

It is well known that pH influences significantly the adsorption processes by affecting both the protonation of the surface groups and the degree of the ionization of the adsorbates [24, 25]. In many cases, the dominant chemical species alter as pH

varies. To investigate the effect of solution pH on REEs removal efficiency by ZCHC, the pH of the solution was varied from 2-7 (in 100 $\mu g \cdot dm^{-3}$ of solution using 1.0 $g \cdot dm^{-3}$ ZCHC dosage for contact time of 4h). The experimental results using ZCHC are shown in **Fig.3-8**.

ZCHC also exhibited a high uptake potential for pH values larger at pH 4. At this concentration, the pH range was kept below 7.0 in order to avoid any bulk precipitation of REE hydroxides. However, the differences in uptake capacity between the different metal surface for its special properties.

Effect of contact time

The effect of contact time on the adsorption capacity of REEs using 1.0 $g \cdot dm^{-3}$ adsorbent (100 $\mu g \cdot dm^{-3}$ of solution) is investigated.

The adsorption capacity of adsorbents for REEs is shown in **Fig.3-9**. The figure contains only the results for Sc and Eu since other REEs showed similar trends. More than 50% (in case of zeolite and chitosan) and 60% (in case of ZCHC) adsorption was observed within first 30 min, and approximately 95% was obtained at 4 h and after that there is no significant change. Hence, the optimized contact time was taken 4 h for the removal of REEs in our experimental work.

Effect of initial concentration

The effect of initial REEs concentrations from 20 $\mu g \cdot dm^{-3}$ to 200 $\mu g \cdot dm^{-3}$ under optimized conditions of pH 4, contact time is 4 h, and adsorbent dosage is 1.0 $g \cdot dm^{-3}$. In general, the uptake of REEs on ZCHC was above 60% over the entire range of concentrations. If pure zeolite or chitosan is used, the uptake percentage is seen to

drop dramatically as the initial concentration of REEs is increased. The association of chitosan with zeolite can be seen as a means by which the uptake performance of the mineral can be significantly enhanced. Data obtained from the variation of initial concentrations were fitted for adsorption isotherms [9] to estimate the relevant parameters mentioned in Section 2.4.

3.3.5 Adsorption isotherms

Adsorption isotherms are commonly used to reflect the performance of adsorbents in adsorption processes. To quantify the sorption capacity of the adsorbents studied for the heavy metals and REEs removal, the most commonly used isotherms, namely Langmuir, Freundlich and Temkin isotherms have been adopted. The Langmuir adsorption isotherm and Freundlich adsorption isotherm were applied to the data obtained in this work. A plot of C_e/q_e versus C_e and $\log_{10}q_e$ versus $\log_{10}C_e$ based on the Langmuir model and Freundlich model are shown in **Fig 3-10**- **Fig 3-13**, respectively.

The adsorption experimental data of Pb^{2+} onto zeolite and ZCHC were well fitted by the Langmuir isothermal adsorption equation, and the correlation coefficients were all > 0.995. As shown in **Table 3-3**, R value for each adsorbent was comparatively large, and a favorable adsorption of Pb^{2+} by these samples was apparent.

The adsorption data obtained for Cr (VI) using zeolite, chitosan and ZCHC were analyzed by Langmuir (**Fig.3-11**) and Freundlich (**Fig.3-12**) equations. The correlation coefficients (R^2) of these isotherms for Cr(VI) on each adsorbent are shown in **Table 3-4** along with other relevant parameters.

From **Table 3-4**, it is found that R^2 value for Cr (VI) on each adsorbent is comparatively large, and favorable adsorption of Cr by adsorbents were presented. The results indicated that the fittings of the data to Langmuir isotherm better than Freundlich isotherms. It was shown that the absorbents ZCHC had a marked increasing effect on the adsorption of Cr (VI), and the ZCHC had more marked increasing effect than zeolite and chitosan.

The adsorption data obtained for REEs using zeolite, chitosan and ZCHC were analyzed by Langmuir (**Fig.3-13**) equations, for simplicity, the figures of Freundlich isotherm of REEs adsorption is omitted. The Langmuir and Freundlich adsorption isotherm parameters, evaluated from the linear plots, are presented in **Table 5**.

Although both Langmuir and Freundlich models well express REEs adsorption onto zeolite, chitosan and ZCHC, correlation coefficients of Langmuir model are higher.

The results suggests that the adsorption of heavy metals and REEs on zeolite, chitosan and ZCHC mainly occurred by monolayer reaction. Furthermore, the maximum adsorption capacity of ZCHC towards Pb^{2+}, Cr (VI) and REEs were higher than that of zeolite and chitosan, there has a significant difference. From the data of q_{max} in **Table 3-3**, **Table 3-4**, **Table 3-5**, it is also found that the adsorption capacity of Pb^{2+}, Cr (VI) and REEs on ZCHC is much higher than thaton pristine zeolite and chitosan. The results indicated that the conventional zeolite and chitosan were compositely treated is effective for enhancing the adsorption capacity of Pb^{2+}, Cr (VI) and REEs.

3.3.6 Kinetic Studies

Kinetic models have been proposed to determine the mechanism of the

adsorption process, which provide useful data to improve the efficiency of the adsorption and feasibility of process scale-up. In the present investigation, the mechanism of the adsorption process was studied by fitting pseudo first-order and second-order reactions to the experimental data.

In order to examine conformity of both models and experimental results, the linear plots of ln (q_e - q_t) - t and t/q_t–t were used for REEs adsorption under the optimized experimental conditions pseudo-first-order and pseudo-second-order kinetic models, shown in **Fig 3-14**, **Fig 3-15**, **Fig 3-16**, respectively. The pseudo-second-order rate constant (k) and the amount of adsorbed lead (q_e), obtained from the intercept and slope of the plot of t/q_t vs. t are listed in **Table 3-6**, **Table 3-7**, **Table 3-8**, along with the regression coefficients (R^2), respectively.

It shows the coefficient of determination (R^2) is more than 0.97 for Pb^{2+} (>0.99), Cr(VI) (>0.99), REEs (>0.97) on zeolite, chitosan, ZCHC. It implies that the adsorption kinetics based on the experimental values are in good agreement with the pseudo second-order kinetic model. The intraparticle diffusion model indicated that the relationship between the concentration of Pb^{2+} (or Cr (VI) or REEs) and the square root of time are linear. This suggests that the adsorption process could be controlled by intraparticle diffusion.

3.4. Mechanism

ZCHC was prepared with sol-gel method by mixing zeolite and chitosan, could improve the mechanical properties of the blending film, which increases the chelating

activity of functional groups such as hydroxyl and amine with metal ions and heavy metal enriching capacity.

The removal mechanism consists of four steps, the esterification of chromate with tannin molecules, the reduction of Cr (VI) into Cr (III), the formation of carboxyl group by the oxidation of tannin molecules and the ion exchange of Cr (III) with hydroxyl and/or carboxyl groups created in tannin gel particles. In this reaction process, it is very important to supply a large amount of proton for promoting the reduction of Cr (VI) into Cr (III). This shows that the pH in the acidic solution can be increased to produce neutral solution through the adjustments of the amount of tannin gel particles and the volume of acidic solution having an appropriate pH for the concentration of Cr (VI) [109].

During the modification process, amino groups of chitosan was cationized and electrostatically attracted by negative charges on the surface of zeolite. However, because of the large size of chitosan, only the negative charges on the extemal surface of zeolite were occupied by chitosan, while the negative charges in internal pores are still accessible for inorganic cationic pollutants.

3.5. Conclusions

The present investigation was carried out to evaluate the efficiency of zeolite/chitosan hybrid composite as adsorbent for aqueous Pb^{2+}, Cr (VI) and REEs. Conclusion: the following matters have been obtained from our work.

1. Zeolite/chitosan hybrid composite (ZCHC) was prepared with sol-gel method

by mixing zeolite and chitosan, investigated the adsorption ability of ZCHC as adsorbent for Pb^{2+}, Cr (VI) and REEs. The removal of Pb^{2+}, Cr (VI) and REEs were more than 95%, 95%, 70% under our experimental conditions, respectively. ZCHC exhibited a higher adsorption capacity and stronger chemical affinity than pristine zeolite and chitosan.

2. The adsorption experimental data of Pb^{2+}, Cr(VI) and REEs onto zeolite, chitosan and ZCHC were full compliance with the Langmuir isothermal adsorption equation, the coefficient of determination (R^2) is more than 0.95 for Pb^{2+}, Cr(VI), REEs on zeolite, chitosan, ZCHC. Isotherm fits of Langmuir models indicated the surface heterogeneity, which suggests that the adsorption of heavy metals and REEs on the surface of the adsorbent belongs to monolayer adsorption in the concentration range studied.

3. The rates of sorption conform to pseudo-second order kinetics, and the correlation coefficients are all >0.97. It implies that the adsorption kinetics based on the experimental values are in good agreement with the pseudo second-order kinetic model. This suggests that the adsorption process could be controlled by intraparticle diffusion.

The results suggest that ZCHC prepared in this work could be suitable as sorbent materials for the removal of heavy metal aqueous solutions. On the whole, the zeolite/chitosan hybrid composite showed their potential to be applied in different water treatment applications for the removal of heavy metals and REEs. This provides very significant information from the viewpoint of environmental protection.

Tables

Table 3-1 Texturals characteristics of adsorbents

Adsorbent	BET surface Area ($m^2 \cdot g^{-1}$)	Pore volume ($cm^3 \cdot g^{-1}$)	Pore size (nm)
Zeolite	5.63	0.0474	26.8
Chitosan	0.612	0.00385	25.2
ZCHC	9.25	0.0485	21.0

Table 3-2 Textural characteristics of ZCHC

Adsorbent	BET surface area [$m^2 \cdot g^{-1}$]	Pore volume [$cm^3 \cdot g^{-1}$]	Pore size [nm]
ZCHC (before adsorption)	9.25	0.0485	21.0
ZCHC (after adsorption)	9.19	0.0479	20.7

Table 3-3 Coefficient of Langmuir isotherm for Pb^{2+} using ZCHC

adsorbent	q_{max} [$mg \cdot g^{-1}$]	K_L [$L \cdot mg^{-1}$]	R
Zeolite	66.5	0.196	0.997
ZCHC	139	0.844	0.999

Table 3-4 Coefficient of Langmuir and Freundlich isotherms for Cr (VI)

	Langmuir isotherm			Freundlich isotherm		
	q_{max} ($mg \cdot g^{-1}$)	K_L ($dm^{-3} \cdot mg^{-1}$)	R^2	K_F ($(mg \cdot g^{-1}) \cdot (dm^{-3} \cdot mg^{-1})^{1/n}$)	$1/n$	R^2
Zeolite	70.0	0.245	0.999	17.4	0.526	0.957
Chitosan	92.2	0.253	0.998	30.6	0.311	0.964
ZCHC	109	0.645	0.994	57.7	0.237	0.955

Table 3-5 Coefficient of Langmuir and Freundlich isotherms for REEs

		Langmuir isotherm			Freundlich isotherm		
		q_{max} [μg·g^{-1}]	K_L [L·μg^{-1}]	R^2	K_F [(μg·g^{-1})·(L·μg^{-1})$^{1/n}$]	1/n	R^2
La	Zeolite	34.8	0.00838	0.973	6.94	0.528	0.959
	Chitosan	52.1	0.0149	0.996	1.81	0.614	0.981
	ZCHC	89.6	0.0397	0.996	1.25	0.634	0.999
Yb	Zeolite	37.8	0.0529	0.983	25.4	0.263	0.959
	Chitosan	57.4	0.0722	0.967	18.2	0.205	0.962
	ZCHC	81.1	0.254	0.998	13.3	0.166	0.891
Lu	Zeolite	37.9	0.0620	0.986	31.1	0.213	0.944
	Chitosan	56.8	0.0887	0.988	20.4	0.145	0.806
	ZCHC	101	0.129	0.993	12.6	0.185	0.897
Eu	Zeolite	43.4	0.0504	0.975	22.5	0.334	0.954
	Chitosan	61.2	0.0473	0.953	13.8	0.260	0.967
	ZCHC	94.4	0.195	0.998	16.8	0.137	0.837
Y	Zeolite	14.9	0.163	0.996	22.1	0.101	0.962
	Chitosan	29.5	0.128	0.997	17.9	0.0766	0.881
	ZCHC	41.4	0.115	0.990	7.81	0.118	0.941
Sc	Zeolite	194	0.539	0.995	39.9	0.531	0.978
	Chitosan	201	0.327	0.999	57.8	0.389	0.957
	ZCHC	209	0.258	0.998	107	0.373	0.961

Table 3-6 Kinetic coefficient for Pb^{2+} adsorption on adsorbents

Adsorbents	q_e (mg·g^{-1})	k (g·mol^{-1}·h^{-1})	R
Zeolite	67.3	9.87×10^{-3}	0.994
Chitosan	96.4	2.08×10^{-2}	0.999
ZCHC	97.9	2.96×10^{-2}	0.999

Table 3-7 Kinetic coefficient for Cr (VI) adsorption on adsorbents

Adsorbents	q_e ($mg \cdot g^{-1}$)	k ($g \cdot mol^{-1} \cdot h^{-1}$)	R
Zeolite	72.6	0.0351	0.999
Chitosan	84.5	0.0724	0.999
ZCHC	97.9	0.0869	0.999

Table 3-8 Kinetic coefficient for REEs adsorption on adsorbents.

		pseudo-first-order			pseudo-second-order		
		q_e ($\mu g \cdot g^{-1}$)	k_1 (h^{-1})	R^2	q_e ($\mu g \cdot g^{-1}$)	k ($g \cdot \mu g^{-1} \cdot h^{-1}$)	R^2
La	Zeolite	9.02	0.372	0.964	16.1	0.702	0.998
	Chitosan	23.5	0.313	0.986	37.4	1.63	0.999
	ZCHC	33.8	0.357	0.931	73.6	2.09	0.996
Yb	Zeolite	26.0	0.394	0.989	38.5	0.620	0.993
	Chitosan	31.1	0.379	0.984	48.6	1.23	0.995
	ZCHC	56.3	0.496	0.967	100	1.25	0.980
Lu	Zeolite	26.7	0.350	0.947	39.6	0.862	0.983
	Chitosan	35.7	0.504	0.977	53.6	0.651	0.985
	ZCHC	58.8	0.552	0.969	93.4	1.01	0.988
Eu	Zeolite	18.8	0.276	0.927	35.2	1.34	0.997
	Chitosan	21.4	0.323	0.943	41.2	2.66	0.998
	ZCHC	46.6	0.371	0.953	94.0	3.00	0.999

	Zeolite	10.6	0.254	0.926	16.9	1.45	0.989
Y	Chitosan	20.8	0.287	0.974	18.3	2.14	0.974
	ZCHC	21.9	0.356	0.949	39.3	3.11	0.995
	Zeolite	37.8	0.677	0.966	103	2.24	0.998
Sc	Chitosan	42.4	0.688	0.969	104	2.40	0.999
	ZCHC	47.7	0.832	0.947	104	3.25	1.00

Figures

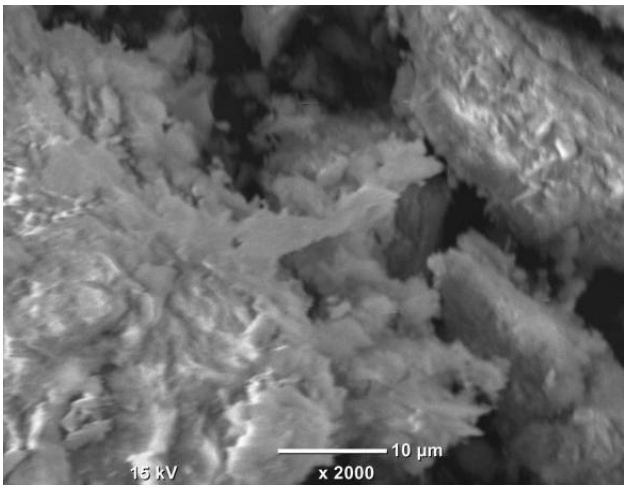

(a)

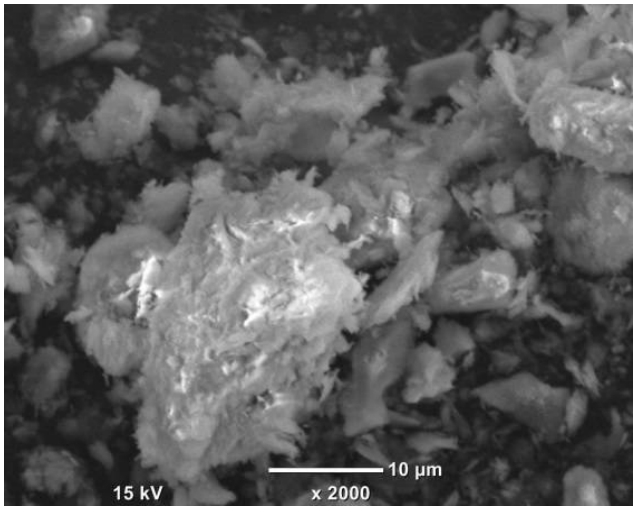

(b)

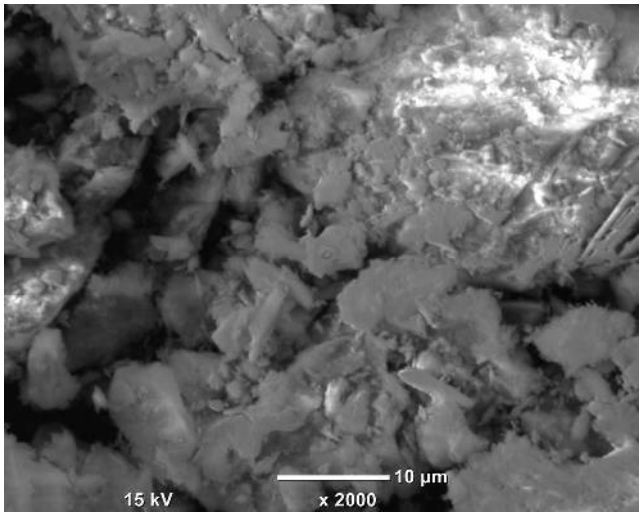

(c)

Figure 3-1 SEM micrographs of the surface of chitosan and ZCHC (a:Zeolite; b: Chitosan; c:ZCHC)

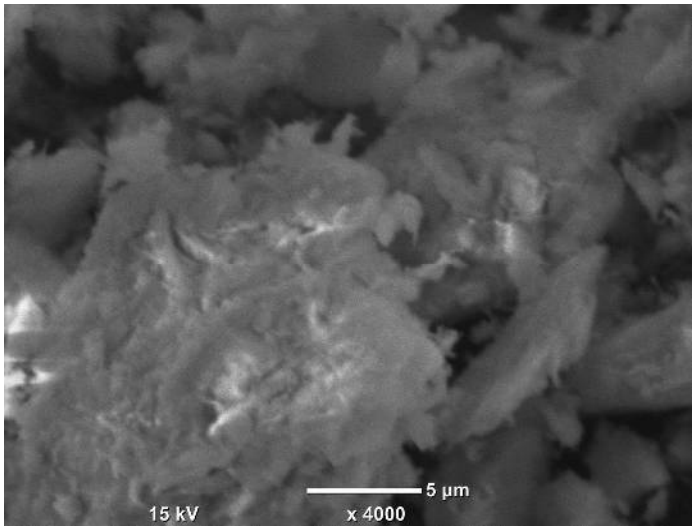

(A)

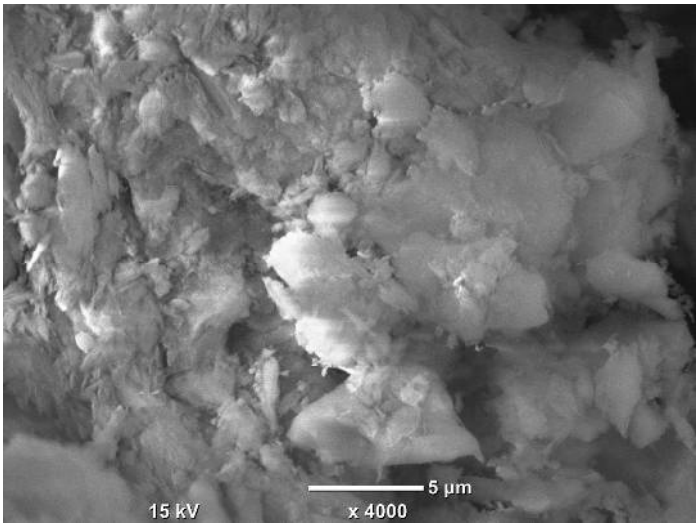

(B)

Figure 3-2 SEM micrographs of the surface of ZCHC: (A) before Pb^{2+}adsorption; (B) after Pb^{2+}adsorption

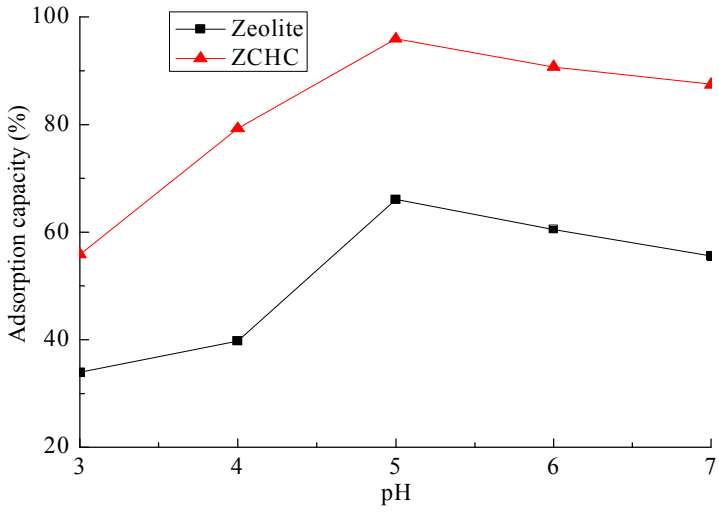

Figure 3-3 Effect of pH on the removal of Pb^{2+} using zeolite and ZCHC

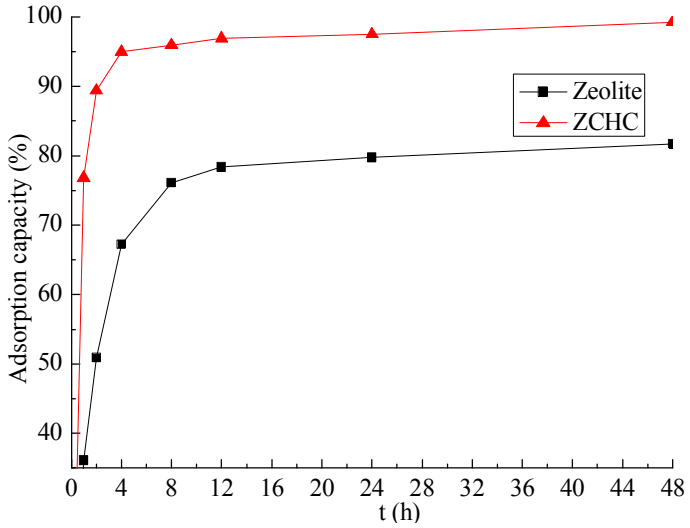

Figure 3-4 Effect of contact time on the removal of Pb^{2+} using zeolite and ZCHC.

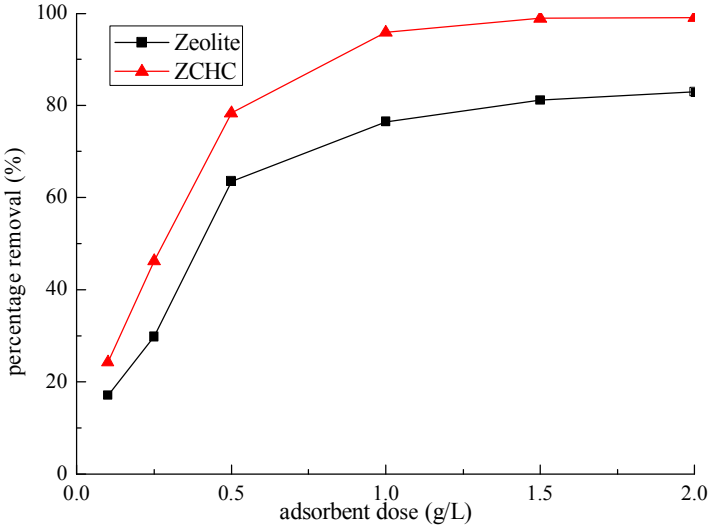

Figure 3-5 Effect of adsorbent dose on the removal of Pb^{2+} using zeolite and ZCHC.

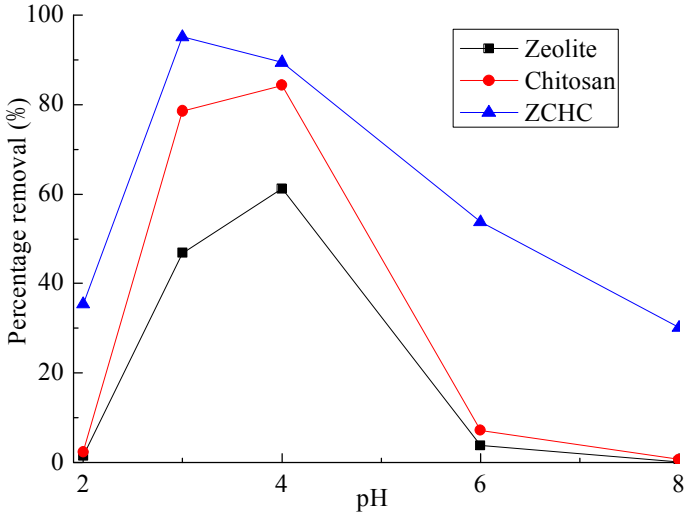

Fig. 3-6 Effect of pH on percent removal of Cr (VI) using adsorbents

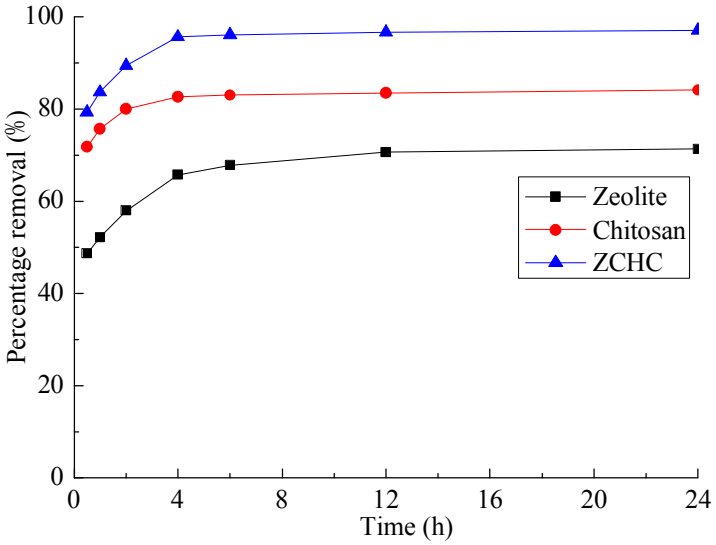

Fig. 3-7 Effect of contact time on percent removal of Cr(VI) using chitosan and adsorbents

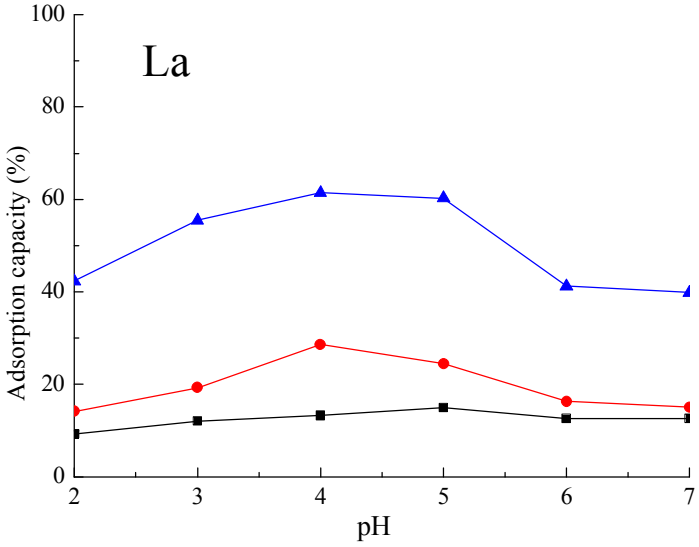

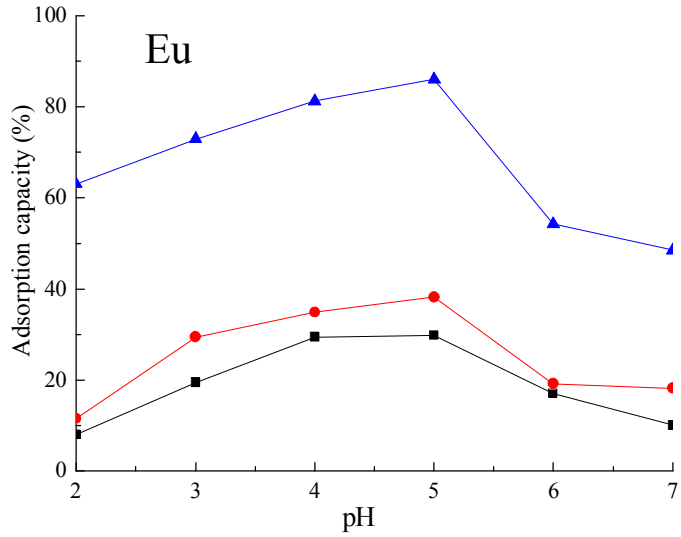

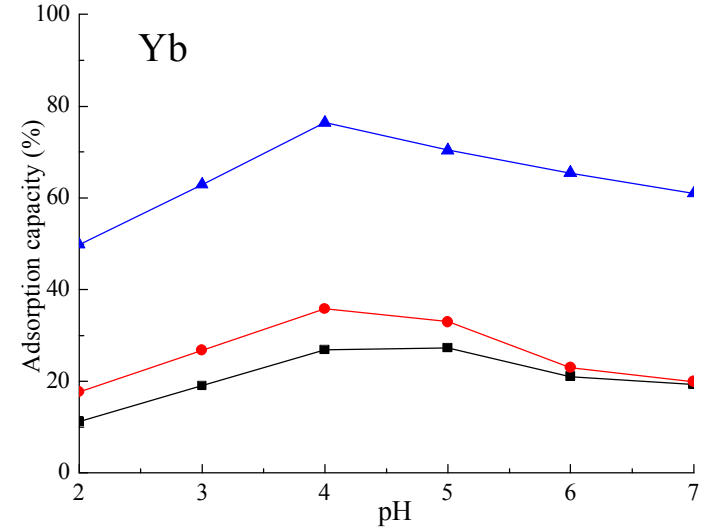
Yb
Adsorption capacity (%)
pH
0
20
40
60
80
100
2
3
4
5
6
7

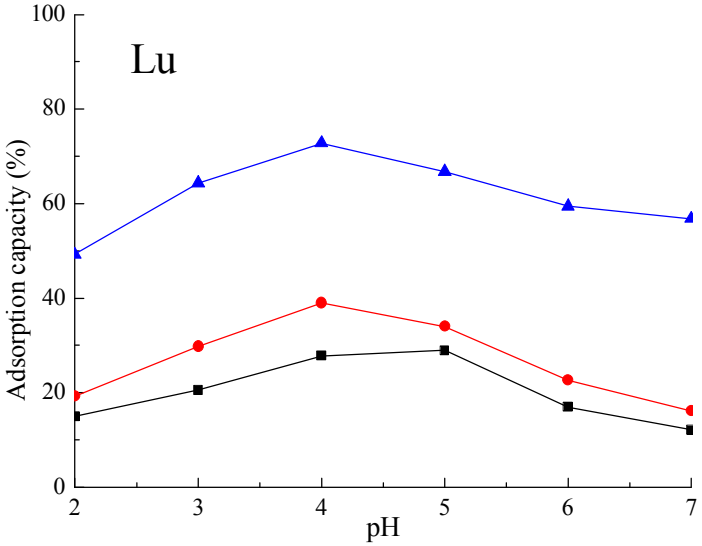
Lu
Adsorption capacity (%)
pH
0
20
40
60
80
100
2
3
4
5
6
7

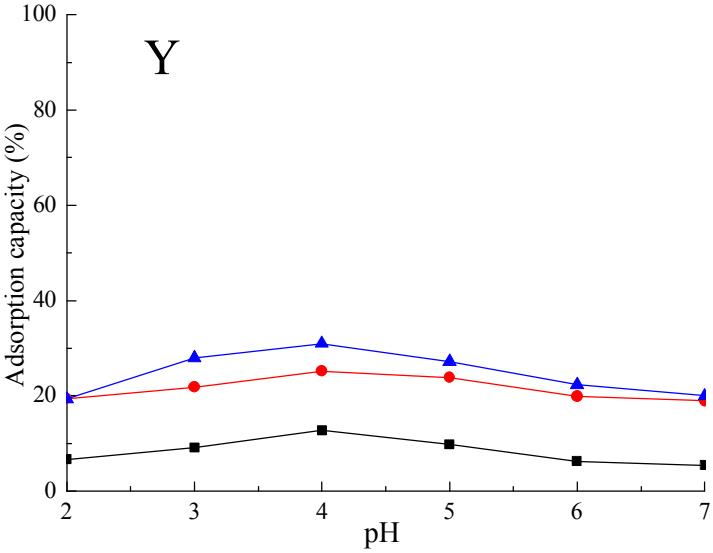
Y
Adsorption capacity (%)
pH
0
20
40
60
80
100
2
3
4
5
6
7

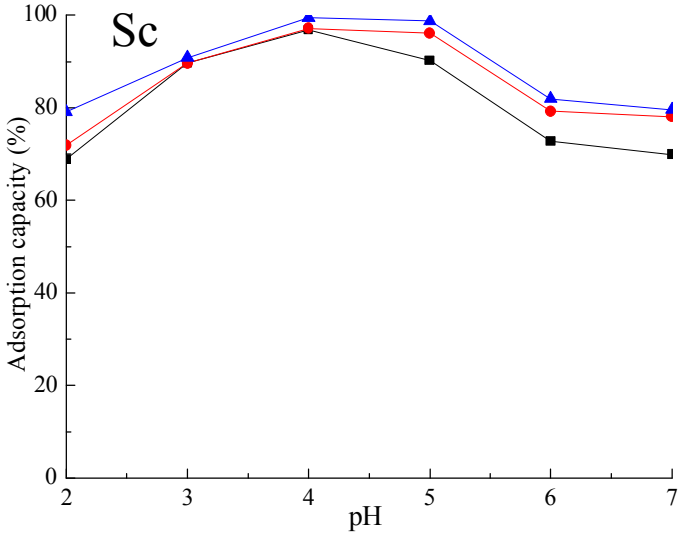

Fig. 3-8 Effect of pH on the removal of REEs using adsorbents (▲: ZCHC; ●:chitosan; ■: zeolite)

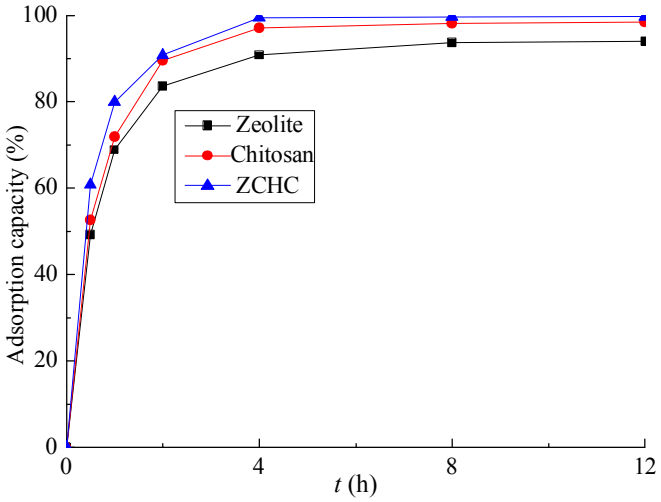

（A）

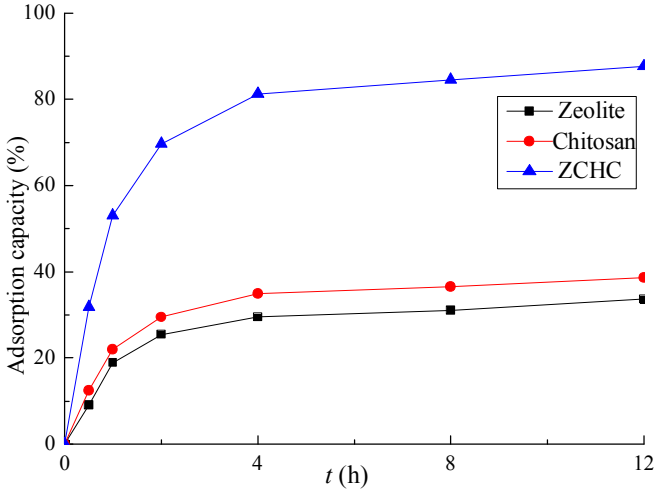

(B)

Fig. 3-9 Effect of contact time on percent removal of Sc using adsorbents (A: Sc; B: Eu)

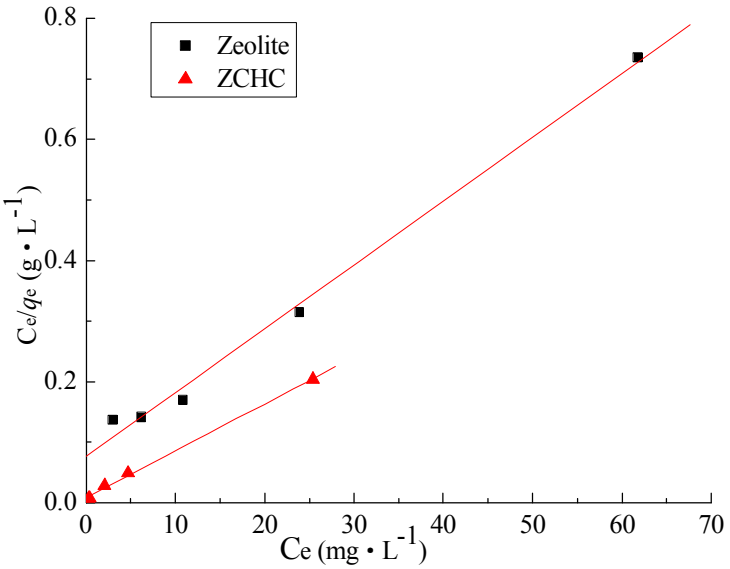

Fig. 3-10 Langmuir isotherm of Pb^{2+} adsorption on zeolite and ZCHC

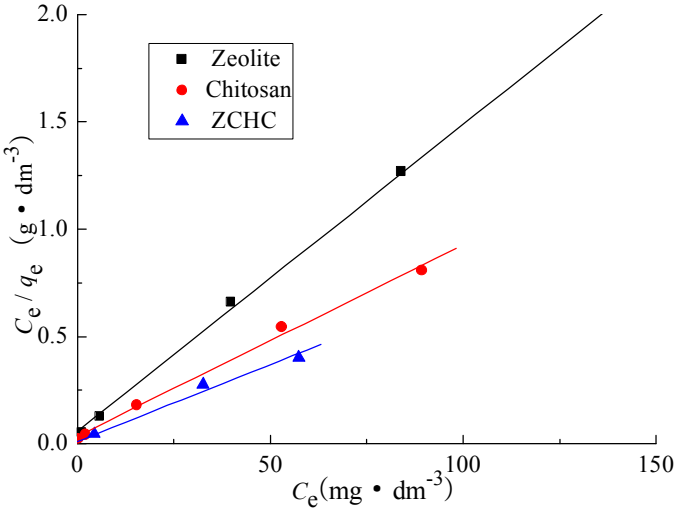

Fig. 3-11 Langmiur isotherm of Cr (VI) adsorption onto adsorbents

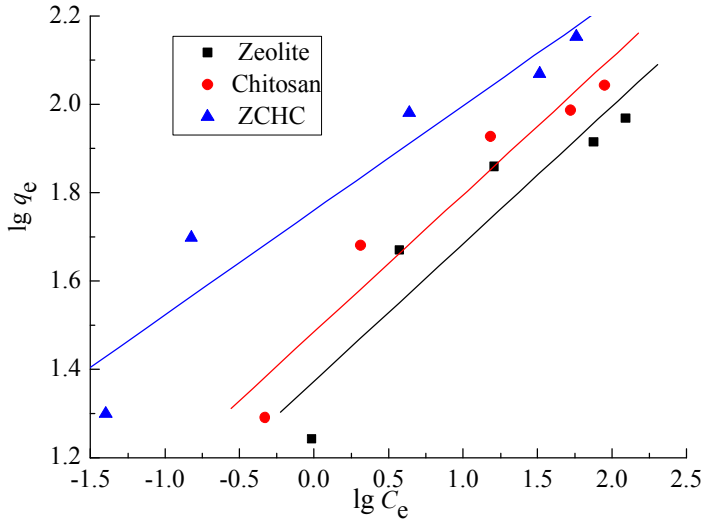

Fig. 3-12 Freundlich isotherm of Cr (VI) adsorption onto adsorbents

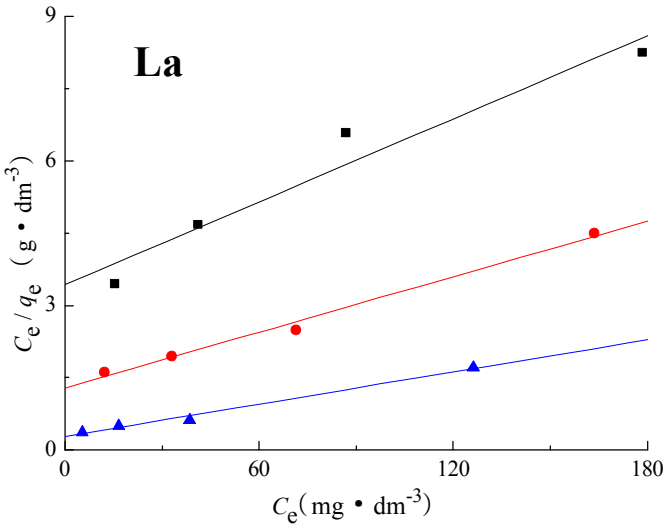
La
9
6
3
0
0
60
120
180
C_e / q_e (g • dm^{-3})
C_e(mg • dm^{-3})

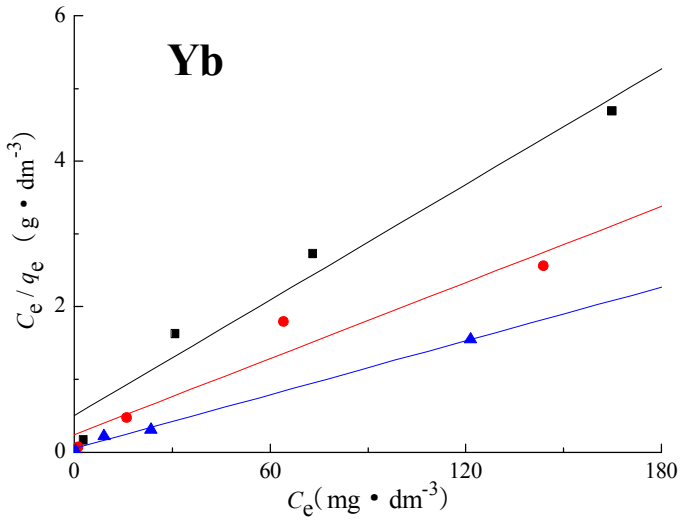
Yb
6
4
2
0
0
60
120
180
C_e / q_e (g • dm^{-3})
C_e(mg • dm^{-3})

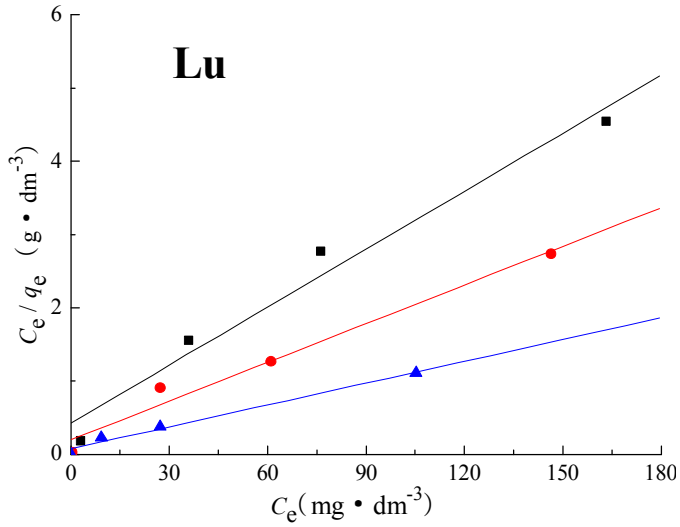
Lu
6
4
2
0
0
30
60
90
120
150
180
C_e / q_e (g • dm^{-3})
C_e(mg • dm^{-3})

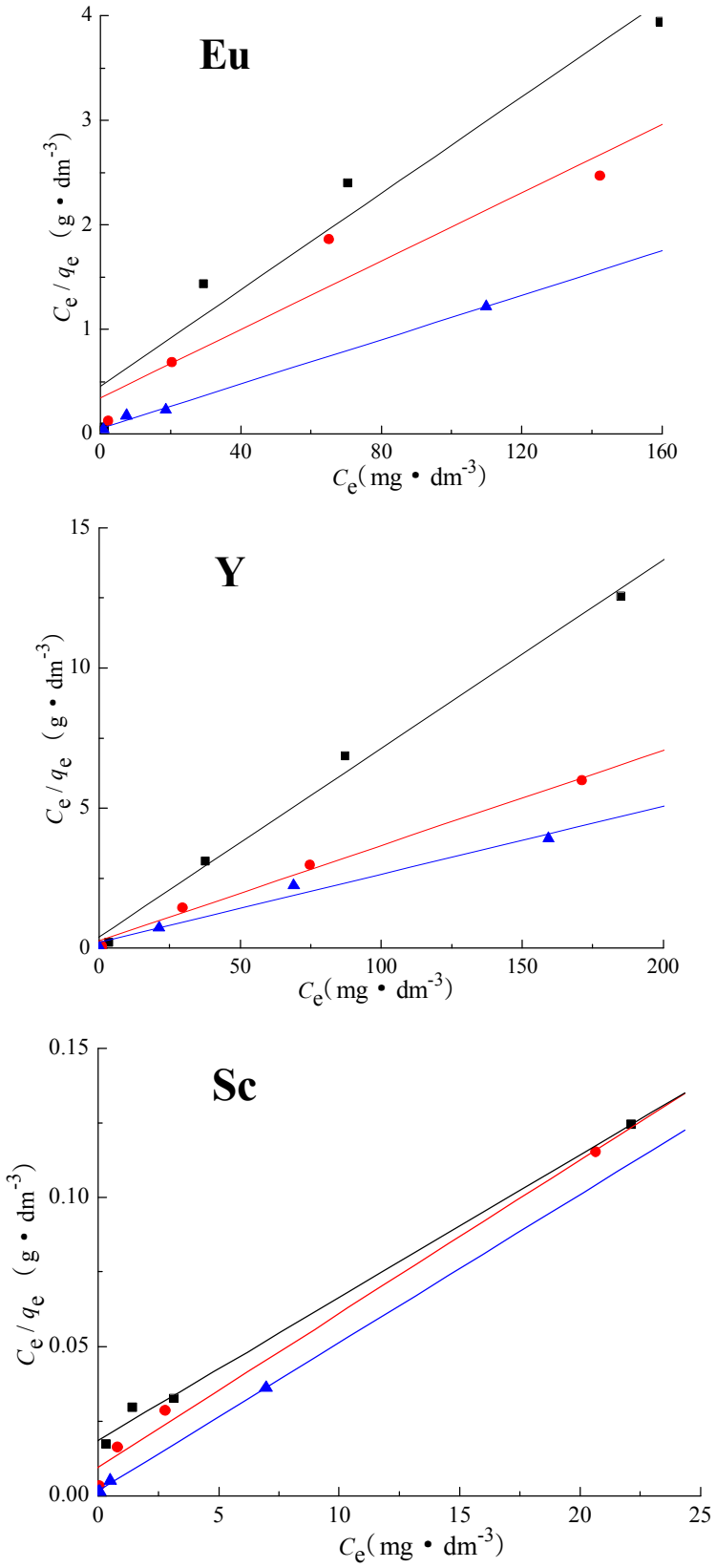

Fig. 3-13 Langmiur isotherm of REEs adsorption onto adsorbents (▲: ZCHC; ●:chitosan; ■: zeolite)

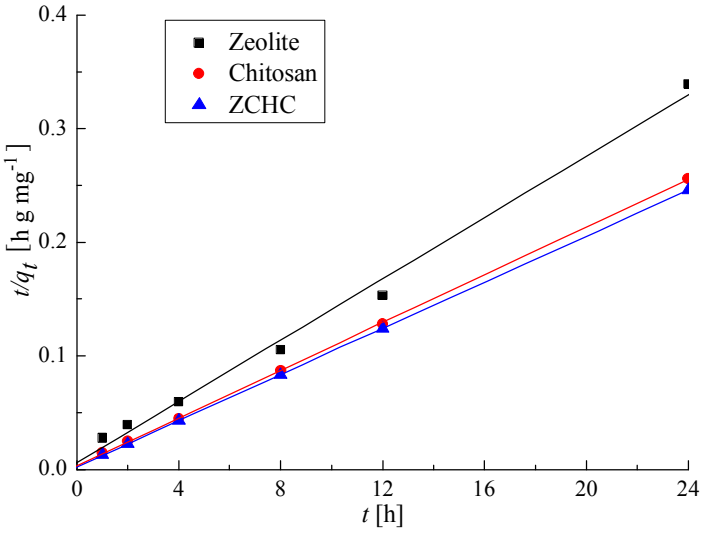

Fig. 3-14 The pseudo-second-order kinetic model of Pb^{2+} for adsorbents

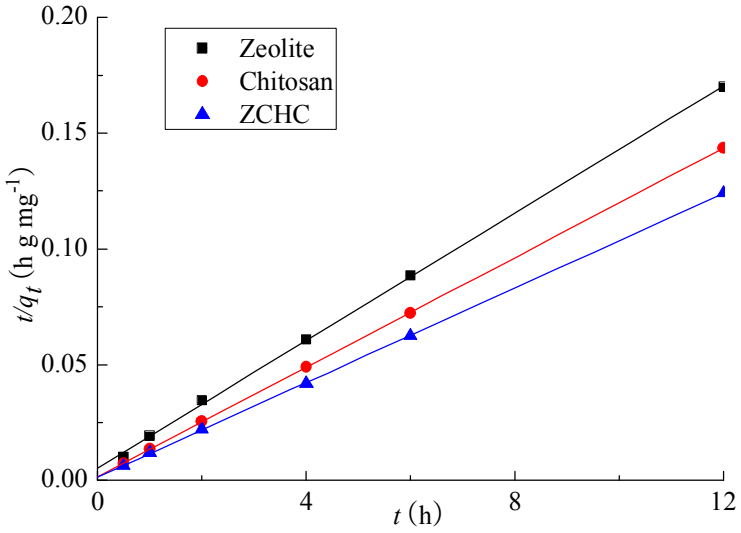

Fig. 3-15 The pseudo-second-order kinetic model of Cr(VI) for adsorbents

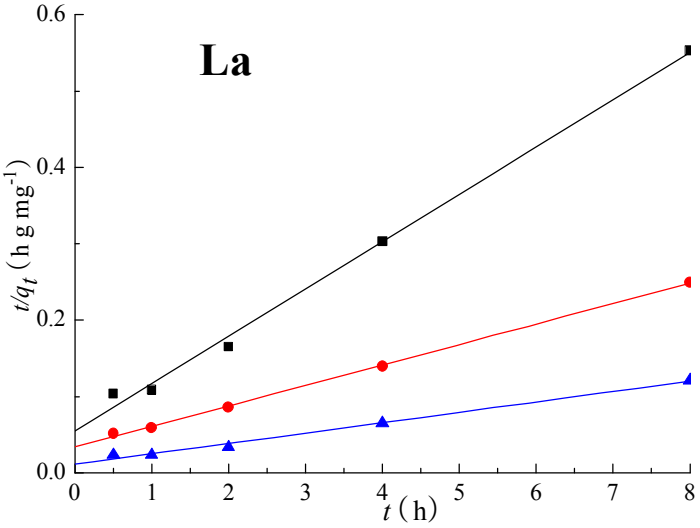

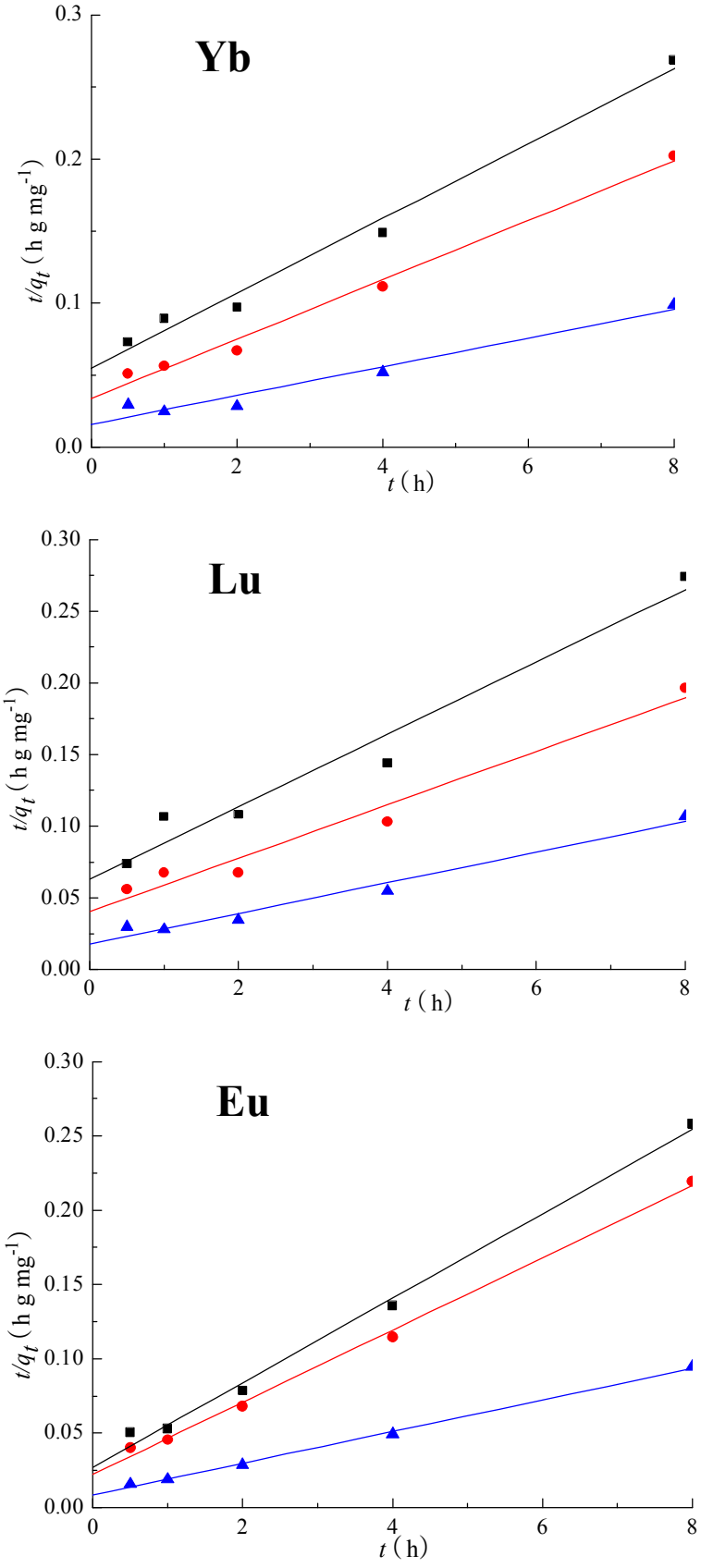
Yb
Lu
Eu
t/q_t (h g mg^{-1})
t (h)
0.0
0.1
0.2
0.3
0.00
0.05
0.10
0.15
0.20
0.25
0.30
0
2
4
6
8

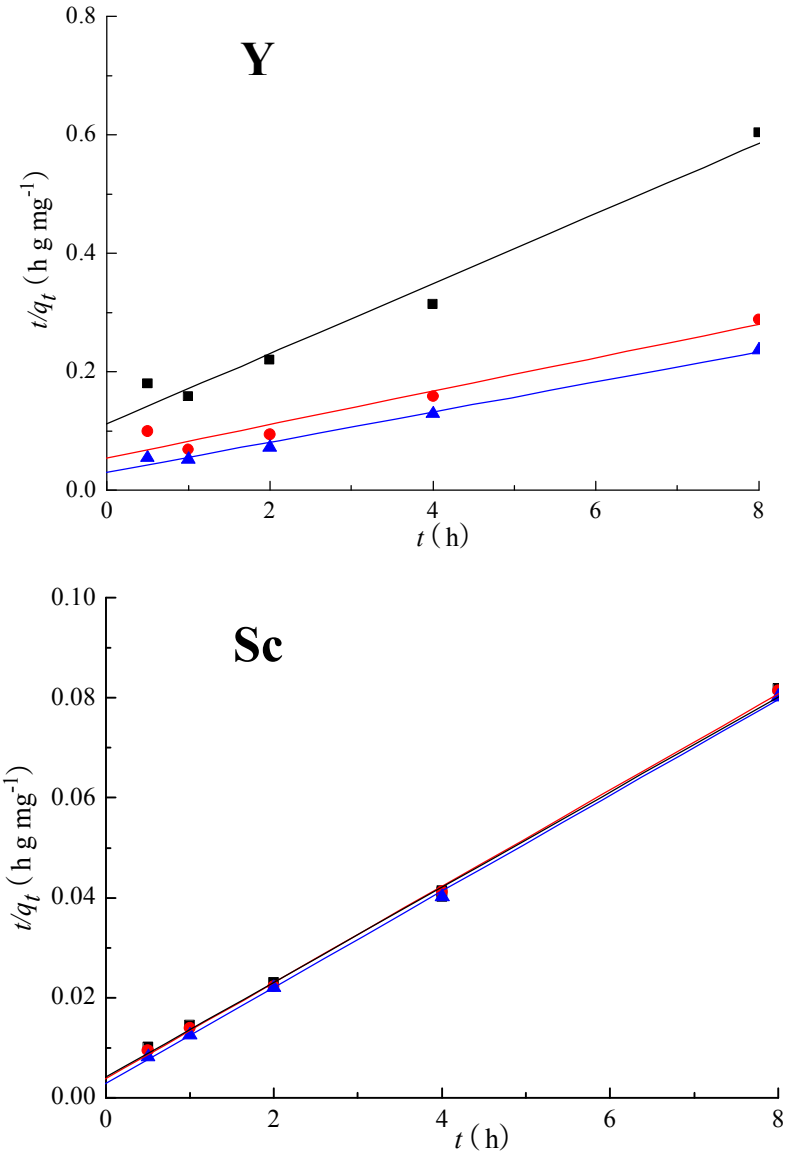

Fig. 3-16 The pseudo-second-order kinetic model of REEs for adsorbents

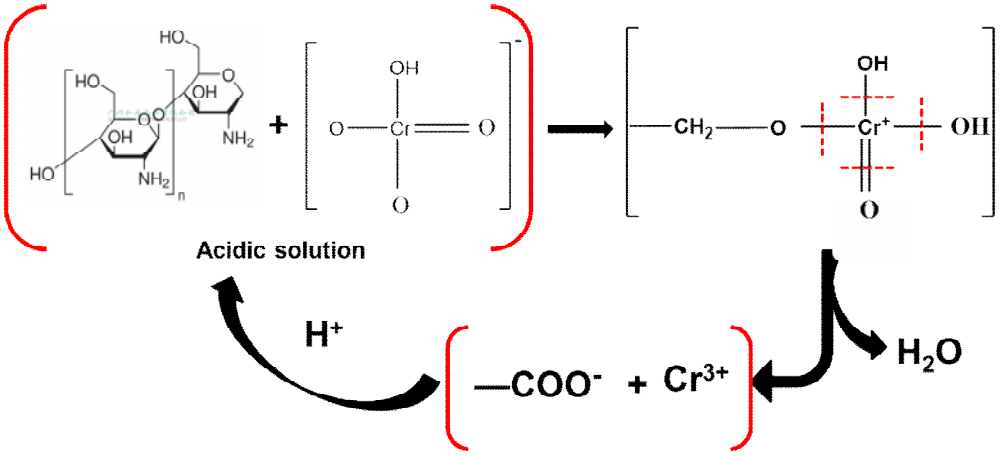

Fig. 3-17 Mechanism of removal of Cr (VI) by biomass gel particle

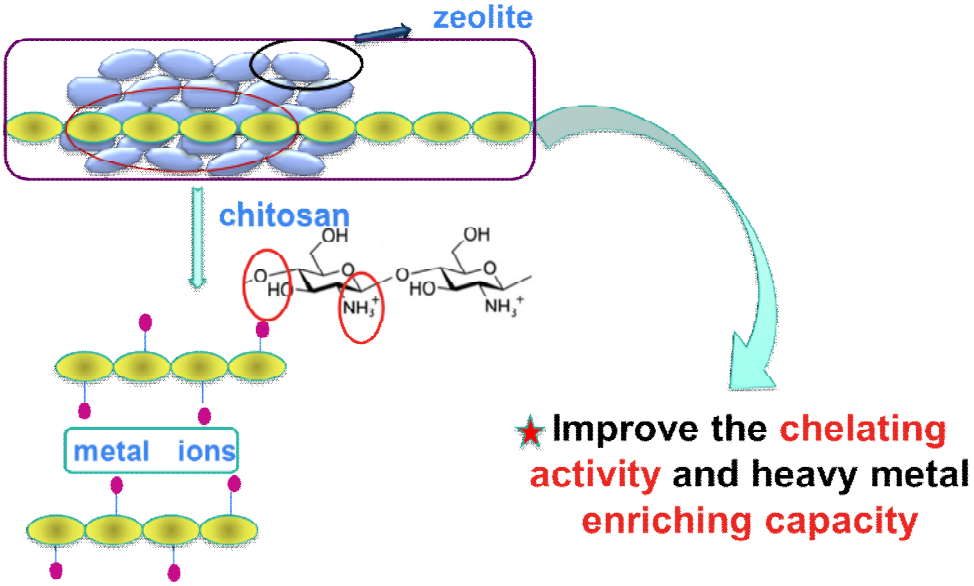

Fig. 3-18 Schematic of the major mechanism for sorption of metal ions onto ZCHC

Chapter 4 Conclusions

In the work of the thesis, the various materials have been extensively examined and applied for adsorption of aqueous containing heavy metals and REEs. In this study, the efficiency of activated carbon modified by $KMnO_4$ as adsorbent for Pb^{2+}, Cr (VI), REEs was investigated by batch techniques. In addition, the present investigation was carried out to evaluate the efficiency of zeolite/chitosan hybrid composite as adsorbent for aqueous Pb^{2+}, Cr (VI) and REEs.

Influence of various variables including pH, adsorbents dose, concentrations of contaminants, adsorption time, temperature and common ions of water on removal of Pb^{2+}, Cr (VI) and REEs was evaluated. The Langmuir and Freundlich models were used for the mathematical description of the adsorption equilibrium of Pb^{2+}, Cr (VI) and REEs to ACs and ZCHC. The suitability of the first- and second-order equations, kinetic model for the adsorption of Pb^{2+}, Cr (VI) and REEs onto ACs and ZCHC are also discussed.

The comparison of maximum adsorption capacities of the adsorbents in present study with that of the other sorbents reported in the literature for heavy metals (ie., Pb^{2+} and Cr (VI)) and REEs (ie., La and Eu) is presented in **Table 4-1—4-4**. From these tables, the adsorbents in this work provide comparable adsorption capacities to other adsorbents. Table 3 shows that the adsorbent used in this work has higher adsorption capacity as compared to those cited in the literature. In particular, it is noteworthy that ACs and ZCHC possess an enhanced sorption capacity for heavy metals and REEs.

The following conclusions were made from the experimental results:

1. Activated carbon were treated with $KMnO_4$, leading to a low-cost adsorbent with a good affinity for heavy metal ions and REEs. The ACs showed excellent adsorption capacity even if large amount of competitive ions exist in system. Particularly, ACs modified with $KMnO_4$ still showed highest adsorption capacity. The obtained material was characterized and used for heavy metals and REEs removal from aqueous solutions.

2. Adsorption of Pb^{2+}, Cr (VI) and REEs by ACs has been shown to depend significantly on the pH and initial adsorbate concentration. Adsorption of heavy metals and REEs onto such materials can generally be attributed to ion exchange with carboxylic and phenolic hydroxyl functional groups.

3. Zeolite/chitosan hybrid composite was prepared with sol-gel method by mixing zeolite and chitosan, investigated the adsorption ability of ZCHC as adsorbent for Pb^{2+}, Cr (VI) and REEs. ZCHC exhibited a higher adsorption capacity and stronger chemical affinity than pristine zeolite and chitosan.

4. The adsorption isotherm of Pb^{2+}, Cr (VI), REEs by ACs was well interpreted by Langmuir and Freundlich models. However, the experimental data of the adsorption of the studied ions onto adsorbents were suitably described by Langmuir isotherm, which suggests that the adsorption of heavy metals and REEs on the surface of the adsorbent belongs to monolayer adsorption in the concentration range studied.

5. The comparison evaluated correlation coefficients based on the studied kinetic models allowed considering the pseudo-second order model suitable for describing

the adsorption processes. This analysis revealed the rate determining step might be chemical and the adsorption processes involved the valency forces through sharing electron between the metal ions and adsorbents.

6. Desorption of Pb^{2+}, Cr (VI) and La (III) from the adsorbent has been found to depend upon the nature of the extracting solution, and ACs still present the high adsorption capacity towards heavy metals through several cycles of adsorption/desorption behavior. ACs could be an efficient adsorbent for heavy metals and REEs.

From this work, it was quantitatively clarified to some extent ACs and ZCHC could be an efficient adsorbent for heavy metal and REEs. It is very significant information from the viewpoint of environmental protection, and can be used for treating industrial waste waters including pollutants, and thus a promising option for the treatment of contaminated waters.

Tables

Table 4-1 Comparison of adsorption capacities various biosorbents towards Pb^{2+}

Biosorbent	Pb^{2+} uptake capacity (mg/g)	Reference
Acidified MWCNTs	49.7	[10]
Cicer arientinum biomass	27.8	[8]
Activated carbon prepared from apricot stone	22.9	[61]
Peanut husks carbon	70.0	[62]
AC_{K3}	101	Present study
ZCHC	139	Present study

Table 4-2 Comparison of adsorption capacities various biosorbents towards Cr (VI)

Biosorbent	Cr(VI) uptake capacity (mg/g)	Reference
Olive Bagasse	88.59	[37]
Eucalyptus Bark	45.50	[74]
Alligator Weed	82.57	[110]
AC_{K3}	134	Present study
Zeolite	70.0	Present study
Chitosan	92.2	Present study
ZCHC	109	Present study

Table 4-3 Comparison of adsorption capacities various biosorbents towards La (Ⅲ)

Biosorbent	La uptake capacity (μg/g)	Reference
carbon black (from recycled tires)	57.8	[3]
Laminaria japonica	12.23	[17]
silica gel/chitosan	69.2	[103]
Chitosan	52.1	Present study
ZCHC	89.6	Present study

Table 4-4 Comparison of adsorption capacities various biosorbents towards Eu (Ⅲ)

Biosorbent	Eu uptake capacity (μg/g)	Reference
ZSM-5 zeolite	24.17	[8]
mesoporous silica SBA-15	15.6	[91]
Bacillus subtilis	58.80	[111]
Zeolite	43.4	Present study
Chitosan	61.2	Present study
ZCHC	94.4	Present study

References

[1] S. Mohan, R. Gandhimathi, Removal of heavy metal ions from municipal solid waste leachate using coal fly ash as an adsorbent, Journal of Hazardous Materials 169 (2009) 351-359.

[2] W.M. Ibrahim, Biosorption of heavy metal ions from aqueous solution by red macroalgae, Journal of Hazardous Materials 192 (2011) 1827-1835

[3] Y. R. Smith, D. Bhattacharyya, T. Willhard, Mano Misra, Adsorption of aqueous rare earth elements using carbon black derived from recycled tires, Chemical Engineering Journal 296 (2016) 102-111

[4] C.R. Cánovas, F. Macías, R. Pérez-López, Metal and acidity fluxes controlled by precipitation/dissolution cycles of sulfate salts in an anthropogenic mine aquifer, Journal of Contaminant Hydrology 188 (2016) 29-43

[5] S.O. Ganiyu, E.D. Hullebusch, M. Cretin, G. Esposito, M. A. Oturan, Coupling of membrane filtration and advanced oxidation processes for removal of pharmaceutical residues: A critical review, Separation and Purification Technology 156 (2015) 891-914

[6] M. Ben-Sasson, X. Lu, S. Nejati, H. Jaramillo, M. Elimelech, In situ surface functionalization of reverse osmosis membranes with biocidal copper nanoparticles, Desalination 388 (2016) 1-8.

[7] E. Repo , J. K. Warchol , A. Bhatnagar, M. Sillanpaa, Heavy metals adsorption by novel EDTA-modified chitosan-silica hybrid materials. J. Colloid Interface Sci., 358 (2011): 261-267.

[8] X. Ren, C. Chen, M. Nagatsu, X. Wang, Carbon nanotubes as adsorbents in environmental pollution management: A review. Chem. Eng. J., 170 (2011) 395-410.

[9] S. Dahiya, R. M. Tripathi, A. G. Hegde, Biosorption of Heavy Metals and Radionuclide from Aqueous Solutions by Pre-treated Arca Shell Biomass. J. Hazard. Mater. 150 (2008) 376-386.

[10] J. Wang, C. Chen, Biosorbents for heavy metals removal and their future. Biotechnol. Adv., 27 (2009) 195-226.

[11] L. Zhou, C. Shang, Z. Liu, G. Huang, and A. A. Adesina, Selective adsorption of uranium (VI) from aqueous solutions using the ion-imprinted magnetic chitosan resins, J. Colloid Interface Sci. 366, (2011) 165-172 .

[12] S. V. Bhat, J. S. Melo, B. B. Chaugule, S. F. Souza, Biosorption characteristics of uranium from aqueous medium onto Catenella repens, a red alga. Journal of Hazardous materials. 158. (2008) 628-635.

[13] S. Haider, N. Bukhari, S. Y. Park and Y. Iqbal, Adsorption of Bromo-phenol Blue from an Aqueous Solution onto Thermally Modified Granular Charcoal, Chem. Eng. Res. Des., 89, (2011) 23-28 .

[14] C. Gerente, V. K. C. Lee, P. L. Cloirec, G. McKay,"Application of chitosan for the removal of metals from wastewaters by adsorption—Mechanisms and models review," Critical Reviews in Environmental Science and Technology, 37, (2007) 41-127.

[15] O.A.A. Elettaa, O.A. Ajayi, O.O. Ogunleye, I.C. Akpan, Adsorption of cyanide from aqueous solution using calcinated eggshells: Equilibrium and optimisation studies,Journal of Environmental Chemical Engineering 4 (2016) 1367-1375.

[16] M. Baláz,, Z. Bujnáková, P. Baláz, A. Zorkovská, Z. Danková, J. Briancin, Adsorption of cadmium(II) on waste biomaterial, Journal of Colloid and Interface Science 454 (2015) 121-133.

[17] K. N. Ghimire, K.Inoue, K. Ohto, T. Hayashida, Adsorption study of metal ions onto crosslinked seaweed Laminaria japonica, Bioresource Technology 99 (2008) 32-37.

[18] M. M. Rahmati, P. Rabbani, A. Abdolali, A. R. Keshtkar,"Kinetics and equilibrium studies on biosorption of cadmium, lead, and nickel ions from aqueous solutions by intact and chemically modified brown algae," Journal of Hazardous materials. 185, (2011) 401-407.

[19] W. Zhang, L. Meng, G. Mu, M. Zhao, P. Zou, Y. Zhang, A facile strategy for fabrication of nano-ZnO/yeast composites and their adsorption mechanism towards lead (II) ions, Applied Surface Science 378 (2016) 196-206.

[20] F.Guzel, H. Yakut, G. Topal, Determination of kinetic and equilibrium parameters of the batch adsorption of Mn(II), Co(II), Ni(II) and Cu(II) from aqueous solution by black carrot (Daucus carota L.) residues, Journal of Hazardous Materials 153 (2008) 1275-1287.

[21] M. R. Yazdani, T. Tuutijärvi, A. Bhatnagar, R. Vahala, Adsorptive removal of arsenic(V) from aqueous phase by feldspars: Kinetics, mechanism, and thermodynamic aspects of adsorption, Journal of Molecular Liquids 214 (2016) 149-156

[22] A. S. K. Kumar, S. J, Jiang, Chitosan-functionalized graphene oxide: A novel adsorbent an efficient adsorption of arsenic from aqueous solution, Journal of Environmental Chemical Engineering, 4 (2016) 1698-1713

[23] N. Geng, P. Wang, C. Wang, J. Hou, J. Qian, L. Miao, Mechanisms of cadmium accumulation (adsorption and absorption) by the freshwater bivalve Corbicula fluminea under hydrodynamic conditions, Environmental Pollution 212 (2016) 550-558

[24] E. Repo, L. Malinen, R. Koivula, R. Harjula, M.Sillanpää, Capture of Co(II) from its aqueous EDTA-chelate by DTPA-modified silica gel and chitosan, Journal of Hazardous Materials 187

(2011) 122-132

[25] G. N. Kousalya, M. R. Gandhi, S. Meenakshi,“Sorption of chromium (VI) using modified forms of chitosan beads”, International Journal of Biological Macromolecules 47, (2010) 308-315.

[26] S. Kumar, V.A. Loganathan, R.B. Gupta, M.O. Barnett, An Assessment of U(VI) removal from groundwater using biochar produced from hydrothermal carbonization, J. Environ. Manage. 92, (2011) 2504-2512.

[27] Q. B. Song, J. H. Li, Environmental effects of heavy metals derived from the e-waste recycling activities in China: A systematic review, Waste Management 34, (2014) 2587-2594.

[28] M. Adrees, S. Ali, M. Rizwan, M. Ibrahim, F. Abbas, Mechanisms of silicon-mediated alleviation of heavy metal toxicity in plants: A review, Ecotoxicology and Environmental Safety 119 (2015) 186-197

[29] L. Zhang, Y. X. Zeng, Z. J. Cheng, Removal of heavy metal ions using chitosan and modified chitosan: A review, Journal of Molecular Liquids 214 (2016) 175-191.

[30] D. R. Baldwin and W. J. Marshall, “Heavy metal poisoning and its laboratory investigation”, Annals of Clinical Biochemistry, 36(3), (1999) 267-300

[31] C.J. Rosen, “Lead in the home garden and urban soil environment”, Communication and Educational Technology Services, University of Minnesota Extension, 2002

[32] J. Zhu, J. Yang and B. Deng, Ethylenediamine-modified Activated Carbon for Aqueous Lead Adsorption, Environ. Chem. Lett., 8 (2010) 277-282

[33] M. Fukushima, K. Nakayasu, S. Tanaka, H. Nakamura, Speciation Analysis of Chromium after Reduction of Chromium (VI) by Humic Acid. Toxicological and Environmental

Chemistry 62, (1997) 207-215.

[34] M. K. Donais, R. Henry, T. Rettberg, Chromium Speciation Using an Automated Liquid Handling System with Inductively Coupled Plasma-Mass Spectrometric Detection. Talanta, 49 (1999) 1045-1050.

[35] R I. Acosta, X. Rodriguez, C. Gutierrez, M. M. Guadalupe, Biosorption of Chromium (VI) from Aqueous Solutions onto Fungal Biomass Bioinorganic Chemistry and Application, 2 (2004) 1-7.

[36] D. P. Mungasavalli, T. Viraraghavan, Y. C. Jin, Biosorption of Chromium from Aqueous Solutions by Pretreated Aspergillus Niger: Batch and Column Studies. Colloids and Surfaces A: Physicochemical and Engineering Aspects, 301 (2007) 214-223.

[37] D. Hakan, I. Demiral, T. Fatma, K. Belgin, Adsorption of Chromium from Aqueous Solution by Activated Carbon Derived from Olive Bagasse and Applicability of Different Adsorption Models. Chemical Engineering Journal, 144 (2008) 188-196.

[38] S. Motomizu, K. Jitmanee, M. Oshima, On-Line Collection/Concentration of Trace Metals for Spectroscopic Detection via Use of STSP (Small-Sized Thin Solid Phase) Column Resin Reactors, Application to Speciation of Cr(III) and Cr(VI). Analytica Chimica Actam, 499 (2003) 149-155.

[39] N. Ertugay, and Y. K. Bayhan, Biosorption of Cr (VI) from Aqueous Solutions by Biomass of Agaricus Bisporus. Journal of Hazardous Materials 154 (2008) 432-439.

[40] M. Pang, N. Kano, and H. Imaizumi, Adsorption of Chromium (VI) from Aqueous Solution Using Zeolite/Chitosan Hybrid Composite, J. Chem. Chem. Eng. 9 (2015) 433-441.

[41] S. U. Yesiller, A.E. Eroglu, T. Shahwan, Removal of aqueous rare earth elements (REEs)

using nano-iron based materials, Journal of Industrial and Engineering Chemistry, 19 (2013) 898-907.

[42] M. Davranche, O. Pourret, G. Gruau, A. Dia, Impact of humate complexation on the adsorption of REE onto Fe oxyhydroxide, Journal of Colloid and Interface Science, 277 (2004) 271-279.

[43] Y. Wan, C. Liu, The effect of humic acid on the adsorption of REEs on kaolin, Colloids and Surfaces A: Physicochem. Eng. Aspects 290 (2006) 112-117.

[44] Kissao Gnandi el al., Distribution patterns of rare earth elements and uranium in tertiary sedimentary phosphorites of Hahotoé-Kpogamé, Togo, *J*ournal of African Earth Sciences, 37 (2003) 1-10

[45] Taylor, S.R., and S.M. Mc Clennan, The Continental Crust: Its Composition and Evolution, Oxford, UK: Blackwell Scientific Publications, 1985.

[46] N. Bahramifar, and Y. Yamini, On-line preconcentration of some rare earth elements in water samples using C18-cartridge modified with l-(2-pyridylazo) 2-naphtol (PAN) prior to simultaneous determination by inductively coupled plasma optical emission spectrometry (ICP-OES), *Anal. Chim. Acta*, 540 (2005) 325-332

[47] M. He, B. Hu, Y. Zeng, and Z. Jiang, ICP-MS direct determination of trace amounts of rare earth impurities in various rare earth oxides with only one standard series, J. Alloys Compd., 390 (2005) 168-174

[48] K. Mohantly, M. Jha, B. C. Meikap, M. N. Biswas, Biosorption of Lanthanides Using Three Kinds of Seaweed Biomasses. Chemical Engineering Journal 117 (2006) 71-77.

[49] R. Kumar, N. R. Bishnoi, G. K. Bishnoi, Biosorption of Chromium(VI) from Aqueous

Solution and Electroplating Wastewater Using Fungal Biomass. Chemical Engineering Journal 135 (2008) 202-208.

[50] S. Dahiya, R. M. Tripathi, A. G. Hegde, Biosorption of Lead and Copper from Aqueous Solutions by Pre-treated Crab and Arca Shell Biomass. Bioresource Technology 99 (2008) 179-187.

[51] P. Sharma, P. Kumari, M. M. Srivastava, S. Srivastava, Ternary Biosorption Studies of Cd(II), Cr(III) and Ni(II) on Shelled Moringa oleifera Seeds. Bioresource Technology 98 (2007) 474-477.

[52] J. Z. Chen, X. C. Tao, J. Xu, T. Zhang, Z. L. Liu, Biosorption of Lead, Cadmium and Mercury by Immobilized Microcystis aeruginosa in a Column. Bioresource Technology 40 (2005) 3675-3679.

[53] A. Sari, M. Tuzen, Removal of Mercury(II) from Aqueous Solution Using Moss (Drepanocladus revolvens) Biomass: Equilibrium, Thermodynamic and Kinetic Studies. Journal of Hazardous Materials 171 (2009) 500-507.

[54] K. Periasamy, C. Namasivayam, Removal of copper(II) by adsorption onto peanut hull carbon from water and copper plating industry wastewater, *Chemosphere*, 32 (1996) 769-789,

[55] A. Sari, M. Tuzen, D. Mendil, M. Soylak, Biosorptive Removal of Mercury(II) from Aqueous Solution Using Lichen (Xanthoparmelia conspersa) Biomass: Kinetic and Equilibrium Studies. Journal of Hazardous Materials 169 (2009) 263-270.

[56] A. Sari, M. Tuzen, Biosorption of Selenium from Aqueous Solution by Green Algae (Cladophora hutchinsiae) Biomass: Equilibrium, Thermodynamic and Kinetic Studies. Chemical Engineering Journal, 158 (2010) 200-206.

[57] A. Sari, M. Tuzen, Biosorption of Pb(II) and Cd(II) from Aqueous Solution Using Green Alga (Ulva lactuca) Biomass. Journal of Hazardous Materials 152 (2009) 302-308.

[58] C. Y. Mevra, K.Yusuf, O. F. Algur, Response Surface Optimization of the Removal of Nickel from Aqueous Solution by Cone Biomass of Pinus sylvestris. Bioresource Technology 97 (2006) 1761-1765.

[59] Y. Sun, S.Yang, G. Sheng, Z. Guo, and X. Wang, The removal of U(VI) from aqueous solution by oxidized multiwalled carbon nanotubes, J. Environ. Radioactivity, 105 (2012) 40-47.

[60] M. Kobya, E. Demirbas, E. Senturk and M. Ince, Adsorption of Heavy Metal Ions from Aqueous Solutions by Activated Carbon Prepared from Apricot Stone, Bioresour. Technol., 96 (2005) 1518-1521

[61] S. Ricordel, S. Taha, I. Cisse and G. Dorange, Heavy Metals Removal by Adsorption onto Peanut Husks Carbon: Characterization, Kinetic Study and Modeling, Sep. Purif. Technol., 24 (2001) 389-401.

[62] W. R. Grace & Co. Enriching Lives, Everywhere. – Zeolite Structure. Grace.com. Retrieved on 2010-12-09.

[63] Levels of Radioactive Materials Rise Near Japanese Plant, The Associated Press (via NYTimes), April 16, 2011

[64] J. Xie, C. J. Li, L. N. Chi and D.Y. Wu, Chitosan modified zeolite as a versatile adsorbent for the removal of different pollutants from water, Fuel 103 (2013) 480-485.

[65] L. Yu, J. Gong, C. F. Zeng, and L. X. Zhang, Preparation of zeolite-A/chitosan hybrid composites and their bioactivities and antimicrobial activities, Materials Science and

Engineering C 33 (2013) 3652-3660.

[66] W. S.Wan Ngah, L. C. Teong, R. H. Toh, and M. A. K. M. Hanafiah, Utilization of chitosan – zeolite composite in the removal of Cu (II) from aqueous solution: Adsorption, desorption and fixed bed column studies. Chemical Engineering Journal 209 (2012) 46-53.

[67] https://en.wikipedia.org/wiki/Chitosan.

[68] Z. Shen, D. P. Kamdem, Development and characterization of biodegradable chitosan films containing two essential oils, International Journal of Biological Macromolecules 74 (2015) 289-296.

[69] H. Ma, J. Sun, Y. Zhang, C. Bian, S. Xia, T. Zhen, Label-free immunosensor based on one-step electrodeposition of chitosan-gold nanoparticles biocompatible film on Au microelectrode for determination of aflatoxin B_1 in maize, Biosensors and Bioelectronics 80 (2016) 222-229.

[70] W. S. Wanngah, S. Fatinathan, Pb(II) Biosorption Using Chitosan and Chitosan Derivatives Beads: Equilibrium, Ion Exchange and Mechanism Studies. Journal of Environmental Sciences 22 (2010) 338-346.

[71] D. Chauhan, M. Jaiswal, S. Nalini, Removal of Cadmium and Hexavalent Chromium from Electroplating Waste Water Using Thiocarbamoyl Chitosans. Carbohydrate Polymers 88 (2012) 670-675.

[72] A. Dhaouadi, L. Monser, N. Adhoum, Removal of rotenone insecticide by adsorption onto chemically modified activated carbons, Journal of Hazardous Materials, 181 (2010) 692-699.

[73] V. Sarin, K. K. Pant, Removal of chromium from industrial waste by using eucalyptus bark. Bioresour. Technol., 97 (2006) 15-20.

[74] D. Duranoğlu, A. W. Trochimczuk, U. Beker, Kinetics and thermodynamics of hexavalent chromium adsorption onto activated carbon derived from acrylonitrile–divinylbenzene copolymer. Chem. Eng. J., 187 (2012) 193-202.

[75] K. R. Hall, L. C. Eagleton, A. Acrivos, T. Vemeulen, Pore and solid-diffusion kinetics in fixed-bed adsorption under constant-pattern conditions, Industrial and Engineering Chemistry Research Fundamentals 5, (1966) 213-223.

[76] https://en.wikipedia.org/wiki/Rate_equation.

[77] S. S. Pillai, M. D. Mullassery, N. B. Fernandez, N. Girija, P. Geetha, and M. Koshy, Biosorption of Cr(VI) from aqueous solution by chemically modified potato starch: Equilibrium and kinetic studies. Ecotoxicology and Environmental Safety 92 (2013) 199-205.

[78] http://en.wikipedia.org/wiki/Rare_earth_element

[79] Sachdeva S., Kumar A. Preparation of nanoporous composite carbon membrane for separation of rhodamine B dye. J. Membr. Sci., 329 (2009) 2-10.

[80] Shashikant R .M., Rajamanya V. S. Biosorption studies of chromium and pentachlorophenol from tannery effluents. Bioresour. Technol., 98 (2003) 1128-1132.

[81] Mellah A., Chegrouche S., Barkat M.The removal of uranium(VI) from aqueous solutions onto activated carbon kinetic and thermodynamic investigations. J. Colloid Interface Sci., 296 (2006) 434-441

[82] Chen C., Li X., Zhao D., Tan X., Wang X. Adsorption kinetic, thermodynamic and desorption studies of Th(IV) on oxidized multi-wall carbon nanotubes. Colloid Surf. A: Physicochem. Eng. Asp., 302 (2007) 449-454.

[83] I. Tuzun, G. Bayramoglu, E. Yalcin, G. Basaran, G. Celik, M. Y. Arica, Equilibrium and

kinetic studies on biosorption of Hg(II), Cd(II) and Pb(II) ions onto microalgae Chlamydomonas Reinhardtii. J. Environ. Manage., 77 (2005) 85-92.

[84] D.A. Britz, A.N. Khlobystov, Noncovalent interactions of molecules with single walled carbon nanotubes, Chemical Society Reviews. 35 (2006) 637-659.

[85] E. Raymundo-Pinero, P. Azaïs, T. Cacciaguerra, D. Cazorla-Amorós, A. Linares Solano, F. Béguin, KOH and NaOH activation mechanisms of multiwalled carbon nanotubes with different structural organisation, Carbon 43 (2005) 786-795.

[86] Y.H. Li, S.G. Wang, Z.K. Luan, J. Ding, C.L. Xu, D.H. Wu, Adsorption of cadmium(II) from aqueous solution by surface oxidized carbon nanotubes, Carbon 41 (2003) 1057–1062.

[87] P. Chingombe, B. Saha and R. J. Wakeman, Surface modification and characterisation of a coal-based activated carbon, Carbon, 43 (2005) 3132-3143

[88] N. Salgado-Gómez, M. G. Macedo-Miranda, M. T. Olguín, Chromium VI adsorption from sodium chromate and potassium dichromate aqueous systems by hexadecyltrimethylammonium-modified zeolite-rich tuff, Applied Clay Science, 95 (2014) 197-204.

[89]N. K. Hamadi, X. D. Chen, M. M. Farid, and M. Q. Lu, Adsorption Kinetics for the Removal of Chromium (VI) from Aqueous Solution by Adsorbents Derived from Used Tyres and Sawdust. Chemical Engineering Journal, 84 (2001) 95-105.

[90] X. L. Tan, D. Xu, C. L. Chen, X. K. Wang, W. P. Hu, Adsorption and kinetic desorption study of $^{152+154}$Eu (III) on multiwall carbon nanotubes from aqueous solution by using chelating resin and XPS methods, Radiochim. Acta, 96 (2008) 23-29.

[91] L. Dolatyari, M. R. Yaftian, S. Rostamnia, Adsorption characteristics of Eu(III) and Th(IV)

ions onto modified mesoporous silica SBA-15 materials, Journal of the Taiwan Institute of Chemical Engineers, 60 (2016) 174-184

[92] Liu Y, Li Q, Cao X, Wang Y, Jiang X, Li M, et al. Removal of uranium(VI) from aqueous solutions by CMK-3 and its polymer composite. Appl Surf Sci, 285 (2013) 258-266.

[93] Abbasizadeh S, Keshtkar AR, Mousavian MA. Preparation of a novel electrospun polyvinyl alcohol/titanium oxide nanofiber adsorbent modified with mercapto groups for uranium(VI) and thorium(IV) removal from aqueous solution. Chem Eng J, 220 (2013) 161–171.

[94] L. Chen, B. Bai, Equilibrium, kinetic, thermodynamic, and in situ regeneration studies about methylene blue adsorption by the raspberry-like TiO_2 yeast microspheres, Ind. Eng. Chem. Res. 52 (2013) 15568-15577

[95] J. Fu, Z. Chen, M. Wang, S. Liu, J. Zhang, J. Zhang, R. Han, Q. Xu, Adsorption of methylene blue by a high-efficiency adsorbent (polydopamine microspheres): kinetics, isotherm, thermodynamics and mechanism analysis, Chem. Eng. J. 259 (2015) 53-61.

[96] E.V. Lazareva, S.M. Zhmodik, N.L. Dobretsov, A.V. Tolstov, B.L. Shcherbov, N.S. Karmanov, E.Yu. Gerasimov, A.V. Bryanskaya, Main minerals of abnormally high-grade ores of the Tomtor deposit, Russian Geology and Geophysics 56 (2015) 844–873.

[97] R. H. Ronald Cohen, Use of microbes for cost reduction of metal removal from metals and mining industry waste streams, Journal of Cleaner Production 14 (2006) 1146-1157

[98] S. M. Abdel Moniem, M. E. M. Ali, T, A. Gad-Allah, A. S. G. Khalil, M. Ulbricht, M.F. El-Shahat, A. M. Ashmawy, H. S. Ibrahim, Detoxification of hexavalent chromium in wastewater containing organic substances using simonkolleite-TiO_2 photocatalyst, Process Safety and Environmental Protection 95 (2015) 247–254.

[99] J. G. Sánchez, F. S. Ochoa, G. H. Cocoletzi, J. F. Rivas-Silva, N. Takeuchi, Ab-initio studies of the Sc adsorption and the ScN thin film formation on the GaN(000-1)-(2 × 2) surface, Thin Solid Films 548 (2013) 317–322.

[100] B. S. Bowman, Applications of surfactant-modified zeolites to environmental remediation, Rev Micropor Mesopor Mater 61(2003) 43–56.

[101] R. D. Soltani, A. R. Khataee, M. Safari, and S.W. Joo, Preparation of bio-silica/chitosan nanocomposite for adsorption of a textile dye in aqueous solutions, International Biodeterioration & Biodegradation 85 (2013) 383–391.

[102] R. N. Aleksandra, J. V. Sava, G. A. Dušan, Modification of chitosan by zeolite A and adsorption of Bezactive Orange 16 from aqueous solution, Composites: Part B 53 (2013) 145–151.

[103] M. R. Gandhi, S. Meenakshi, Preparation and characterization of La(III) encapsulated silica gel/chitosan composite and its metal uptake studies, Journal of Hazardous Materials 203-204 (2012) 29-37.

[104] M. R. Gandhi, S. Meenakshi, Preparation and characterization of silica gel/chitosan composite for the removal of Cu(II) and Pb(II), Journal of Hazardous Materials 50 (2012) 650-657.

[105] G. Wang, J. Liu, X. Wang, Z. Y. Xie, and N. Deng, Adsorption of Uranium (VI) from Aqueous Solution onto Cross-Linked Chitosan. Journal of Hazardous Materials 168 (2009) 1053-1058.

[106] N. Salgado-Gómez, M. G. Macedo-Miranda, and M. T. Olguín, Chromium (VI) Adsorption from Sodium Chromate and Potassium Dichromate Aqueous Systems by

Hexadecyltrimethylammonium - modified Zeolite-rich Tuff. Applied Clay Science 95 (2014) 197-204.

[107] N. K. Hamadi, X. D. Chen, M. M. Farid, and M. Q. Lu, Adsorption Kinetics for the Removal of Chromium (VI) from Aqueous Solution by Adsorbents Derived from Used Tyres and Sawdust. Chemical Engineering Journal, 84 (2001) 95-105.

[108] D. Xu, X. Tan, C. Chen, and X. Wang, Adsorption of Pb(II) from Aqueous Solution to MX-80 Bentonite: Effect of pH, Ionic Strength, Foreign Ions and Temperature. Appl. Clay Sci. 41 (2008) 37-46.

[109] Y. NAKANO, K. TAKESHITA and T. TSUTSUM, Adsorption mechanism of hexavalent chromium by redox within condensed-tannin gel, Water Research 35 (2001) 496–500

[110] X. Wang, Y. Tang and S. Tao, Kinetics, equilibrium and thermodynamic study on removal of Cr (VI) from aqueous solutions using low-cost adsorbent Alligator weed, Chemical Engineering Journal 148 (2009) 217–225

[111] T. Yao, X. Wu, X. Chen, Y. Xiao, Y. Zhang, Y. Zhao and F. Li, Biosorption of Eu(III) and U(VI) on Bacillus subtilis: Macroscopic and modeling investigation, Journal of Molecular Liquids 219 (2016) 32–38.

Acknowledgements

In the past three years and half, I have been studied in Kano Lab at the Graduate School of Science and Technology, Niigata University, Japan. Allow me to express my appreciations and thanks on my graduations!

Firstly, I would like to express my deepest gratitude to Associated Professor Naoki Kano for his sincerely guidance, valuable advice and encouragement, and I am very thanks to Professor Hiroshi Imaizumi for his help for me throughout my doctoral course. I would like to thank Professor Mineo Sato, Professor Tatsuya Kodama, and Professor Kazuaki Yamagiwa for their advices and suggestions of this thesis.

Secondly, I also want to give my appreciations to peoples who give me many instruction, helping and encourage for my experiments. They are Kunihiko Fuzii, Manabu Ooizumi and Miyoko Masui in Office for Environment and Safety of Niigata University for the on the use of ICP-AES and ICP-MS, my co-members my Chinese friends in our lab.

Finally, the best thanks to my parents and friends in China for their support of my studying abroad.